University of Alberta

Photodegradation of Free Chlorine and the Possible Application for the Validation
of Ultraviolet (UV) Reactors

by

Yangang Feng

A thesis submitted to the Faculty of Graduate Studies and Research
in partial fulfillment of the requirements for the degree of

Doctor of Philosophy

in

Environmental Engineering

Department of Civil & Environmental Engineering

Edmonton, Alberta
Spring 2007

Canada

This work is dedicated to my wife, Zhewen Kang.

ABSTRACT

Free chlorine is commonly used for microorganism reduction in water and wastewater treatment, and it is usually observed to be degraded significantly by UV light. Therefore, this study investigated the possibility to use the photodegradation of free chlorine (PFC) for the validation of UV reactors. First, the quantum yield of free chlorine and the influencing factors were investigated in this study. The quantum yield was observed to be affected significantly by pH, the concentration of free chlorine, and the concentration of organic contaminants. The temperature also affected the quantum yield when organics were in the free chlorine sample. When the wavelength of UV light varied from 220 to 300 nm, the quantum yield was not observed to change significantly. Second, the photodegradation products of free chlorine under 254 nm UV light were also studied. The mass balance of the photodegradation products indicates that the chloride (Cl^-) and chlorate (ClO_3^-) ions are the major end products in the photodegradation of free chlorine. Last, the possibility of the PFC method used for the validation of UV reactors was investigated on a bench-scale low-pressure UV system for various operating conditions (flow rate, UV transmittance and TOC). As a comparison, the UV reactor was also validated by *Bacillus subtilis* spores (a surrogate often used in biodosimetry for the validation of UV reactors) for corresponding operating conditions. The results obtained in this research show that the reliability of the proposed method is independent of the operating conditions and it can work as well as conventional biodosimetry for monitoring of the performance of UV reactors.

ACKNOWLEDGEMENT

I would like to express my sincere gratitude to my supervisor, Dr. James R. Bolton, for his valuable suggestions and guidance provided throughout my research program. I will always be grateful for his warm-hearted encouragement, unbelievable understanding and endless support in these years. I also would like to take this unique opportunity to give my deep thankfulness to my co-supervisor, Dr. Daniel W. Smith, for his excellent suggestions and direction provided during my research.

I extremely appreciate Dr. Stephen A. Craik for his very helpful suggestions in my experiments and his kind help to allow me to use the equipments in his laboratory for this research. I would also like to give my special thanks to Ms. Maria Demeter who helped me tirelessly in my laboratory experiments. Without her suggestions and guidance, my experiments will never be performed so smoothly and comfortably. I would also like to extend my appreciation to Mr. Gary Solonynko and Mr. Nick Chernuka for their kindly assistance in my study and research in these years.

Finally I would acknowledge the Natural Sciences and Engineering Research Council (NSERC) for financial support and the Department of Civil & Environmental Engineering for providing the facilities for my study and research. Also, I would give my special thanks to my family, friends, and colleague students for their help, encouragement and friendship.

TABLE OF CONTENTS

LIST OF TABLES

LIST OF FIGURES

ACRONYMS

AWWA	American Water Works Association
BD	Biodosimetry
CDF	Chlorine Demand Free
CFD	Computational Fluid Dynamics
CFU	Colony Forming Units
DBPs	Disinfection By-products
HAAs	Haloacetic Acids
LP/MP	low pressure/medium pressure
LT2ESWTR	Long Term 2 Enhanced Surface Water Treatment Rule
MOR	Microorganism Reduction
PFC	Photodegradation of Free Chlorine
REF	Reduction Equivalent Fluence
RED	Reduction Equivalent Dose
THMs	Trihalomethanes
TOC	Total Organic Carbon
USEPA	US Envionmental Protection Agency
UV	Ultraviolet
UVT	Ultraviolet Transmittance

CHAPTER 1 INTRODUCTION

1.1 Background

Ultraviolet (UV) disinfection in water treatment, including research and applications, can be traced back for about 100 years ago (Lorch 1987, USEPA 2003a, and Whitby and Scheible 2004). However, because of many reasons, such as the technologies of UV equipment manufacture, verification of the UV light efficacy, other cheaper alternative microorganism reduction (MOR) methods, etc., it was not widely applied in the world until recently. However, in recent decades, especially with the discoveries of some carcinogenic disinfection by-products (DBPs) caused by chemical MOR methods (such as chlorine and ozone) and the outbreaks of infection from protozoan cysts and oocysts (shown in Table 1.1), efforts have been accelerated to find an effective disinfection method to protect the safety of public drinking water supply. At the Annual Conference of American Water Works Association (AWWA) in 1998, it was the first time that the UV irradiation was clearly reported to be very effective with *Cryptosporidium spp.* (Bolton et al. 1998). This important discovery stimulated the investigation of UV irradiation for the reduction of some refractory microbes in drinking water treatment in the following years. Around 2000, considerable work on UV inactivation of *Cryptosporidium spp.* (Clancy et al., 2000; Bukhari et al., 1999; Craik et al., 2001) and *Giardia spp.* (Craik et al., 2000; Finch and Belosevic, 1999; Campbell and Wallis, 2002) using mouse infectivity or cell culture showed that low or medium-pressure UV lamps, or pulsed UV technology are very effective for the inactivation of these

1

pathogens, which are usually very resistant to the conventional treatment processes, such as chlorine treatment. Therefore, UV irradiation began to be recognized again for the inactivation of protozoan pathogens, especially *Giardia lamblia* and *Cryptosporidium parvum*. As of 2002, it was estimated that over 3,000 drinking water facilities had employed UV irradiation in Europe for disinfection (Masschelein, 2002). In North America, thousands of UV disinfection processes have been applied to control the contamination of refractory pathogenic microorganisms (especially *Cryptosporidium spp.* and *Giardia spp.*) and disinfection byproducts in drinking water (USEPA 2003b and 2003c). With the increased public awareness and concerns about the drinking water safety, one can surmise that UV disinfection will be more and more popular in the world and the number of applications in water utilities will also increase explosively.

Table 1.1 Some severe waterborne outbreaks caused by protozoan cysts and oocysts occurred in the world

Year	Pathogen	Brief introduction of the event	Reference
1987, U.S.	*Cryptosporidium spp.* oocysts were identified in samples of treated public water with use of a monoclonal-antibody test.	An outbreak of gastroenteritis affected an estimated 13,000 people in a county of 64,900 residents in western Georgia.	Hayes et al. 1989
1993, U.S.	An ineffective filtration process led to the inadequate removal of *Cryptosporidium spp.* oocysts in one of two municipal water treatment plants	An estimated 403000 residents of the 5-county greater Milwaukee, Wisconsin area developed cryptosporidiosis after drinking contaminated municipal water.	Osewe et al. 1996
2001, Canada	*Cryptosporidium spp.* oocysts were detected in the finished drinking water of this region.	About 2000 persons were infected with gastroenteritis in an area of North Battleford, Saskatchewan.	Stirling et al. 2001
2004, Norway	The *Giardia lamblia* cysts were found in treated water up to 5 cysts per 10 liters.	A serious waterborne outbreak of giardiasis occurred in the Norwegian city of Bergen resulting in over 1000 people becoming ill.	Kalisvaart 2005
2004, U.S.	The groundwater was found to be contaminated by *Giardia spp.*, *Campylobacter spp.*, *Salmonella* etc.	About 1450 people were infected with gastroenteritis after visiting the South Bass Island (Ohio) between July and September 2004	CRC, 2005a
2005, U.K.	The drinking water reservoir was contaminated by human wastes containing *Cryptosporidium hominis*	Over 70,000 people in 40 towns in the north western region of Wales, UK have been told to boil their drinking water due to an outbreak of cryptosporidiosis	CRC, 2005b

3

However, UV disinfection is not always so powerful as to inactivate all kinds of microorganisms. As shown in Figure 1.1, for different pathogenic microorganisms, the sensitivities to UV irradiation vary greatly. For example, for *E. coli*, one only needs a fluence (UV dose) of about 7 mJ cm^{-2} to achieve 3-log removal, but for adenovirus 40 (PLC/PRF/5 cell line as the host), the fluence (UV dose) should be about 150 mJ cm^{-2} to get the same inactivation level. This indicates that it is very important for a UV reactor to deliver enough fluence (UV dose) to get the required inactivation level for the target pathogens. If a UV reactor fails to deliver the required fluence (UV dose), one cannot be assured that the treated drinking water is microbiologically safe. For instance, some regulations, such as ÖNORM M 5873-1 (Austria) and DVGW-W294 (Germany), prescribe that the minimum fluence (UV dose) delivered in a UV reactor should be 40 mJ cm^{-2} for the removal of 3-log *Cryptosporidium spp.* and 3-log *Giardia spp.* (DVGW 1997 and ÖNORM 2003). The Long Term 2 Enhanced Surface Water Treatment Rule (LT2ESWTR) enacted by U.S. Environmental Protection Agency (EPA) also requires UV systems employed in water utilities to demonstrate that the UV reactor can deliver enough fluence (UV dose) under different operating conditions to provide the level of inactivation required in a given application (USEPA 2003b). Therefore, in order to satisfy the regulation requirements and to verify the disinfection performance of UV reactors, it is very necessary to validate the fluences (UV doses) delivered by the UV reactor under different operating conditions. In practice, validation testing also is an exceedingly important step for the design and operation of UV facilities.

4
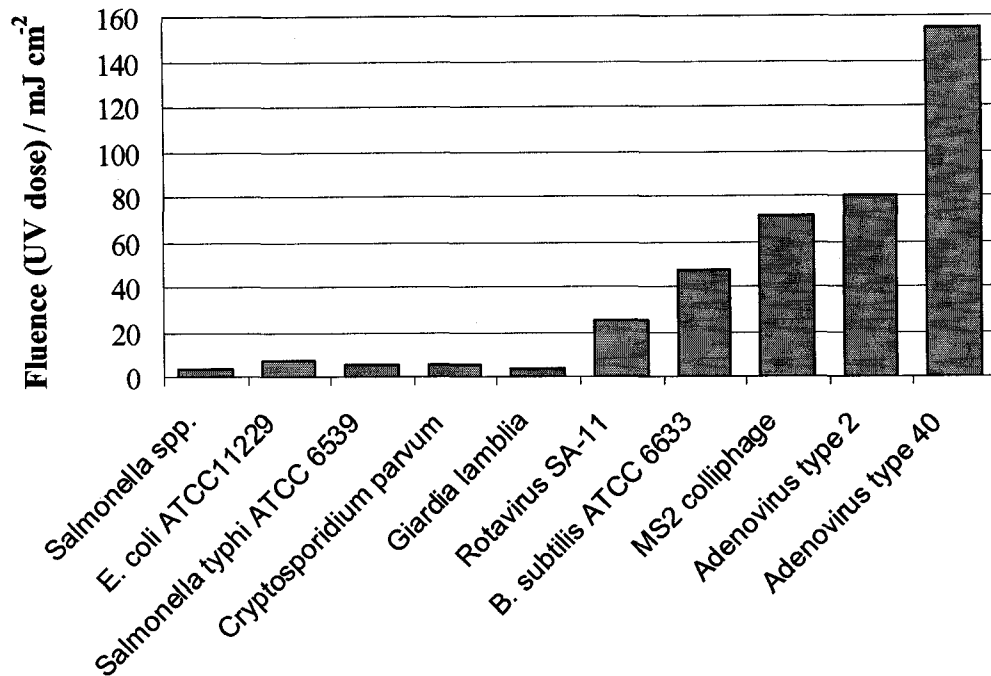
Figure 1.1[1] **Fluences (UV doses) needed for the 3 log inactivation of various pathogenic microorganisms (after Chevrefils et al. 2006)**

Biodosimetry is currently a widely used method for the validation of UV reactors in water treatment utilities. In this method, a surrogate microorganism, such as *Bacillus subtilis* spores, MS2 bacteriophage, or *E. coli*, are usually spiked into the testing water and flow through the validated UV reactor. Then, the log-inactivation of the surrogate microbe achieved by the UV reactor is determined, based on the concentrations of the viable microorganisms in the influent and effluent of the UV reactor. The fluence or UV dose delivered in the UV reactor, termed the Reduction Equivalent Fluence (REF) or reduction equivalent dose (RED), can be obtained by relating the log-inactivation value to the predetermined fluence-response curve of the surrogate microbe. This is the most

---

[1] In the above figure, the hosts of Rotavirus SA-11, MS2 phage, Adenovirus type 2, and Adenovirus type 40 respectively are MA-104 cell line, E. coli ATCC 15597, A549 cell line, and PLC/PRF/5 cell line.

5

reliable method available at present for the full-scale validation of UV reactors, and it is usually provided as a standard approach by some current regulatory guidance manuals. However, this is a relatively expensive and time-consuming process, and it cannot be operated on-line in water treatment utilities because of the biohazard. In addition, this method has been effectively used for the validation of UV reactors at flow rates less than 20 MGD, whereas little evidence has shown that it works effectively at much higher flow rates (Mamane-Gravetz and Linden, 2004). Even though it may be possible to be utilized at large flow rates, there are problems in growing the large quantities of surrogate microorganisms required to validate a large UV reactor. Furthermore, culture conditions for surrogates can affect their sensitivity to UV irradiation and, as a result, the accuracy of the validation data could be adversely affected (Severin et al., 1983; Nicholson and Galeano, 2003). Since the response of many microorganisms is nonlinear to UV fluence and a UV reactor always has a distribution of fluences, there could be a deviation to use the REF (RED) determined by surrogate microorganisms to reflect the disinfection efficiency of a UV reactor for other pathogenic microorganisms. Thereby, it is desirable to find an easier, quicker and more inexpensive approach for the validation testing of UV reactors to compensate for the disadvantages of biodosimetry.

1.2 Research objectives

Chlorine has been used for drinking water MOR treatment for nearly a century and it still is the most widely used method throughout the world today. In practical operations or in laboratory studies, one can usually observe that chlorine can be clearly degraded by UV irradiation. Thus, the objective of this research was to investigate the

6

possibility of using the photodecomposition of free chlorine as a method to validate the fluence (UV dose) delivered in UV reactors. Specifically, this research was: (1) to determine the quantum yields of free chlorine decomposed by UV light and the influencing factors, (2) to investigate photodecomposition mechanisms and products of free chlorine, and (3) to compare the validation results of a UV reactor obtained by the free chlorine method and biodosimetry (using *Bacillus subtilis* spores).

1.2.1 Quantum yields of free chlorine and the influencing factors

Free chlorine consists of hypochlorous acid (HOCl) and its conjugate base, the hypochlorite ion (OCl⁻), and the relationship of these components mainly depend on pH. The quantum yields of free chlorine were measured at various pH values, and a mathematic model was established to estimate the quantum yield of free chlorine for any pH condition. The influencing factors, such as TOC, temperature, concentration of free chlorine, and wavelength, were investigated, and the effects of these factors on the quantum yield of free chlorine were carefully analyzed.

1.2.2 Photodecomposition mechanisms and products of free chlorine

The degradation products generated from the photolysis of free chlorine (HOCl and OCl⁻) were quantitatively determined and the mass balance of the end-products was performed. The effects of pH, TOC, and concentration of free chlorine on the photodecomposition products were examined in detail. In addition, based on the experimental results, this research presented proposed photodecomposition mechanisms for both HOCl and OCl⁻.

7

1.2.3 Validation testing of UV reactors by free chlorine

Free chlorine was used to validate a bench-scale UV reactor for various operating conditions, and the effects of flow rate, UV transmittance, and water quality (TOC) on the validation testing were explored. The UV reactor was also validated by biodosimetry (*B. subtilis*) for similar operating conditions, and a comparison of the validation results obtained by free chlorine and *B. subtilis* was conducted. According to the statistical analysis of the validation results, the possibility of using free chlorine for the validation of UV reactors was studied.

1.3 References

Bolton, J.R., Dussert, B.W., Bukhari, Z., Hargy, T. and Clancy, J.L. 1998. Inactivation of *Cryptosporidium parvum* by medium-pressure ultraviolet light in finished drinking water, *Proc. AWWA 1998 Annual Conference*, Dallas, TX, Vol. A, pp 389–403.

Bukhari, Z., Bolton, J.R., Dussert, B.W. and Clancy, J.L. 1999. Medium-pressure UV for oocyst inactivation. *J. AWWA*, **91(3)**: 86–94.

Campbell, A.T. and Wallis, P. 2002. The effect of UV irradiation on human-derived Giardia lamblia cysts. *Wat. Res.*, **36(4)**: 963–969.

Chevrefils, G., Caron, E., Wright, H., Sakamoto, G., Payment, P., Barbeau, B. and Cairns, B. 2006. UV dose required to achieve incremental log inactivation of bacteria, protozoa and viruses. *IUVA News*, **8(1)**: 38–45.

Clancy, L.J., Bukhari, Z., Bolton, J.R., Dussert, B.W. and Marshall, M.M. 2000. Using UV to inactivate Cryptosporidium. *J. AWWA*, **92(9)**: 97–104.

Craik, S.A., Weldon, D., Finch, G.R., Bolton, J.R. and Belosevic, M. 2001. Inactivation of Cryptosporidium parvum oocysts using medium- and low-pressure ultraviolet radiation. *Wat. Res.*, **35(6)**: 1387–1398.

Craik, S.A., Finch, G.R., Bolton, J.R. and Belosevic, M. 2000. Inactivation of Giardia muris cysts using medium-pressure ultraviolet radiation in filtered drinking water. *Wat. Res.*, **34(18)**: 4325–4332.

CRC 2005a. Public Health Newsletter of the CRC for Water Quality and Treatment, Health Stream (March 2005, issue 37), http://www.waterquality.crc.org.au/hs/hs3 7web.htm

CRC 2005b. Public Health Newsletter of the CRC for Water Quality and Treatment, Health Stream (December 2005, issue 40), http://www.waterquality.crc.org.au/hs/ hs40web.htm

Finch, G.R. and Belosevic, M. 1999. Presentation to the U.S. EPA Stage 2 FACA: ultraviolet technology work group, September 10, 1999, U.S. EPA, Washington, DC

GVGW - Deutscher Verein des Gas- und Wasserfaches e.V. 1997. UV systems for disinfection in drinking water supplies - requirements and testing (English version translated and edited by J. R. Bolton). Postfach 14 01 51, D-53056 Bonn, Germany.

Hayes, E.B., Matte, T.D., O'Brien, T.R., McKinley, T.W., Logsdon, G.S., Rose, J.B., Ungar, B.L., Word, D.M., Pinsky, P.F., Cummings, M.L. 1989. Large community outbreak of cryptosporidiosis due to contamination of a filtered public water supply. *N. Engl. J. Med.*, **320(21)**: 1372–1376.

Kalisvaart, B. 2005. Giardia contamination of Bergen waterworks prompts quick implementation of UV disinfection system. *IUVA News*, **7(2)**: 7–8.

Lorch, W. (editor) 1987. Handbook of eater purification (2nd edition). Ellis Horwood Limited, Market Cross House, Cooper Street, Chichester, West Sussex, PO19 1EB, Endland. pp 530–531.

Mamane-Gravetz, H. and Linden, K.G. 2004. UV disinfection of indigenous aerobic spores: implications for UV reactor validation in unfiltered waters. *Wat. Res.*, **38(12)**: 2898–2906.

Masschelein, W.J. 2002. Ultraviolet light in water and wastewater sanitation. CRC Press LLC, 2000 NW Corporate Blvd., Boca Raton, Florida 33431.

Nicholson, L.W. and Galeano, B. 2003. UV resistance of Bacillus anthracis spores revisited: validation of Bacillus subtilis spores as UV surrogates for spores of B. anthracis sterne. *Appl. Environ. Microbiol.*, **69(2)**: 1327–1330.

ÖNORM 2003. Austrian National Standard: prÖNORM M 5873-2 E. 2003. Plants for disinfection of water using ultraviolet radiation: requirements and testing. Austrian Standards Institute, Vienna, Austria, www.on-norm.at

Osewe, P., Addiss, D.G., Blair, K.A., Hightower, A., Kamb, M.L., Davis, J.P. 1996. Cryptosporidiosis in Wisconsin: a case-control study of post-outbreak transmission. *Epidemiol. Infect.*, **117(2)**: 297–304.

Severin, B.F., Suidan, M.T. and Engelbrecht, R.S. 1983. Kinetic modeling of UV disinfection of water. *Wat. Res.*, **17(11)**: 1669–1678.

Stirling, R., Aramini, J., Ellis, A., Lim, G., Meyers, R., Fleury, M. and Werker, D. 2001. Waterborne Cryptosporidiosis outbreak, North Battleford, Saskatchewan, spring, 2001. Canada Communicable Disease Report, 15 November 2001, Volume 27 - Number 22.

USEPA 2000. U.S. Environmental Protection Agency, National primary drinking water regulations: ground water rule; proposed rules, *Fed. Reg.*, **65(91)**, 2000.

USEPA 2003a. Ultraviolet Disinfection Guidance Manual. EPA 815-D-03-007, June 2003 draft, 1200 Pennsylvania Avenue NW Washington, DC 20460-0001.

USEPA 2003b. National primary drinking water regulations: Long Term 2 Enhanced Surface Water Treatment Rule; proposed rule; *Fed. Reg.*, **68(154)**, August 11, 2003.

USEPA 2003c. National primary drinking water regulations (NPDWRs): Stage 2 Disinfectants and Disinfection Byproducts Rule; NPDWRs: Approval of Analytical Methods for Chemical Contaminants; Proposed Rule. *Fed. Reg.*, **68(159)**, August 18, 2003.

Whitby, G.E. and Scheible, O.K. 2004. The history of UV and wastewater. *IUVA News*, **6(3)**: 15–26.

CHAPTER 2 PHOTODECOMPOSITION OF FREE CHLORINE

AND VALIDATION OF UV REACTORS – AN OVERVIEW

2.1 Introduction

Chlorine has been used in water MOR treatment for more than one century, and now it still is extensively used throughout the world. However, due to the increasing public concerns on the harmful chlorinated disinfection by-products (DBPs) and the inability of chlorine to inactivate some refractory pathogens (such as *Giardia spp.* and *Cryptosporidium spp.*), other disinfection methods have been developed and employed in recent decades. Although it is not a newly emerged MOR technology, UV technology has been given considerable attention in recent years because of its excellent disinfection capability for the reduction of those pathogens which are resistant to chlorine. UV light is very effective with many pathogenic microorganisms, such as *E. coli*, *Giardia* spp., Hepatitis A virus, *Legionella spp.*, etc. Nevertheless, it is not all-powerful; for instance, Adenovirus 40 is very resistant to UV irradiation, but it is quite sensitive to chlorine. Accordingly, in order to provide a higher level of pathogen protection and a level of disinfection redundancy, UV and chlorine are usually combined as multiple disinfection barriers in many water utilities.

It is well recognized in water treatment and swimming pool disinfection that aqueous chlorine is not stable under sunlight or UV irradiation. For example, in the E. L. Smith Water Treatment Plant (EPCOR Water Services, Edmonton), it is usually observed that the concentration of chlorine in the pre-chlorinated water has a significant decrease

12

after flowing through the UV reactors. The UV reactors used in water utilities must be validated to show that they can deliver enough fluence (UV dose) to achieve the required inactivation levels for the target pathogens. Usually, biodosimetry is employed for the validation of UV reactors, which is a relatively money- and time-consuming approach. Based on the phenomenon of photodecomposition of free chlorine with UV irradiation, this study proposes to use free chlorine for the validation of UV reactors. This chapter will present an overview of the photodecomposition of free chlorine and the validation of UV reactors. Specifically, this literature review will mainly involve (1) photolysis of free chlorine with UV light, (2) the sequential process of chlorination and UV irradiation applied in drinking water disinfection and the DBPs generated in this process, (3) biodosimetry for the validation of UV reactors, and (4) other validation methods.

2.2 Photolysis of free chlorine with UV light

2.2.1 Components of free chlorine in water disinfection

In water disinfection, free chlorine is defined as the concentration of residual chlorine in water present as dissolved gas (Cl_2), hypochlorous acid (HOCl) and hypochlorite ion (OCl^-). These three forms of free chlorine exist in water according to the following equilibria:

[2.1] $Cl_2 + H_2O \leftrightarrow HOCl + H^+ + Cl^-$

[2.2] $HOCl \leftrightarrow H^+ + OCl^-$
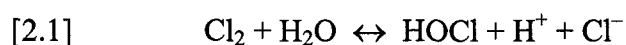
The relative proportions of these three components depend primarily on the pH and temperature. As an example, Figure 2.1 shows the effect of pH on the form of free chlorine at 25°C.

13
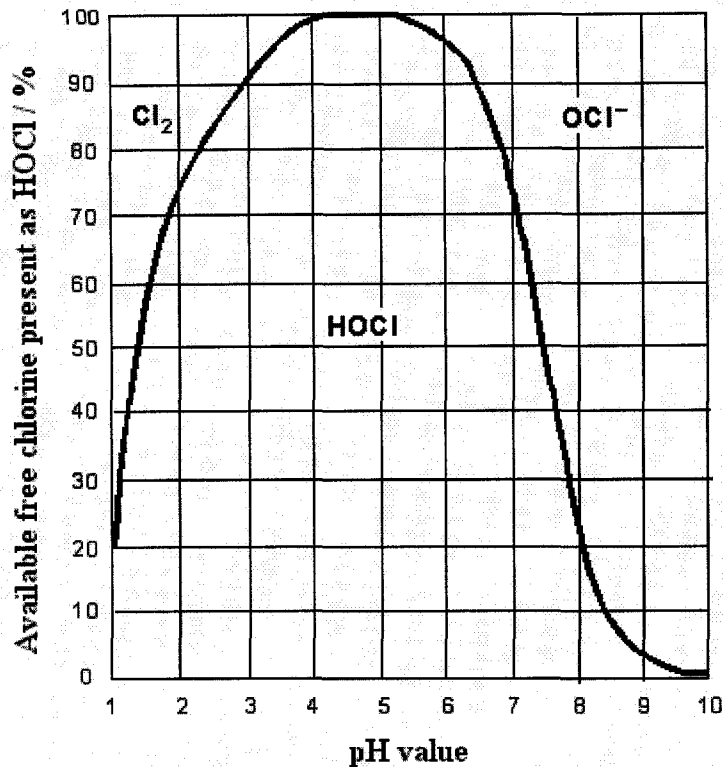
Figure 2.1 The effect of the pH on the components of free chlorine (Edstrom 2006)

From Figure 2.1, free chlorine consists of Cl_2 and HOCl at lower pH (< 4), but is composed of HOCl and OCl⁻ at higher pH (> 5). HOCl is the predominant component of free chlorine at pH 4 to 5. Since the pH of drinking water varies in the range of 7 to 8.5, the primary components of free chlorine of concern in drinking water are HOCl and OCl⁻.

2.2.2 Photodecomposition of aqueous free chlorine

There are abundant studies associated with the photodissociation of gaseous HOCl for the possible role that HOCl may play in the ozone depletion in the stratosphere (Molina and Molina 1978; Molina et al. 1980; Butler and Phillips 1983; Guo 1993; and Tanaka et al. 1998). Most of these studies were performed from the viewpoint of physical chemistry to investigate the mechanism, degradation products, and reaction rate of the

14

photolysis of gaseous HOCl with UV light. However, in drinking water treatment HOCl and OCl⁻ are present in an aqueous phase. Hence, the photodissociation of HOCl and OCl⁻ could be very different from that in the gas phase because of the different environment. Although it has been observed that chlorine concentrations decrease significantly under the sunlight or UV irradiation in many practical operations, there are few studies performed to investigate systematically the photodecomposition of aqueous chlorine.

Buxton and Subhani (1972) conducted a detailed study on the photolysis of aqueous solutions of hypochlorite ions. Based on their experimental results, the aqueous hypochlorite ion (OCl^-) was supposed to be degraded with 254 nm UV light in the following processes:

[2.3] $ClO^- + h\nu$ (UV photons) $\rightarrow$ $\cdot Cl + O^-$ or $Cl^- + O(^1D)$

[2.4] $\cdot Cl + ClO^- \rightarrow Cl^- + \cdot OCl$

[2.5] $\cdot OH + ClO^- \rightarrow OH^- + \cdot OCl$

[2.6] $2 \cdot OCl \leftrightarrow Cl_2O_2$

[2.7] $2 Cl_2O_2 + 2 H_2O \rightarrow 2 Cl^- + ClO^- + ClO_3^- + 4 H^+ + O_2$

[2.8] $O^- + H_2O \leftrightarrow \cdot OH + OH^-$

[2.9] $O^- + ClO^- \rightarrow \cdot OCl + O^{2-}$ $(H^+ + O^- + ClO^- \rightarrow \cdot OCl + OH^-)$

[2.10] $O(^1D) + H_2O \rightarrow H_2O_2$

[2.11] $H_2O_2 + ClO^- \rightarrow H_2O + Cl^- + O_2$
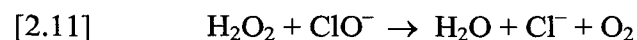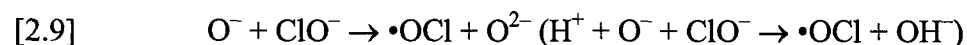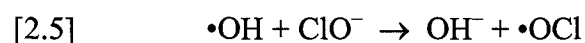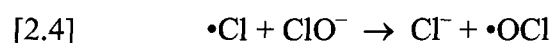
Buxton and Subhani (1972) performed their research in purified water without the influence of organic materials. In addition, the concentration of OCl^- ($\sim 10^{-3}$ M) was not very high in their research. From the above described mechanism, the end-products of the

15

photodecomposition of OCl$^-$ should be chloride (Cl$^-$), chlorate (ClO$_3^-$), and oxygen (O$_2$). However, with a high chloride (Cl$^-$) concentration, chloride ions present in water can rapidly react with hydroxyl radicals ($\cdot$OH) as described in the following equations (Oppenländer 2003):

[2.12] $\cdot$OH + Cl$^-$ → $\cdot$ClOH$^-$

[2.13] $\cdot$ClOH$^-$ + H$^+$ → $\cdot$Cl + H$_2$O

In practical operations, there always are some naturally organic compounds dissolved in the raw water. With the presence of organic compounds, the photoreactions of free chlorine under the UV irradiation may be very complex. Oliver and Carey (1977) studied the photochlorination of ethanol, n-butanol, and benzoic acid at pH 4, and they found that chlorine was distinctly consumed by these organic materials under UV irradiation. According to their observations, the following two chain-reactions were proposed for the photodecomposition of HOCl:

[2.14]   HOCl + hv (UV photons) → $\cdot$OH + $\cdot$Cl

$\cdot$OH radical chain:

[2.15] $\cdot$OH + RH → $\cdot$R + H$_2$O

[2.16] $\cdot$R + HOCl → RCl + $\cdot$OH

$\cdot$Cl radical chain:

[2.17] $\cdot$Cl + RH → $\cdot$R + HCl

[2.18] $\cdot$R + HOCl → ROH + $\cdot$Cl
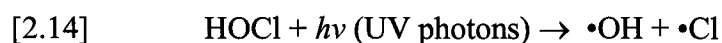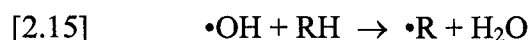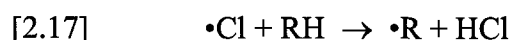
The above reactions indicate when there is some organic matter in the water, more chlorine could be consumed in the photochemical reactions. Some research has confirmed this assumption. Giles and Danell (1983) found that almost 99% of the total

16

chlorine in municipal water was eliminated in a study concerning dechlorination in water by UV irradiation. Kobayashi and Okuda (1972) found that some compounds (such as formic acid, fumaric acid, and glucose), which do not thermally consume chlorine at all, can react with chlorine under UV light to generate some chlorinated products. In addition, in an experiment in which UV disinfection was employed in water chlorinated upstream of the UV disinfection unit, Zheng et al. (1999a) found that the higher the UV dose (fluence) applied the greater the chlorine dose required to keep a fixed chlorine concentration in the effluent water; at the highest UV dose (fluence) of 4825 mJ/cm^2 employed, the chlorine demand was about 5 times that obtained without UV irradiation. However, some individuals reported contrary observations. Cassan et al. (2006) found that the free and active chlorine levels were significantly increased when a medium-pressure UV lamp was used to irradiate chlorinated swimming pool water. In that case, the researchers thought that the increase of free chlorine was caused by the photolysis of combined chlorine. In addition, Örmeci et al. (2005) reported that the decay of chlorine at typical UV disinfection fluences (less than 100 mJ cm^{-2}) was negligible.

2.2.3 Quantum yield of free chlorine and the influencing factors

The quantum yield of free chlorine can be defined as the number of moles of free chlorine decomposed per einstein[2] of UV photons absorbed by the free chlorine sample. Generally speaking, the quantum yield should be less than one (1.00), but if some chain-reactions, such as those described above, are involved in the photodecomposition of free chlorine, the quantum yield could be greater than one (1). Accordingly, the quantum yield of free chlorine could be different in different water matrices. This has been verified in

---

[2] One einstein is one mole (6.023 x 10^{23}) photons.

17

many operations and studies. For example, after examining the effects of fifty-one (51) kinds of organic compounds on the photodecomposition of chlorine, Kobayashi and Okuda (1972) found that aqueous chlorine exposed to UV irradiation was greatly consumed in the presence of some compounds (such as acetone, ethanol, and *n*-butyl acetate), but some compounds (such as acetic acid and succinic acid) did not affect the photodecomposition of chlorine at all. In addition, other factors, such as temperature, the wavelength of UV light and the concentration of free chlorine, could also have significant effects on the quantum yield of free chlorine.

When the chlorine sample was prepared using purified water and the concentration was about 10^{-3} M, Buxton and Subhani (1972) determined the quantum yields of hypochlorite ions (OCl^-) at ambient temperature. The quantum yields they measured were 0.60 ± 0.02, 0.39 ± 0.01, and 0.85 ± 0.02 at wavelengths of 365, 313, and 254 nm, respectively. Their results show that the wavelength of UV light has a significant effect on the quantum yield of OCl^- photolysis. In another study, Nowell and Hoigné (1992a) observed that the quantum yields of HOCl and OCl^- were affected by pH due to the dependence of the ratio of $HOCl/OCl^-$ on pH. They reported that the pseudo-first-order rate constant for the photolysis of HOCl was 2×10^{-4} s^{-1} and that of OCl^- 1.2×10^{-3} s^{-1} when the chlorine samples prepared in filtered lake waters were exposed to sunlight in which the most effective wavelength was approximately 330 nm. The most interesting observation they reported was that the pseudo-first-order rate constants of HOCl and OCl^- were very close when the samples were irradiated by 254 nm UV light in the absence of radical scavengers. The researchers thought that the reason for the dependence of the pseudo-first-order rate constants on wavelength was because of the molar

18

absorption coefficients of HOCl and OCl⁻. But another potential reason they did not consider is a possible difference in quantum yields of HOCl and OCl⁻ at different wavelengths. In their further research, Nowell and Hoigné (1992b) found that the production ratio[3] of •OH generated by OCl⁻ is only about 0.1 and HOCl (pH 5) yielded 0.7 •OH in sunlight and 0.9 •OH with 255 nm UV light. This also confirms that pH is a significant influencing factor on the quantum yield of free chlorine.

Theoretically, the variation of temperature in practical operations of drinking water disinfection should not influence photochemical reactions significantly. However, the situation becomes quite complicated, when some organic compounds are involved in the process of photodecomposition of free chlorine. Giles and Danell (1983) reported that the photodechlorination efficiency by UV light did not have a significant change, when the experimental temperature varied from 7.5 to 20.6°C. However, the study of Kobayashi and Okuda (1972) indicates that the amount of aqueous chlorine consumed by organic compounds under UV irradiation could be different for different temperature conditions. These seemingly inconsistent experimental results could be caused by the temperature-dependence of chain-reactions originated by the radicals produced in the photolysis of chlorine. For example, some compounds could react with the radicals generated by the photolysis of chlorine, and then the intermediate products can still consume chlorine in the following reactions; but some compounds could only react with the radicals and produce some stable products and not react with chlorine any more. Obviously, for the first case, the decomposition of chlorine will be affected by temperature, but for the latter one, the temperature will play only a minor role for

---

[3] The number of reactive free radicals generated per molecule of aqueous chlorine photolytically degraded

19

chlorine photodecomposition. In addition to the temperature, the research results obtained by Zheng et al. (1999a) show that the initial chlorine concentration before exposure to UV light is also a significant factor in the decomposition of chlorine. For example, at a UV dose of 2000 mJ cm^{-2} (medium-pressure UV lamp), they observed that the chlorine demands are about 16 and 25 mg L^{-1} for the samples with initial chlorine concentrations of 27 and 46 mg L^{-1}, respectively.

2.3 Sequential disinfection process of chlorination and UV irradiation and DBPs generated in this process

2.3.1 Application of chlorination and UV irradiation for water disinfection

From the safety and economics point of view, the combination of chlorine and UV disinfection is usually used as multiple barriers for the MOR treatment of drinking water utilities. For example, free chlorine is usually added to drinking water before the UV reactor to remove the UV-resistant microbes and tastes/odors or after the UV reactors to keep the chlorine residual in the distribution systems of many water utilities. In some research, the process of UV treatment followed by chlorination was observed to have a synergistic effect for some refractory pathogens. Ballester and Malley (2004) found a 4-log reduction of adenovirus type 2 by UV irradiation at a typical fluence of 40 mJ cm^{-2} followed by sequential addition of chorine (total chlorine 3 mg L^{-1}). They found that this multiple disinfection scheme can protect public health effectively and meet the stringent USEPA requirements. The synergistic inactivation effect also has been identified by the work of Cheung (2004) for the inactivation of MS2 colliphage cell suspensions. However, when these multiple disinfection barriers were used for the reduction of *Cryptosporidium*

20

parvum oocysts and *Bacillus subtilis* spores, no significant synergistic inactivation effects were observed (Kashinkuti et al. 2004). In order to remove the UV-resistant pathogens and control unpleasant tastes and odors, chlorine is also usually added to the raw water before the UV disinfection unit. The E. L. Smith Water Treatment Plant (Edmonton, AB, Canada) is a good example in this respect, where chlorine is added before filtration followed by UV treatment (EPCOR 2006). According to Mah (2005), a water treatment plant with a capability of 150 million L per day in Lethbridge (AB, Canada) was upgraded to employ free chlorine, UV treatment and chloramines sequentially for drinking water disinfection in 2003. In the practical operation, this composite process proved to be very economical to reach the required disinfection target. In a wastewater treatment project, Plummer et al. (2005) also demonstrated that the process of chlorination prior to UV treatment was more cost-effective than UV treatment alone.

2.3.2 Effect of UV irradiation and chlorine on DBPs formation

There are many studies that report on disinfection by-products (DBPs) caused by chlorine or UV irradiation in drinking water treatment. Some organohalogens (trihalomethanes, haloacetic acids, haloacetonitriles, N-chloramines, etc.), inorganic (chlorate) and non-halogenic (aldehydes, alkanoic acids, carboxylic acids etc.) by-products can be generated by the use of chlorine. Of these DBPs, the trihalomethanes (THMs) and haloacetic acids (HAAs) are two kinds of well known DBPs that are stringently limited for the safety of public water supplies (Lister 1956; Adam et al. 1992).

Compared to chlorine, the DBPs caused by UV treatment are almost negligible. No significant DBPs caused by UV treatment were observed at low fluences (less than 200 mJ/cm^2); whereas, at high fluences (more than 500 mJ/cm^2) some aldehydes and

21

carboxylic acids are produced (Liu et al. 2002 and Lehtola et al. 2003). In a study of UV treatment for wastewater disinfection, Linden et al. (1998) did not detect any significant DBPs at UV fluences over 2800 mJ cm^{-2}, even though the wastewater samples were rich in organics that could be precursors to DBPs. Table 2.1 gives a summary of their work, which was conducted over a large range of fluences and wastewater water qualities (primary, secondary and tertiary treated effluents). Malley (1995) investigated the UV disinfection of groundwater and surface water treated by coagulation and filtration at the fluences as high as 200 mJ cm^{-2}, but he also failed to find any other significant DBPs except small amount of formaldehyde. In addition, many studies have shown that UV disinfection does not result in mutagenic or toxic by-products (Haider et al. 2002, Kool et al. 1985, Cairns et al. 1993, and Buchanan et al. 2006). UV treatment at wavelengths below 240 nm can convert nitrate to nitrite (Groocock 1984 and Vanderveer et al. 2005), which can react with nitrosatable compounds in the human stomach to form potential carcinogenic N-nitroso compounds (WHO 2003). However, Sharpless et al. (2001 and 2003) found that the formation of nitrite was affected by UV wavelengths, fluences, DOC concentrations and pH, and in the normal operations of drinking water disinfection, it should not be a serious problem to threaten the drinking water safety.

Many investigations have been performed on the effect of the sequential disinfection processes of UV treatment and chlorination on the formation of DBPs. Table 2.2 summarizes a part of results obtained by different researchers under various experimental conditions. On the whole, the formation of DBPs can be affected by the sequence of the UV and chlorination treatments and some other factors including pH, contact time, temperature, concentration and properties of organic compounds,

22

concentration of chlorine and residual chlorine, etc. For the process of UV treatment followed by free chlorine or chloramines, most studies concluded that there was no significant effect on the formation of DBPs, such as THMs, HAA, carboxylic acids, aldehydes, and TOX, at the typical fluences employed in water disinfection. Nevertheless, some had the inconsistent opinions. For example, Cheung (2004) found that the sequential disinfection process, regardless of the sequences of UV treatment and chlorination, significantly increased the production of DBPs when humic acid was used as the organic source.

Table 2.2 Summary of DBPs studies for the wastewater treatment by UV light (Linden et al. 1998)

Site	Lamp	Fluence mJ cm^{-2}	Analysis	Results
Oak Ridge	LP	13 to 61	Organic screen (LC), VOC (HEC/GC)	No major change
Elsinore	LP	~ 2800	Organic screen (HPLC, GC/MS), VOC (EPA5030/8260), semi- and non-VOC (LC/MS)	No major change. Unidentified peak at 2800 dose
Goldbar	MP	70	VOC (GC/MS), semi-VOC (extraction GC/MS)	No major change. Increase in acetone.
Santa Rosa	MP	100, 200	VOC (EPA 8260), semi-VOC (EPA8270), carboxylic acid (EPA300M), chlorinated DBP(EPA551), HAA (EPA552), inorganic anions (EPA300B), aldehydes(GC/ECD)	Aldehydes increased with UV dose. No other major change.
Fairfield	LP, MP	150 to 898	Organic screen (HPLC, GC/MS)	No major change.
Santa Rosa	LP	150, 300	Organic screen (HPLC, GC/MS)	No major change.
Vallejo	LP, MP	150 to 1138	Organic screen (HPLC, GC/MS)	No major change.
Sacramento	LP, MP	144 to 903	Organic screen (HPLC, GC/MS)	No major change.
Greenville	MP	60 to 80	Organic screen (HPLC, GC/MS)	No major change.

24

Table 2.3 Summary of the effects of sequential disinfection process on the formation of DBPs

Treatment sequence	Water matrix	UV irradiation	Chlorination	Effects on the formation of DBPs	Reference
UV + chlorine	Richard Miller Treatment Plant (Ohio, US), filtered	LP or MP 40/140 mJ cm^{-2}	Free chlorine 2 mg L^{-1}	No changes on THMs, HAA9, carboxylic acids, aldehydes, and TOX.	Kashinkunti et al. 2004
UV + chlorine	East Moorabool reservoir system (Victoria, Aust.), 0.45 μm membrane filtered	LP or VUV, fluences up to 240 mJ cm^{-2}	Free chlorine 4 mg L^{-1}	VUV can reduce both THMs and HAAs, but LP only can reduce THMs.	Buchanan et al. 2006
Chlorine + UV	N/A	LP or MP	Free chlorine 1 mg L^{-1}	No significant changes.	Mackey et al. 2000
UV + chlorine	N/A	LP 130 mJ cm^{-2}	Free chlorine	DBPs formation rate and quantities increased without the adjustment of chlorine residuals; otherwise, no significant changes were observed.	Malley et al. 1995
UV + chlorine; chlorine + UV	Synthetic water with humic acid	LP	Free chlorine or monochloramine	A notable increase for chloroform, dichloroacetic acid, trichloroacetic acid and cyanogen chloride; and the more significant increase in the pre-chlorination process.	Cheung 2004

25

Table 2.2 Continued ...

UV + chlorine	Synthetic water with humic acid, Suwannee River humic acid and natural organic matter; Yau Kom Tau water treatment works (HK)	LP or MP 60 mJ cm^{-2}	Free chlorine or monochloramine 7 mg L^{-1}	Chloroform, dichloroacetic acid, trichloroacetic acid and cyanogen chloride significantly increased; the formation of DBPs could depend on the chlorine application sequences and the NOM properties.	Liu et al. 2006
Chlorine + UV	Mannheim Water Treatment Plant (Ont., Canada), filtered	MP ~2000 mJ cm^{-2}	Free chlorine 6 to 48 mg L^{-1}	UV irradiation had a relatively minor effect on the THMs and HAAs at fluences lower than 100 mJ cm^{-2}, but the effect became significant at high fluences	Zheng et al. 1999a
UV + chlorine	Mannheim Water Treatment Plant (Ont., Canada), filtered; synthetic water with humic acid and alginic acid	MP ~3000 mJ cm^{-2}	Free chlorine 5 to 10.5 mg L^{-1}	Chlorine demand depended on the species and concentration of organic materials; the formation of THMs and HAAs was independent of the sequential disinfection process.	Zheng et al. 1999b
UV + chlorine	Synthetic water with humic acid and alginic acid	LP, MP and pulsed UV 40 to more than 1000 mJ cm^{-2}	Free chlorine	For fluences of less than 1000 mJ cm^{-2}, UV irradiation did not affect the THMs and HAAs formation in the subsequent chlorination processes	Liu et al. 2002

26

2.4 Biodosimetry for the validation of UV reactors

UV technologies are becoming better recognized as effective and economic tools in the multiple barrier arsenal for the protection of public health against pathogens and chemical contaminants in the public water supply. An important component for the design and operation of UV reactors is validation testing, which is usually performed to check if a UV reactor can provide enough fluence to achieve the designed disinfection levels under different operating conditions. Biodosimetry, the use of microbiological response as an indicator for the measurement of irradiation, is a widely used method for UV reactor validation. This is a most reliable method available at present for the full-scale validation of UV reactors and usually is provided as an important approach by most regulatory guidance, such as those in the USEPA Long Term 2 Enhanced Surface Water Treatment Rule (LT2ESWTR), the German DVGW W294 Regulations, and the Austrian ÖNORM M 5873-1 regulations (USEPA 2006, DVGW 1997 and ÖNORM 2003).

2.4.1 Fluences delivered in UV reactors and the validation testing

The fluence in UV reactors can be defined as the product of fluence rate (UV irradiance[4], mW cm^{-2}) and the irradiation time (s) (reactor volume/flow rate). In ideal conditions, this model assumes ideal radial mixing and the fluences incident on microorganisms or contaminants are considered to be uniformly distributed in UV reactors. For example, the collimated beam UV apparatus, with thoroughly mixed samples, is very close to the behavior of an ideal UV reactor. However, actually this is almost always not the case in practical operations. In a real UV reactor, each

---

[4] This is also termed 'UV intensity' (e.g., by the USEPA); however, this is not a well-defined term.

microorganism or particle can pass through the reactor in a unique trajectory because of the hydraulic profiles and irradiance gradients within the UV reactor, and thus the fluence imparted to a given microorganism will not be same as for others. This is to say, there always is a distribution of fluences in a real UV reactor. This is shown visually in Figure 2.3 (Lawryshyn and Cairns 2003), which is a UV dose (fluence) histogram of a real UV reactor obtained by Computational Fluid Dynamics (CFD) modeling. The range of the fluence distribution shows the level of *mixing efficiency*, which is defined as the ratio of the average fluence received by microorganisms to the theoretical fluence, within a UV reactor. The narrower the distribution, the better the mixing efficiency will be. However, in practice, it is hard to determine experimentally what fluence is incident on an individual microorganism because of the non-ideal behavior of real UV reactors and the complexity of their designs. Therefore, the fluence delivered by a UV reactor is usually expressed as an average *reduction equivalent fluence* (REF) as measured by biodosimetry.

The validation process determines the log inactivation achieved for a specific pathogen and relates it to the operating conditions at the time of the testing (e.g., UV transmittance at 254 nm, output of UV lamps, and flow rate). This is very important in the design and application of UV reactors for drinking water disinfection. Engineers use the validation data to determine if a UV reactor is properly designed to deliver the required fluence under the design conditions, and drinking water utilities also use the validation results to relate the flow rate, sensor UV irradiance, and UV transmittance measured in the UV reactor operation to the UV dose delivery, in order to obtain the desired disinfection credit. So far, regulatory frameworks have been built around the

28

validation process, and a number of protocols have been developed to establish the minimum testing requirements.
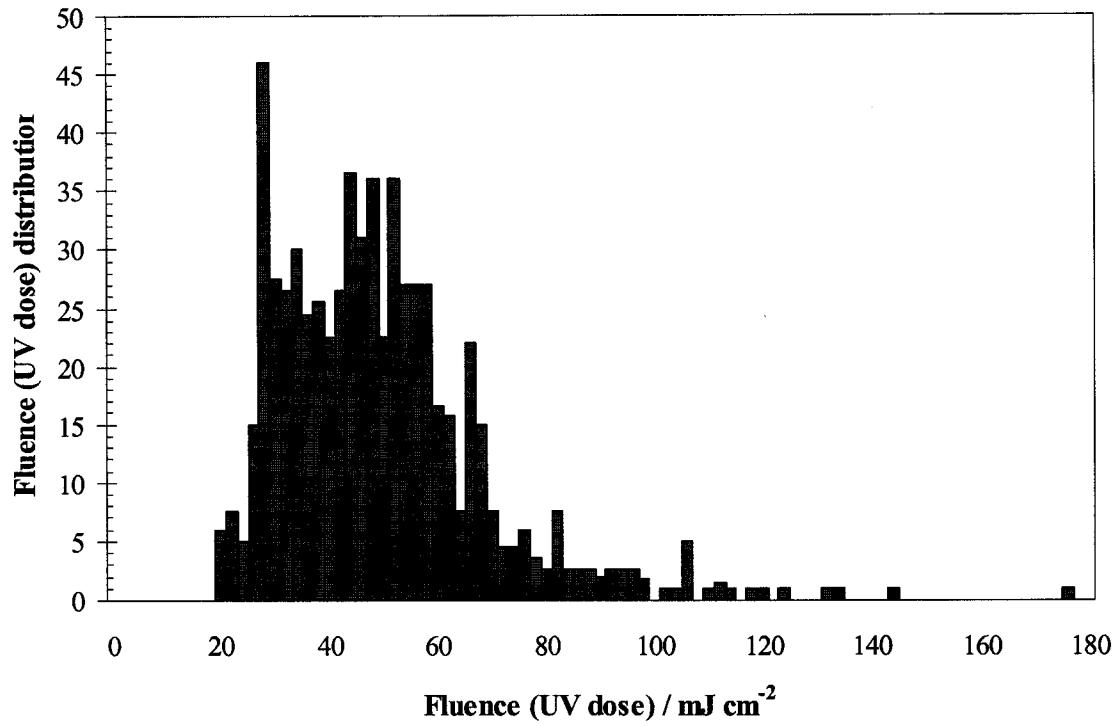
Figure 2.2 CFD generated histogram of the UV dose delivered to microbes in a UV reactor (after Lawryshyn and Cairns 2003).

In order to obtain the designed inactivation level for water treatment utilities, the Long Term 2 Enhanced Surface Water Treatment Rule (LT2ESWTR) requires that the UV reactor performance must be validated to ensure that it delivers the required fluence (USEPA 2006). Table 2.3, developed by USEPA (2006), shows the fluence requirements for *Cryptosporidium spp.*, *Giardia spp.*, and virus during the validation testing of UV reactors. For reactor validation, the LT2ESWTR specifies that validation testing must determine the range of operating conditions that can be monitored by the UV reactor, where the reactor delivers the required fluence, and the reactor that is validated must

29

conform uniformly to the reactors used by the utility. In addition, the test microorganism used in validation testing must have UV dose-response characteristics that have been quantified with a low-pressure mercury vapor lamp. During the validation testing, the range of permitted operating parameters will be determined. The minimum conditions that are required to be validated are flow, UV irradiance (as measured by a sensor), and lamp status (e.g., 80% power). Although there are some differences from the USEPA regulations in detail, the regulations promulgated by European countries, such as ÖNORM M 5873-1 (Austria) and DVGW-W294 (Germany), also specify similar requirements for UV disinfection systems regarding the minimal delivered fluence (UV dose) and UV reactor validation testing (Sommer et al. 2004 and DVGW 1997).

Table 2.3 Fluence (mJ cm^{-2}) requirements for *Cryptosporidium spp.*, *Giardia lamblia*, and virus inactivation credit used in validation tests[5] (USEPA 2006)

Microorganism	Log reduction							
	0.5	1.0	1.5	2.0	2.5	3.0	3.5	4.0
Cryptosporidium spp.	1.6	2.5	3.9	5.8	8.5	12	15	22
Giardia lamblia	1.5	2.1	3.0	5.2	7.7	11	15	22
Viruses	39	58	79	100	121	143	163	186

2.4.2 Biodosimetry for the validation of UV reactors

Biodosimetry is an already well established and widely used method for the validation of UV reactors (Qualls and Johnson 1983, Sommer and Cabaj 1993 and Sommer et al. 1998). Usually, MS2 phage, *Bacillus subtilis* spores or *E. coli*, is used as the challenge microorganism which is spiked into the influent of the validated UV reactor.

---

[5] In the above table, it should be noted that there are safety factors that will be applied to these fluence (UV dose) requirements to determine what fluence must be achieved during validation testing.

30

Then, the reduction equivalent fluence (REF) delivered in the UV reactor can be determined by the inactivation rate of the challenge microorganism. Generally speaking, this process consists of three key steps, and Figure 2.4 briefly shows each step involved in the validation process (USEPA 2003).

1. A challenge microorganism is selected as the surrogate in validation testing and its sensitivity to UV treatment is determined in the form of a fluence–response curve. Usually, a well mixed bench-scale reactor, such as that in a collimated beam UV apparatus, is used for this purpose. In this step, volumes of samples (an aqueous suspension of the challenge microorganism) are exposed to UV light at different fluences; the log reductions of the viable microorganisms at these fluences are measured; and then the log reduction versus fluence is plotted as the fluence-response curve (Bolton and Linden 2003).

2. The challenge microorganism is injected into the influent of the validated UV reactor and the logarithmic inactivation of the microorganism is determined for each operating condition (flow rate, UV transmittance, lamp age, etc.). Meanwhile, the test water carrying the challenge microorganism flows through the validated UV reactor under several sets of controlled conditions, which cover the range of possible practical operating conditions. Subsequently, some samples are collected from the influent and effluent of the UV reactor and the log reductions of the challenge microbe are determined by measuring the concentration of the viable challenge microbe in these samples.

3. The reduction equivalent fluence (REF) is determined by comparing the inactivation of the challenge microorganism passing through the UV reactor with

31

the laboratory fluence-response curve to determine which fluence delivered by the collimated beam reactor gives the same microbe inactivation. For a different validation conditions a different REF may be obtained and so several values of the REF will be obtained under various validation conditions.

32
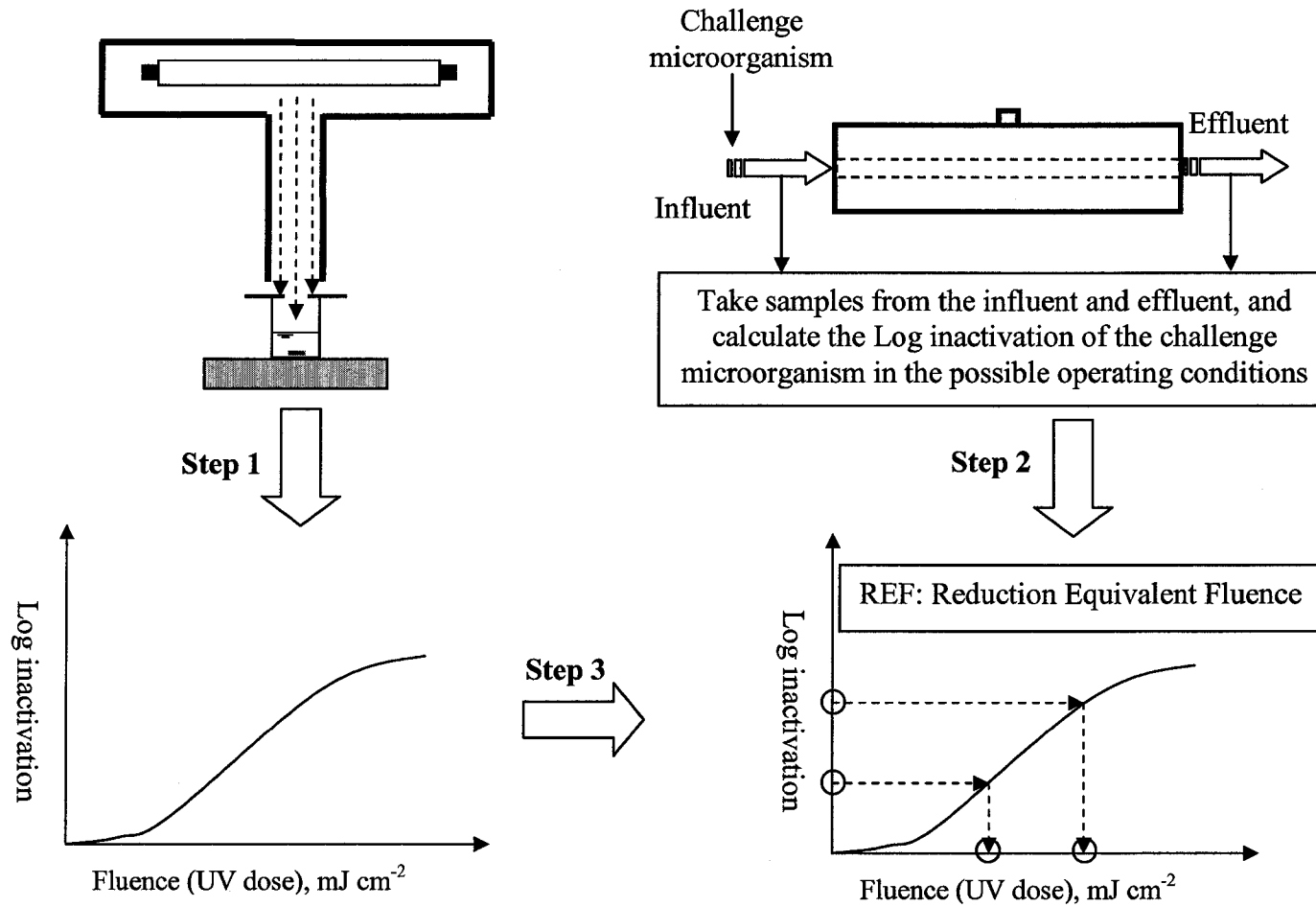
Figure 2.1 Steps of the biodosimetry for UV reactor validation

Combined with a safety factor, which is used to account for the uncertainty occurring in translating a REF measured during a validation test to a given level of pathogen inactivation in real operating conditions, these REF values can be used for monitoring the performance of UV reactors in daily operations. The USEPA (2003) provides two approaches (Tier 1 and Tier 2) for addressing uncertainty with a safety factor to determine the log inactivation credit. Tier 1 is a very simple method, since the required fluences (shown in Table 2.4) are predetermined by applying the preset safety factors. For the approach of Tier 2, it becomes relatively complex, and the safety factors need to be calculated based on the uncertainties associated with the whole validation process.

Table 2.4 Tier 1 REF targets for LP, LPOH and MP UV lamps, mJ cm^{-2} (USEPA 2003)

Log Inactivation Credit	REF Target for LP or LPHO lamps			REF Target for MP lamps		
	Cryptosporidium spp.	*Giardia spp.*	Viruses	*Cryptosporidium spp.*	*Giardia spp.*	Viruses
0.5	6.8	6.6	55	7.7	7.5	63
1.0	11	9.7	81	12	11	94
1.5	15	13	110	17	15	128
2.0	21	20	139	24	23	161
2.5	28	26	169	32	30	195
3.0	36	34	199	42	40	231
3.5	—	—	227	—	—	263
4.0	—	—	259	—	—	300

34

2.4.3 Comments on the biodosimetry

On the whole, biodosimetry has proved its effectiveness and reliability in a considerable number of applications and has been widely accepted as a regulated validation approach in many countries. It can be conducted either off-site at a dedicated test facility or on-site at the utility interested in implementing UV disinfection. Table 2.5 presents a summary of potential advantages and disadvantages associated with these two kinds of validation testing (Scheible et al. 2003).

Table 2.5 The Comparison of On-site and Off-site Validation Testing (Scheible et al. 2003)

Testing option	Advantages	Disadvantages
Off-site testing at a dedicated facility	Greater flexibility and most efficiency; provides performance data to support the design of a facility; ability to test over a wide range of operating conditions including inlet/outlet piping configurations	May require re-validation (on- or off-site) if site-specific conditions had not been previously tested
On-site validation at the subject application	Match exact piping hydraulic conditions; the UVT will more accurately represent the UV installation; providing testing support equipment on-site allows for future testing, if needed	UV installation has to be completed before benefit of validation; dosing, mixing and sampling requires modification of piping up- and down-stream of reactor; limited to water quality available; costs tend to be higher; logistics may be very difficult

As discussed above, biodosimetry must employ a challenge microorganism as the indicator of UV irradiation to determine the UV delivery (REF) in a UV reactor. Since

35

the irradiance field within a UV reactor is usually not homogenous, the microbes, as they flow through the reactor, follow different paths and are exposed to different fluences. The REF obtained by biodosimetry just gives an indication of the average UV fluence in the reactor. But it should be emphasized that the REF is not the arithmetic mean of the fluence distribution, but the mean of fluence distribution weighted with the survival curve of the challenge microorganism. The wider the fluence distribution and the higher the UV sensitivity of the challenge microbe, the lower the measured REF will be; but if there is a shoulder on the survival curve and the fluence distribution includes the shoulder, the measured REF could be higher (Cabaj et al. 1996). This indicates that without the fluence distribution of a UV reactor, the REF measured by one challenge microorganism cannot be used to make definitive predictions of the fluences delivered to another microbe unless both have the same sensitivity to UV irradiation (Wright and Lawryshyn 2000). As a result, the USEPA (2003) suggests calculating an REF bias factor, which can be used to convert the REF of the challenge microorganism to the REF of the target microorganism, to account for these issues. This bias factor usually is selected from a "worst case" of the fluence distribution, and thereby, the power of UV reactor designed based on the REF corrected by the bias factor could be much higher than the regulated or required value.

In addition, the application of biodosimetry could be restricted because of the size of the validated UV reactors. Although the biodosimetry approach has proved to be very effective for the reactors rated at flows less than 90 ML d^{-1}, very little evidence has been presented to show that it works as well as this at the much larger flow rate (Mamane-Gravetz and Linden, 2004). Even though possible, it is not practical to grow a large amount of challenge microorganisms in the laboratory over extended periods to validate a

36

large UV reactor. Furthermore, culture conditions for surrogates can affect their sensitivity to UV irradiation and as a result, the reliability of the validation results (REF) could be influenced (Severin et al. 1983; Nicholson and Galeano 2003). Finally, biodosimetry is a relatively expensive and time-consuming method, and it cannot be used as an on-line approach to monitor the performance of UV reactors. Therefore, there is always an opportunity to look for better methodologies for the validation of UV reactors to improve/replace the currently used biodosimetry method.

2.5 Other validation methods

Because the conventional biodosimetry uses laboratory cultured microorganisms, such as *Bacillus subtilis* spores or MS2 colliphage, spiked into test water to validate UV reactors, it is limited by the microbe titer which is possible to grow, thus limiting the size of the reactor that can be validated. Therefore, some (Blatchley and Hunt 1994, Nieminski et al. 2000 and Mamane-Gravetz and Linden 2004) have suggested using indigenous aerobic spores naturally occurring in raw/unfiltered water sources as an alternative indicator for the validation testing of UV reactors, especially for unfiltered water supplies planning large UV reactors. According to their investigations, it was determined that the indigenous aerobic spores in raw/unfiltered water, could be used for validation testing, and might also be used as a regular tool to monitor and report the daily performance of UV reactors. An advantage of this suggested method is that there is no need to carry out considerable work for the preparation of challenge microorganisms. Therefore, this could be more time-saving and economical than conventional biodosimetry.

37

However, there still are some limitations or disadvantages for the indigenous method. First of all, the variation of inactivation kinetics of the indigenous microorganism strains would introduce some uncertainty in the validation results. This could lead this method to be not very practical for the validation testing of UV reactors. Also, as shown in Figure 2.5, the indigenous aerobic spores are usually found to be more resistant to UV treatment than the laboratory cultured surrogates, such as *Bacillus subtilis* spores or MS2 colliphage. Accordingly, an even unrecognized fluctuation of the log-inactivation could lead to a large variation of the REF determined by indigenous microbes. The UV-resistant indigenous microbes also have a common drawback similar to other UV-resistant biodosimeters, in that they are incapable of substantiating the higher level inactivation of UV-sensitive microbes exposed to the same fluence (Wright and Lawryshyn 2000 and Mackey et al. 2002). In addition, the application of the indigenous microbes for the validation of UV reactors could be restricted by water qualities. Sometimes, this method does not work very well, since there are not enough indigenous microbes in the raw water to provide measurable inactivation credits for the validation testing. In order to reduce the impact of vegetative bacteria in raw water, the samples collected in the process of validation testing need to be carefully pre-treated before enumerating the colonies of indigenous spores. For example, Mamane-Gravetz and Linden (2004) suggest incubating the samples at 35 to 37°C for 30 min and then pasteurizing at 65°C for 15 min before the enumeration of colonies. Obviously, this pretreatment process could introduce some unknown and/or uncontrollable factors to affect the experimental reliability. Another disadvantage is that the validation results

38

obtained in one utility could have little or no meaning for other utilities, since the species

and characteristics of spores could be totally different in different water sources.
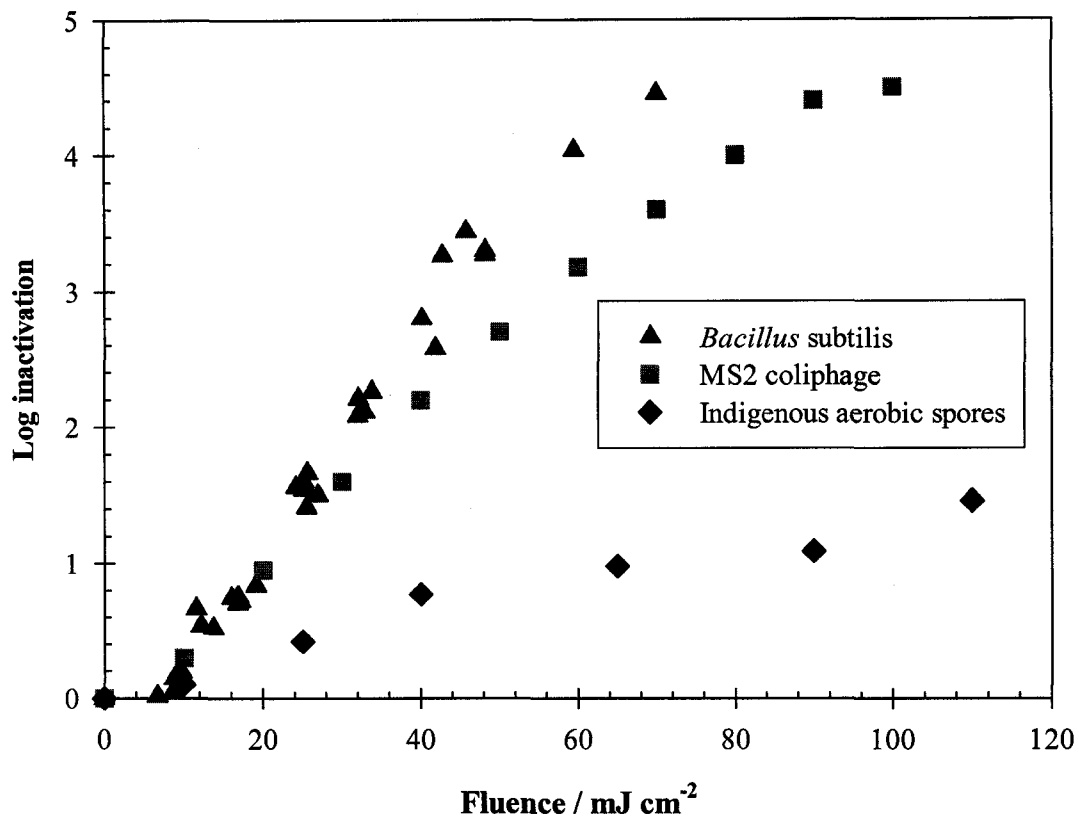
Figure 2.4 Log inactivation of indigenous aerobic spores, *Bacillus* subtilis spores, and MS2 colliphage as a function of UV fluence. ▲ *Bacillus* Subtilis spores (this research), ■ MS2 colliphage (USEPA, 2003) and ◆ Indigenous aerobic spores (Mamane-Gravetz and Linden, 2004).

Because it usually takes a long time to complete a validation test by biodosimetry,

some (Severin et al. 1983, Blatchley et al. 1998, Bolton 2000, Lawryshyn and Cairns

2003, Fenner and Komvuschara 2005, etc.) have developed various mathematic models

validated by biodosimeters (*Bacillus subtilis* spores, MS2 colliphage, or other surrogates)

to evaluate the performance of UV reactors under various operating conditions. These

models usually account for the elements of fluid behavior, water quality, and microbe

39

inactivation kinetics. They can be used to accelerate greatly the process of UV reactor planning and design and to monitor the performance of UV reactor easily in real time. As an example, Figure 2.6 (Lawryshyn and Cairns 2003) shows the correlation of UV doses determined by biodosimetry and UV doses calculated by a validated CFD model under varying flow rates, UV transmittance, and lamp settings. In this example, the UV doses determined by conventional biodosimetry and those calculated by a validated CFD model have a relatively good linear relationship. This shows that validated mathematical models can be a useful tool for the conceptual and quantitative determination of UV reactors. The significant advantage of mathematical models is that they are very convenient, time-saving and economical to be used for evaluating UV reactor design alternatives, predicting the results of reactor improvements, and developing a fundamental understanding of flow and fluence. However, mathematical models cannot reflect the physical manifestation of fluence in UV reactors, and also are difficult to integrate effects of particles in influent. Another disadvantage is that these models need to be validated by biodosimeters under all possible operating conditions before being applied; otherwise no one knows the reliability of the results generated by those models. Also, the mathematical models cannot be used alone as a monitoring tool.

40
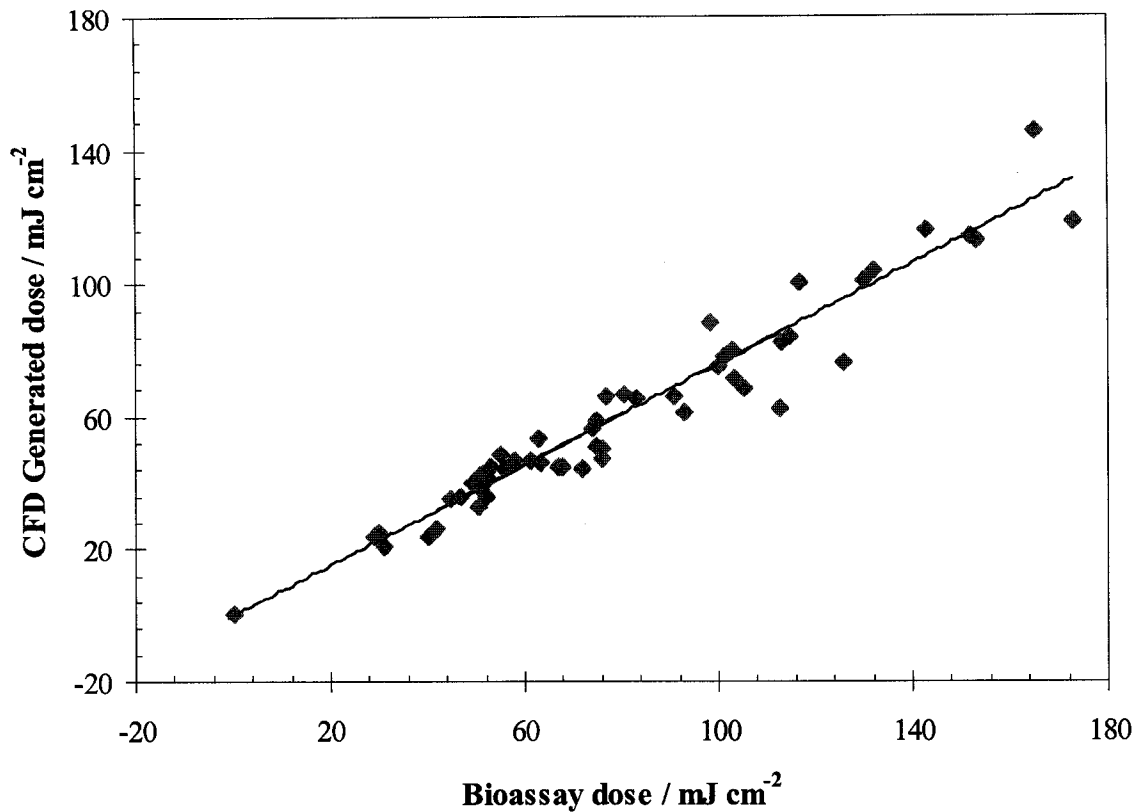
Figure 2.5 Biodosimetry UV dose vs. CFD generated UV dose (after Lawryshyn and Cairns, 2003)

The sensor set-point strategy also is a method usually used for determining the performance of UV reactors in practical operations. In this method, the fluence is calculated based on the average residence time and the irradiance measured by a UV sensor, which is installed at certain position of a UV reactor. The position of UV sensor is very important for this method, and a wrong sensor position can lead to significant errors. However, it is not easy to determine the optimal position of the UV sensor. According to the results reported by Ducoste and Linden (2005), only a small range of possible locations exist where the sensor can be placed to achieve a relatively reliable REF, regardless of the water quality. However, the predicted optimal location is a function of

41

the local irradiance. That means although the UV sensor is still at the same position as before, some misleading results could be obtained by this method, if the lamp power changes so as to alter the local irradiance. It should also be emphasized that an important assumption of this method is that the fluid in validated UV reactors is hydraulically well mixed. Therefore, even though the UV sensor is still at the optimal location, the reliability of this method could be greatly reduced if the UV reactor performs poorly with poor hydraulic mixing. Figure 2.7 (Lawryshyn and Cairns, 2003) shows visually the effects of the UV sensor location and hydraulic condition on the predicted results. Another disadvantage is that the sensor set-point method cannot directly show the germicidal fluence delivered by UV reactors and sometimes needs to be validated by biodosimeters.
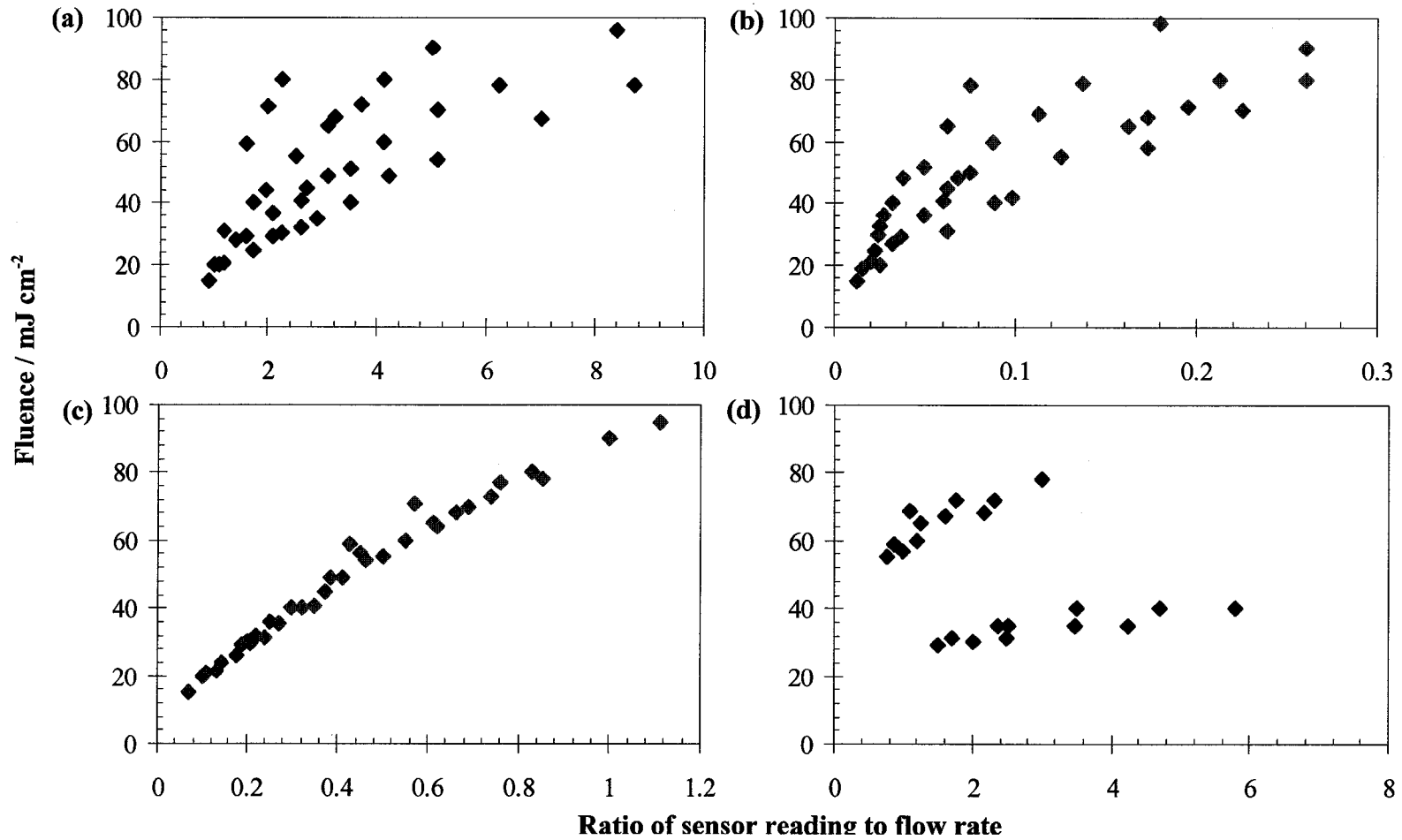
Figure 2.2 Effects of UV sensor location[6] and hydraulic status on the REF. (a) 5 cm; (b) optimal sensor location; (c) 20 cm; and (d) a poorly operated UV reactor (after Lawryshyn and Cairns, 2003)

[6] Here the sensor location is the distance from the sensor to the lamp being monitored. The data shown in these charts were generated numerically through CFD and simplified optical models (Lawryshyn and Cairns, 2003).

Chemical actinometry has been used for about 70 years as a simple, flexible and accurate approach for the measurement of UV irradiation and dozens of chemical actinometers have been developed to be employed in solid-, liquid- and gas-phase conditions for many purposes (Kuhn et al. 2004). Simply speaking, a chemical actinometer is a chemical system that undergoes a photochemical reaction for which the quantum yield is very well known, and thus the UV irradiation (photon flow) can be determined easily by measuring the chemical yield after exposure to UV light. Some chemical actinometers, such as ferrioxalate, persulfate and iodide/iodate actinometers, are usually applied for the validation of UV reactors in drinking water disinfection (Bolton, 2001). Many attempts have been reported to utilize chemical actinometry as a useful tool in design evaluations and comparative studies of UV disinfection systems. Harris et al. (1987) conducted some validation tests at various flow rates using the potassium ferrioxalate actinometer, and they obtained reproducible fluence estimates which were very consistent with the validation results obtained by *Bacillus subtilis* biodosimetry. Linden and Darby (1997) found that very similar estimations of effective germicidal fluences for a medium-pressure UV lamp were obtained by MS2 biodosimetry and uridine actinometry, when the relative absorbance spectra of the uridine and MS2 phage were accounted for. In addition, Jin et al. (2006) also observed that the germicidal fluence rates obtained by uridine and iodide/iodate actinometers, integrated with mathematical models, were very close to those determined by *Bacillus subtilis* biodosimetry. Compared with biodosimetry, a major advantage for chemical actinometry is that it is convenient, economical and time-saving. In addition, unlike biodosimetry, which only can provide some information associated with the average fluence rate, the chemical actinometry

44

methods can determine the fluence rate distribution within a UV reactor if it is properly applied. For example, Stefan et al. (2001) and Rahn et al. (2006) successfully determined the fluence rate distribution in a batch UV reactor with a medium-pressure or low-pressure UV lamp using the iodide/iodate actinometer under various operating conditions, and both sets of their experimental results obtained by actinometry had a satisfactory agreement with the data obtained by irradiance models. Using potassium ferrioxalate actinometer, Quan et al. (2004) also experimentally determined the fluence distribution in a UV reactor, and the results matched very well with the computational results obtained by three different mathematic models. However, in spite of its advantages, the disadvantages of chemical actinometry are also very predominant. First of all, the costs of some chemicals used in actinometers, such as ferrioxalate, iodide and iodate salts, still are relatively high, and it is impractical for regular use in field situations. Second, some actinometer solutions, such as potassium ferrioxalate and potassium peroxodisulfate, are not stable and need to be freshly prepared every one or two days. In addition, the photoproducts of some actinometers are unstable and are influenced by operating conditions. This could cause a significant deviation between the data determined by actinometry and the real values. Third, the quantum yields of some chemical actinometers could be dependent on the operating conditions, such as the actinometer concentration, UV irradiation, wavelength, water quality, etc. For instance, Rahn et al. (2003) reported that the quantum yield of iodide/iodate actinometer decreased from 0.73 down to 0.30 when the wavelength of UV light varied from 254 to 284 nm; at the same time, the quantum yield also appeared to have a marked decrease, when the concentration of iodide was lower than 0.15 M. Another limitation of chemical actinometry is that some

actinometers cannot reflect directly the effective germicidal fluence because of the differences between the absorbance spectra of the actinometer and the DNA of target pathogens. In addition, some chemical actinometer solutions or the photoproducts could be harmful to the water environment, and the effluent of actinometry may need to be treated carefully. This could increase the cost and difficulty of chemical actinometers implemented for the validation of UV reactors (especially the UV reactors with large flow rates).

2.6 Conclusions

UV irradiation has been used increasingly for the water and wastewater microorganism reduction treatment. As a key component for the design and operation of UV reactors, validation testing also attracts great attention. Generally speaking, there are three kinds of methods usually used for the estimate of fluences delivered in UV reactors. Biodosimetry is the most widely used and most reliable approach available at the present. It also has been regulated as a primary method for the validation of UV reactors in some countries. However, the implementation of biodosimetry is a time- and money-consuming process. In order to get an effective and economical validation technique, some have developed mathematical models validated by biodosimetry to determine the performance of UV reactors. For this method, the big problem is that mathematic models cannot be used for the UV reactor validation alone, and they still need to be corrected by biodosimetry. Chemical actinometry is a convenient and accurate method for the measurement of UV fluence, and some actinometers, such as potassium ferrioxalate and uridine, have been successfully tested for the validation of UV reactors in several studies. But some disadvantages or limitations extremely restrict the application of actinometry in

46

practical operations. Therefore, there is still a need to explore a reliable, convenient and cost-effective approach that can be used for the validation of UV reactors in practical operations.

The sequential process of chlorination and UV irradiation is often employed for drinking water disinfection. When chlorination was located prior to UV treatment, a significant decrease of chlorine concentration was observed in several studies and operations because of the photodecomposition of chlorine. In addition, the formation of DBPs, regardless of the sequence of UV treatment and chlorination, was examined in several investigations. The reported results are controversial, since some researchers did not observe any significant effect of the sequential process on the formation of DBPs (e.g., THMs and HAAs), but some obtained contrary conclusions. This could be due to the different experimental conditions, such as temperature, pH, characteristics of organic compounds, concentration of chlorine, UV fluence, etc. Consequently, it is necessary to conduct a systematic study associated with the formation of DPBs in a sequential disinfection process.

Based on the investigation on the approaches applied for the validation of UV reactors and utilizations of chlorination and UV irradiation in drinking water disinfection, a novel method could be developed for the estimation of the performance of UV reactors by using free chlorine as an indicator of UV irradiation. Before using free chlorine to validate UV reactors, the quantum yield of free chlorine decomposed by UV light should be very well determined in advance. The by-products generated by the photodegradation of free chlorine should also be carefully identified, and the effects on the drinking water quality should be studied.

47

2.7 References

Adam, L.C., Fábián, I., Suzuki, K. and Gordon, G. 1992. Hypochlorous acid decomposition in the pH 5–8 region. *Inorg. Chem.*, **31(17)**: 3534–3541.

Ballester, N.A. and Malley, J.P. 2004. Sequential disinfection of adenovirus type 2 with UV-chlorine-chloramine. *J.–AWWA*, **96(10)**: 97–103.

Blatchley, E.R. and Hunt, B.A. 1994. Bioassay for full-scale UV disinfection systems. *Wat. Sci. Technol.*, **30(4)**: 115–123.

Blatchley, E.R., Do-Quang, Z., Janex, M.L. and Laîné, J.M. 1998. Process modeling of ultraviolet disinfection. *Wat. Sci. Technol.*, **38(6)**: 63–69.

Bolton, J.R. 2001. Ultraviolet Applications Handbook. Bolton Photosciences Inc., Edmonton, AB, Canada T6R 2M5.

Bolton, J.R. and Linden, K.G. 2003. Standardization of methods for fluence (UV Dose) determination in bench-scale UV experiments. *J. Environ. Engng.*, **129(3)**: 209–216.

Bolton, J.R. 2000. Calculation of ultraviolet fluence rate distributions in an annular reactor: significance of refraction and reflection. *Wat. Res.*, **34(13)**: 3315–3324.

Buchanan, W., Roddick, F. and Porter, N. 2006. Formation of hazardous by-products resulting from the irradiation of natural organic matter: Comparison between UV and VUV irradiation. *Chemosphere*, **63(7)**: 1130–1141.

Butler, P.J.D. and Phillips, L.F. 1983. Upper limit for the atomic oxygen yield in the 308 nm photolysis of HOCl. *J. Phys. Chem.*, **87(1)**:183–184.

Cabaj, A., Sommer, R. and Schoenen, D. 1996. Biodosimetry: model calculations for UV water disinfection devices with regard to dose disitributions. *Wat. Res.*, **30(4)**: 1003–1009.

Cairns, W.L., Sakamoto, G., Comair, C.B. and Gehr, R. 1993. Assessing UV disinfection of a physico-chemical effluent by medium pressure lamps using a collimated beam and pilot plant. Trojan Technologies Inc. 3020 Gore Road, London, Ontario Canada N5V 4T7.

Cassan, D., Mercier, B., Castex, F. and Rambaud, A. 2006. Effects of medium-pressure UV lamps radiation on water quality in a chlorinated indoor swimming pool. *Chemosphere*, **62(9)**: 1507–1513.

Cheung, L.M. 2004. Investigation of virus inactivation and byproducts formation under sequential disinfection using UV irradiation and free chlorine or monochloramine. M.Phil thesis, Hong Kong University of Science and Technology.

DVGW 1997. UV disinfection devices for drinking water supply—Requirements and testing. Bonn, Germany: German Gas and Water Management Union (DVGW).

Edstrom Industries, Inc. 2006. Forms of chlorine in water. 819 Bakke Avenue Waterford, WI 53185-5913 http://www.edstrom.com/Resources. cfm?doc_id=164 (available on Aug. 15, 2006).

EPCOR 2006. EPCOR Water Service, Edmonton, AB, Canada. http://www.epcor. com/Communities/Alberta/Operations/Water+Treatment+Plants/Edmonton/ELSmith/ StrathmoreWTProcess.htm (available on Aug 15, 2006)

Fenner, R.A. and Komvuschara, K. 2005. A new kinetic model for ultraviolet disinfection of grey water. *J. Environ. Engng.*, **131(6)**: 850–864.

Giles, M.A. and Danell, R. 1983. Water dechlorination by activated carbon, ultraviolet radiation and sodium sulphite. *Wat. Res.*, **17(6)**: 667–676.

Guo, H. 1993. Time-dependent quantum dynamical study of the photodissociation of HOCl. *J. Phys. Chem.*, **97(11)**: 2602–2608.

Haidera, T., Sommer, R., Knasmüller, S., Eckl, P., Pribil, W., Cabaj, A. and Kundi, M. 2002. Genotoxic response of Austrian groundwater samples treated under standardized UV (254 nm) – disinfection conditions in a combination of three different bioassays. *Wat. Res.*, **36(1)**: 25–32.

Harris, G.D., Adams, V.D., Moore, W.M. and Sorensen, D.L. 1987. Potassium ferrioxalate as chemical actinometer in ultraviolet reactors. *J. Environ. Engng.*, **113(3)**: 612–627.

Jin, S., Mofidi, A.A. and Linden, K.G. 2006. Polychromatic UV fluence measurement using chemical actinometry, biodosimetry, and mathematical techniques. *J. Environ. Engng.*, **132(8)**: 831–841.

Kashinkuti, R.D., Linden, K.G., Shin, G.A., Metz, D.H., Sobsey, M.D., Moran, M.C., Samuelson, A.M. 2004. Investigating multibarrier inactivation for Cincinnati-UV, by-products, and biostability. *J–AWWA*, **96(6)**: 114–127.

Kobayashi, T. and Okuda, T. 1972. A continuous method of monitoring water quality by chlorine consumption under ultraviolet radiation. *Wat. Res.*, **6(1)**: 197–209.

Kool, H.J., Kreijl, C.F. and Hrubec, J. 1985. Mutagenic and carcinogenic properties of drinking water in water chlorination. R.L. Jolley, R.J. Bull, W.P. Davis, S. Katz, M.H., Roberts, Jr., and V.A. Jacobs (Eds.). Chemistry, Environmental Impact and Health Effects, Lewis Publishers, Chelsea, Michigan, USA, 5,187–205.

Kuhn, H.J., Braslavsky, S.E. and Schmidt, R. 2004. International union of pure and applied chemistry organic and biomolecular chemistry division subcommittee on photochemistry: chemical actinometry. *Pure Appl. Chem.*, **76(12)**: 2105–2146.

Lawryshyn, Y.A. and Cairns, B. 2003. UV disinfection of water: the need for UV reactor validation. *Wat. Sci. Technol.: Wat. Supply*, **3(4)**: 293–300.

Lehtola, J.M., Miettinen, I.T., Vartiainen, T., Rantakokko, P., Hirvonen, A. and Martikainen, P.J. 2003. Impact of UV disinfection on microbially available phosphorus, organic carbon, and microbial growth in drinking water. *Wat. Res.*, **37(5)**: 1064–1070.

Linden, K.G., Soriano, G.S., Dodson, G.S. and Darby, J.L. 1998. Investigation of disinfection by-product formation following low and medium pressure UV irradiation of wastewater. Proceedings of the WEF Disinfection Specialty Conference, Baltimore.

Lister, M.W. 1956. Decomposition of sodium hypochlorite: the uncatalyzed reaction. *Can. J. Chem.*, **34(4)**: 465–478.

Liu, W., Cheung, L.M., Yang, X. and Shang, C. 2006. THM, HAA and CNCl formation from UV irradiation and chlor(am)ination of selected organic waters. *Wat. Res.*, **40(10)**: 2033–2043.

Liu, W., Andrews, S.A., Bolton, J.R., Linden, K.G., Sharpless, C. and Stefan, M.I. 2002. Comparison of disinfection byproduct (DBP) formation from different UV technologies at bench scale. *Wat. Sci. Technol.: Wat. Supply*, **2(5–6)**: 515–521.

Mackey, E.D., Cushing, R.S. and Crozes, G.F. 2000. Practical aspects of UV disinfection. AWWARF AWWA West Explorer Drive, Suite 200, Boise, ID 83713.

Mackey, E.D., Hargy, T.M., Wright, H.B., Malley, J.P. and Cushing, R.S. 2002. Comparing Cryptosporidium and MS2 bioassays – implications for UV reactor validation. *J. –AWWA*, **94(2)**: 62–69.

Mah, L. 2005. Alberta water treatment plant maintained production during UV installation. *Environ. Sci. Engng.*, **18(5)**: 19–20.

Malley, J.P., Shaw, J.P. and Ropp, J.R. 1995. Evaluation of by-products produced by treatment of ground waters with ultraviolet irradiation. AWWARF, Denver, CO.

Mamane-Gravetz, H. and Linden, K.G. 2004. UV disinfection of indigenous aerobic spores: implications for UV reactor validation in unfiltered waters. *Wat. Res.*, **38(12)**: 2898–2906.

Molina, L.T. and Molina, M.J. 1978. Ultraviolet spectrum of HOCl. *J. Phys. Chem.*, **82(22)**: 2410–2414.

Molina, M.J., Ishiwata, T. and Molina, L.T. 1980. Production of OH from photolysis of HOCl at 307–309 nm. *J. Phys. Chem.*, **84(8)**: 821–826.

Nicholson, L.W. and Galeano, B. 2003. UV resistance of Bacillus anthracis spores revisited: validation of Bacillus subtilis spores as UV surrogates for spores of B. anthracis sterne. *Appl. Environ. Microbiol.*, **69(2)**: 1327–1330.

Nieminski, E.C., Bellamy, W.D. and Moss, L.R. 2000. Using surrogates to improve treatment plant performance. *J. –AWWA*, **92(3)**: 67–78.

Nowell, L.H. and Hoigné, J. 1992a. Photolysis of aqueous chlorine at sunlight and ultraviolet wavelengths—I. Degradations rates. *Wat. Res.*, **26(5)**: 593–598.

Nowell, L.H. and Hoigné, J. 1992b. Photolysis of aqueous chlorine at sunlight and ultraviolet wavelengths—II. Hydroxyl radical production. *Wat. Res.*, **26(5)**: 599–605.

Oliver, B.G. and Carey, J.H. 1977. Photochemical production of chlorinated organics in aqueous solutions containing chlorine. *Environ. Sci. Technol.*, **11(9)**: 893–895.

ÖNORM 2003. Austrian national standard: prÖNORM M 5873-2, 2003. Plants for disinfection of water using ultraviolet radiation: requirements and testing, Part 2: Medium pressure mercury lamp plants. Austrian Standards Institute, Vienna, Austria.

Oppenländer, T. 2003. Photochemical Purification of Water and Air Advanced Oxidation Processes (AOPs): Principles, Reaction Mechanisms, Reactor Concepts. Wiley–VCH Verlag GmbH & Co. KGaA, Weinheim.

Örmeci, B., Ducoste, J.J. and Linden, K.G. 2005. UV disinfection of chlorinated water: impact on chlorine concentration and UV dose delivery. *J. Wat. Supply: Res. Technol.—AQUA*, **54(3)**: 189–199.

Plummer, J., Padden, M. and Brown, T. 2005. MQP: JYP-0402 UV wastewater treatment. http://www.wpi.edu/Academics/Depts/CEE/mqp_04-05_gallery/ppt%20files/UV%20 Waste.ppt (available at Aug. 15, 2006)

Qualls, G.R. and Johnson, J.D. 1983. Bioassay and dose measurement in UV disinfection. *Appl. Environ. Microbiol.*, **45(3)**: 872–877.

Quan, Y., Pehkonen, S.O. and Ray, M.B. 2004. Evaluation of three different lamp emission models using novel application of potassium ferrioxalate actinometry. *Ind. Engng. Chem. Res.*, **43(4)**: 948–955.

Rahn, R.O., Bolton, J.R. and Stefan, M.I. 2006. The iodide/iodate actinometer in UV disinfection: determination of the fluence rate distribution in UV reactors. *Photochem. Photobiol.*, **82(2)**: 611–615.

53

Rahn, R.O., Stefan, M.I., Bolton, J.R., Goren, E., Shaw, P.S. and Lykke, K.R. 2003. Quantum yield of the iodide–iodate chemical actinometer: dependence on wavelength and concentration. *Photochem. Photobiol.*, **78(2)**: 146–152.

Scheible, K., Wright, H., Cabaj, A. and Hoyer, O. 2003. Validation facilities for drinking water UV systems. *IUVA News*, **5(4)**: 24–28.

Severin, B.F., Suidan, M.T. and Engelbrecht, R.S. 1983. Kinetic modeling of UV disinfection of water. *Wat. Res.*, **17(11)**: 1669–1678.

Sharpless, C.M. and Linden, K.G. 2001. UV photolysis of nitrate: effects of natural organic matter and dissolved inorganic carbon and implications for UV water disinfection. *Environ. Sci. Technol.*, **35(14)**: 2949–2955.

Sharpless, C.M., Bastow, T.L. and Linden, K.G. 2001. Nitrite production during polychromatic UV disinfection of drinking water: effect of pH and natural organic matter," Proceedings American Water Works Association Annual Meeting, Washington, DC.

Sharpless, C.M., Page, M.A. and Linden, K.G. 2003. Impact of hydrogen peroxide on nitrite formation during UV disinfection. *Wat. Res.*, **37(19)**: 4730–4736.

Sommer, R. and Cabaj, A. 1993. Evaluation of the efficiency of a UV plant for drinking water disinfection. *Wat. Sci. Technol.*, **27(3–4)**: 357–362.

Sommer, R., Cabaj, A., Haider, T. and Hirschmann, G. 2004. UV drinking water disinfection – requirements, testing and surveillance: exemplified by the Austrian National Standards M 5873-1 and M 5873-2. *IUVA News*, **6(4)**: 27–35.

Sommer, R., Haider, T., Cabaj, A., Pribil, W. and Lhotsky, M. 1998. Time dose reciprocity in UV disinfection of water. *Wat. Sci. Technol.*, **38(12)**: 145–150.

54

Stefan, M.I., Bolton, J.R. and Rahn, R.O. 2001. Use of the iodide/iodate actinometer together with spherical cells for determination of the fluence rate distribution in UV reactors: validation of the mathematical model. Conference proceeding, First International Congress on Ultraviolet Technologies, Washington, DC.

Tanaka, Y., Kawasaki, M., Matsumi, Y., Fujiwara, H., Ishiwata, T., Rogers, L.J., Dixon, R.N. and Ashfold, M.N.R. 1998. The ultraviolet photodissociation of Cl2O at 235 nm and of HOCl at 235 and 266 nm. *J. Chem. Phys.*, **109(4)**: 1315–1323.

USEPA 2003. Ultraviolet disinfection guidance manual. U.S. Environmental Protection Agency, Mail Code 4607M, 1200 Pennsylvania Avenue NW, Washington, DC 20460-0001. EPA 815-D-03-007, June 2003 Draft.

USEPA 2006. National primary drinking water regulations: Long Term 2 Enhanced Surface Water Treatment Rule. Federal Register, Environmental Protection Agency, 40 CFR Parts 9, 141, and 142 [EPA-HQ-OW-2002-0039; FRL-8013-1] RIN 2040-AD37.

Van der Veer, A.J., Ijpelaar, J.F., Medema, G.J. and Kruithof, J.C. 2005. Nitrite formation, a useful tool in medium pressure UV fluence control. *Water Intelligence Online*, http://www.iwaponline.com/wio/2005/04/wio200504008.htm (available on Aug. 19, 2006).

WHO 2003. Nitrate and nitrite in drinking-water. Background document for preparation of WHO Guidelines for drinking-water quality. Geneva, World Health Organization (WHO/SDE/WSH/03.04/56).

Wright, H. and Lawryshyn, Y.A. 2000. An assessment of the bioassay concept for UV reactor validation. Proceedings, Disinfection 2000: Disinfection of Wastes in the New

Millenium, New Orleans, LA, March 15–18. Water Environment Federation, Alexandria, VA.

Zheng, M., Andrews, S.A. and Bolton, J.R. 1999a. Impacts of medium-pressure UV and UV/H_2O_2 on THM and HAA formation in pre-UV chlorination drinking water, Proceedings WQTC, Tampa FL.

Zheng, M., Andrews, S.A. and Bolton, J.R. 1999b. Impacts of medium-pressure UV and UV/H_2O_2 treatments on disinfection byproduct formation. Proceedings of AWWA annual conference, Chicago, IL.

CHAPTER 3 QUANTUM YIELD OF AQUEOUS FREE CHLORNE

DECOMPOSED BY UV LIGHT AT 254 NM[7]

3.1 Introduction

As discussed in Chapter 1, the primary purpose of this research is to develop a method, using free chlorine, for the estimation of delivered fluences in UV reactors. That is, free aqueous chlorine will be employed as a chemical actinometer to validate the performance of UV reactors in this research. It is well known that a vital requirement for a chemical actinometry is that the quantum yield of the actinometer is determined accurately. Although the quantum yield of aqueous free chlorine has been reported in some previous studies (Nowell and Hoigné 1992a and Buxton and Subhani 1972a), it is still not very well known, since those studies did not conduct a detailed investigation on the quantum yield of aqueous free chlorine, and the reported results were not consistent with each other. Accordingly, it is necessary to perform a systematic study on the quantum yield of aqueous free chlorine before using it for validation testing.

As it is known, in drinking water disinfection with the pH varying from 7 to 8, free chlorine mainly consists of hypochlorous acid (HOCl) and its conjugate base, the hypochlorite ion (OCl^-). The relative amount of HOCl and OCl^- are strongly dependent on the pH and follow the equilibrium

[3.1] $HOCl \rightleftharpoons OCl^- + H^+$ ($pK_a = 7.5$ at $25°C^8$)

---

[7] A version of a part of this chapter has been submitted for publication. Feng, Y., D. W. Smith and J. R. Bolton. *J.Environ. Engng. Sci.* (2006)

[8] Morris (1966), Snoeyink and Jenkins (1980), Sawyer et al. (1994).

Of the aqueous free chlorine species, HOCl is mainly responsible for disinfection in the chlorination process. According to the above reaction, the fraction (f) of HOCl in aqueous chlorine solution is

$$[3.2] \qquad f = \frac{[\text{HOCl}]}{[\text{OCl}^-]+[\text{HOCl}]} = \frac{1}{1+10^{\text{pH}-\text{pK}_a}}$$

As shown in Figure 3.1, the dependence of free chlorine species on pH has been plotted based on Eq. 3.2. This figure shows that the relative amount of HOCl gradually increases with decreasing pH to the point that at pH 5 $(f > 0.99)$; however, at higher pH values the OCl$^-$ ion becomes the predominant species.
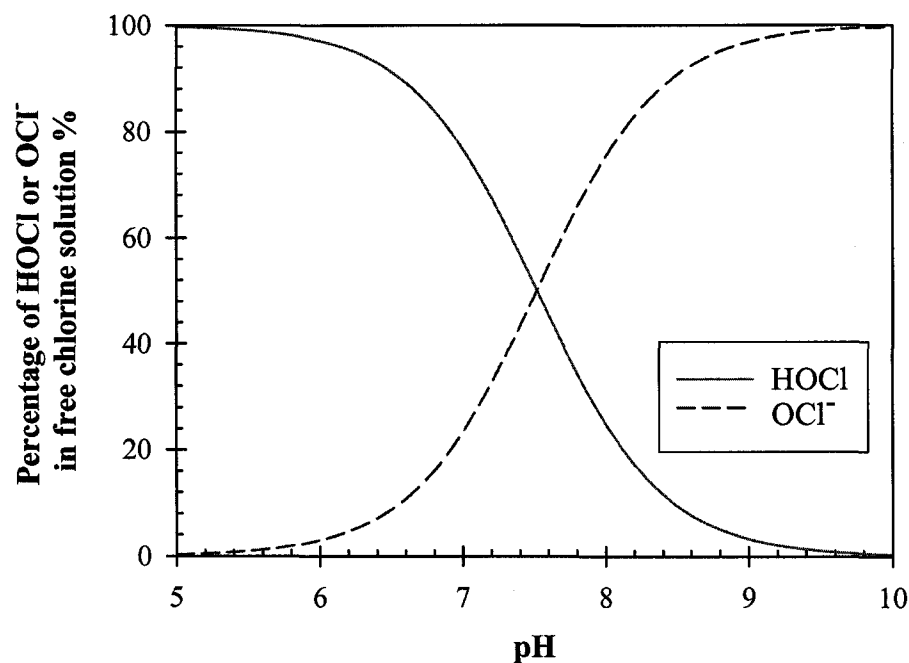
Figure 3.1 The dependence of relative amount of aqueous free chlorine species (HOCl and OCl⁻) on pH value

Since, in practice, the pH is such that both HOCl and OCl$^-$ are present in most water or wastewater treatment, the overall quantum yield of free chlorine decomposed is

58

more important than the quantum yield of individual free chlorine species, which was usually reported in previous studies. In addition, the concentration of free chlorine may have an influence on the quantum yield because of possible chain reactions. Therefore, the main objective of this chapter is to investigate the effects of pH and concentration of free chlorine in solution on the overall photolysis quantum yield at 254 nm. Then, a mathematic model will be derived based on the experimental results for the estimate of the overall quantum yield of free chlorine. To achieve this purpose, the following experiments will be performed:

1. Determination of the absorbance spectra of $HOCl$ and OCl^-;

2. Measurement of the molar absorption coefficients of both chlorine species;

3. Examination of the overall quantum yields of aqueous free chlorine solution for various pH values;

4. Development a mathematic model and verifying its reliability for the quantum yield prediction; and

5. Investigation of the effect of organic compounds on the quantum yield of free chlorine.

3.2 Materials and methods

3.2.1 Reagents and apparatus

All chemicals used in this research were analytical reagent grade. Deionized water (DI water) generated by a Maxima Ultra Pure Water System (Model: Elcastat Maxima HPLC, Fisher Scientific Co., Canada) was used for chemical solution preparations and general experimental analysis. For some special purposes, such as the dilution of free

59

chlorine samples, the chlorine demand free (CDF) DI water (produced according to APHA et al., 1995a) was used. The free chlorine solutions used in this study were prepared by adding an appropriate aliquot of fresh sodium hypochlorite solution (5.65 to 6%, Fisher Scientific Co., Canada) to a CDF volumetric flask containing sufficient DI water. DPD free chlorine reagent and DPD total chlorine reagent (for 25 mL sample, Hach[®], Anachemia Canada Inc.) were usually used to determine the concentration of chlorine species, and the other compounds used in this research were stock chemicals of analytical grade. A *quasi* collimated beam UV apparatus (Model PSI-1-120, Calgon Carbon Corporation, USA) equipped with a 10 W low-pressure UV lamp (Ster-L-Ray Germicidal Lamp, model G12T6L 15114, Atlantic Ultraviolet Corporation, USA) was used to generate a nearly parallel beam of UV light at 254 nm. The UV irradiance at the center of the UV beam on the surface of free chlorine sample was measured using a radiometer (International Light, Model IL 1400A) equipped with a UV detector (International Light , Model SED240), which was calibrated at 254 nm. An Ultraspec 2000 UV-Visible spectrophotometer (Pharmacia Biotech, Fisher Scientific Co., Canada) and either a 10.0 or a 50.0 mm path length quartz cell (Fisher Scientific Co., Canada) were used to determine the absorbance of aqueous chlorine solutions. The absorbance spectra of HOCl and OCl⁻ were determined using a Hewlett-Packard 8452A diode array spectrophotometer (Hewlett Packard, France). In addition, some CDF glassware, treated by being exposed to about 100 mg/L chlorine solution overnight, rinsed with chlorine demand free water, and then dried in an oven at about 180°C, and some other routine apparatuses, such as a pH meter (Accumet[®] Research AR50, Fisher Scientific Co.,

60

Canada), an electronic balance (Model: EP613C, Ohaus Corporation, US) and a magnetic stirrer (Isotemp®, Fisher Scientific Co., Canada), were also used in this research.

3.2.2 Preparation of buffer solutions

In this study, the quantum yields of aqueous free chlorine at pH 5, 7, 8, 9 and 10 were determined. Table 3.1 shows the chemicals used for the preparation of buffer solutions at the various pH values. The amount of chemicals for each buffer solution was calculated based on the chemistry of the weak acid-base equilibrium. For example, for a weak acid HA that ionizes in water

[3.3] $HA \leftrightarrow H^+ + A^-$

and therefore, the ionization constant (K_a) is

[3.4] $K_a = \dfrac{[H^+][A^-]}{[HA]}$

By rearranging equation [3.4], the molar ratio of A^- (conjugate base of HA) to HA can be obtained as follows:

[3.5] $\dfrac{[A^-]}{[HA]} = 10^{pH-pK_a}$

where pKa = $-\log(K_a)$. If one assumes that the concentration of buffer solution needed to be prepared is C, that is

[3.6] $[HA] + [A^-] = C$

by combining Eqs. 3.5 and 3.6, the moles of HA and its conjugate base, A^-, can be calculated. Then, the buffer solution can be prepared by adding the appropriate amount of weak acid (or base) and its conjugate base (or acid) to chlorine demand free water in a 1000 mL volumetric flask, and adjusting the pH of the solution to the required value

61

using 0.005N sulfuric acid (H_2SO_4) or 0.005N sodium hydroxide (NaOH). The concentrations of the buffer solutions used in this study were usually lower than 0.02 M, hence the ionic strength is not considered in the above calculation process.

Table 3.1 Chemicals used for the preparation of buffer solutions

pH value of buffer solution	Chemicals	Ionization Equilibrium	pK_a
5	CH_3COOH and CH_3COONa	$CH_3COOH \leftrightarrow H^+ + CH_3COO^-$	4.74
7	NaH_2PO_4 and K_2HPO_4	$H_2PO_4^- \leftrightarrow H^+ + HPO_4^{2-}$	7.21
8	NaH_2PO_4 and K_2HPO_4	$H_2PO_4^- \leftrightarrow H^+ + HPO_4^{2-}$	7.21
9	H_2SO_4 and NaH_2BO_3	$H_3BO_3 \leftrightarrow H^+ + H_2BO_3^-$	9.24
10	$NaHCO_3$ and Na_2CO_3; or H_2SO_4 and NaH_2BO_3	$HCO_3^- \leftrightarrow H^+ + CO_3^{2-}$; or $H_3BO_3 \leftrightarrow H^+ + H_2BO_3^-$	10.33 or 9.24

3.2.3 Preparation of free chlorine samples

In this study, the free chlorine samples were freshly prepared for each experiment. First, the concentration of the fresh sodium hypochlorite solution (5.65 to 6%) obtained from Fisher Scientific Co. (Canada) was determined accurately using the DPD method by careful quantitative dilution of the original solution after it was received from the supplier. Then, based on the concentration of a free chlorine sample to be prepared, the volume of the original sodium hypochlorite solution to be used for the sample preparation was

62

calculated, and the sample was made up by the gradual dilution method. For example, if 0.25 mL of the original sodium hypochlorite solution was needed for the preparation of 1000 mL of a free chlorine sample based on the calculations, 5.0 mL of original sodium hypochlorite solution was transferred using a volumetric transfer pipette (Kimax®, Fisher Scientific Co., Canada) to be diluted to 100 mL by a buffer solution or CFD DI water and then 5.0 mL of the diluted solution was transferred to a 1000 mL volumetric flask for the preparation of the desired free chlorine solution. The corresponding buffer solution was used for the preparation of a free chlorine sample at a certain pH value; otherwise, CFD DI water was used for the preparation of samples.

3.2.4 UV exposure and irradiance measurements

Two aliquots of free chlorine solution were used for each run: one for exposure to UV light and the other as a dark control sample. The former sample was placed under the open end of the plastic collimating tube of the UV collimated beam apparatus in the center of the beam, and the latter sample was placed in the dark on a bench that was far away from the UV apparatus. The surface of the solution to be exposed was about 300 mm from the UV lamp. The exposure time of the UV light on the free chlorine solution was controlled by means of a pneumatic shutter located at the top of the collimating tube beneath the UV lamp, and was activated using a stopwatch. During the exposure period, a 3 mm × 12 mm Teflon™-coated stir bar was added into each of these two samples to provide sufficient stirring. At the beginning and end of the UV exposure, the concentration of free chlorine in each sample was measured in order to determine the amount of free chlorine photodecomposed. The incident irradiance was measured by positioning the radiometer vertically, such that the reference calibration marker on the

63

radiometer detector head was placed at the same level as the top surface of the sample solution. During these experiments, two similar beakers (internal diameter 31.2 mm, 50 mL, Pyrex®, Fisher Scientific Co., Canada) were used as the photolysis reactor and the control reactor. In addition, the beaker exposed to UV light was covered with an opaque cap, containing a 14.2 mm diameter hole in the center of the cover to let UV light pass onto the sample in the beaker. This was done to avoid any interaction of the UV beam with the sides of the beaker. To allow for the same conditions as the UV irradiated sample, a similar cap was also employed for the dark control sample. About 25 mL of the free chlorine sample was added into the beaker for each run. The schematic and view of the collimated beam UV apparatus used in this research are shown in Figures 3.2 (a) and (b), respectively.
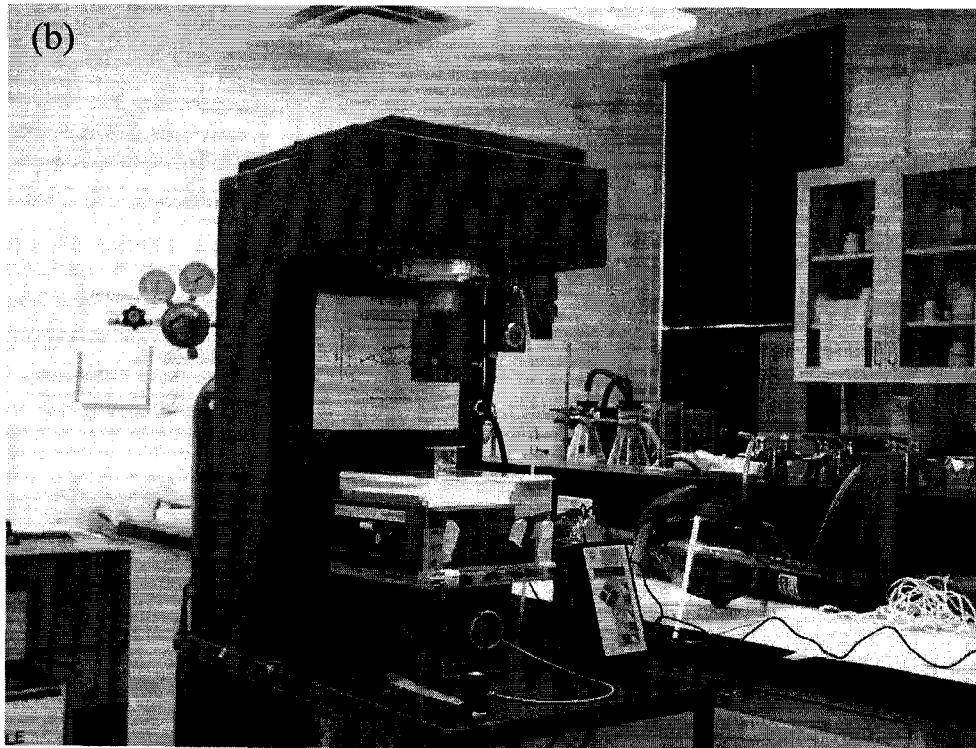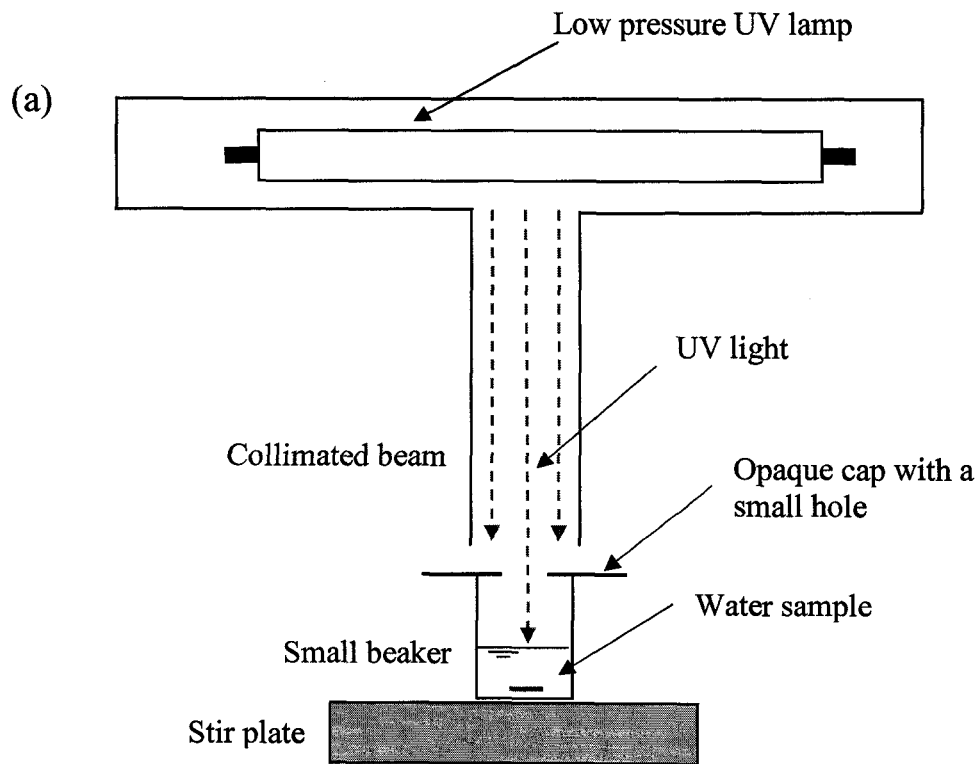
Figure 3.2 Collimated beam apparatus: (a) Schematic of the working principle and (b) View of the equipment in this research

65

3.2.5 Determination of the concentration of chlorine samples

In this study, the concentration of free chlorine in water samples was determined by one of two methods:

1. The DPD colorimetric method was usually used when the concentration was less than 50 mg L^{-1}.

2. The absorbance of chlorine species at certain wavelength was used for the concentration determination when the concentration was $\geq$50 mg L^{-1}.

For the DPD colorimetric method, the concentration of chlorine was determined using a spectrophotometer, based on the absorbance caused by the colorimetric reaction of DPD reagent with chlorine. The detailed procedure is provided in *Standard Methods for the Examination of Water and Wastewater* (APHA et al. 1995b). Briefly, the determination of the free chlorine residual is as follows:

1. A 25 mL aliquot of sample was transferred to a 40 mL vial;

2. A pouch of DPD Free Chlorine Reagent (for 25 mL sample, powder, Hach®, Anachemia Science Co.) was added to the vial;

3. The solution was mixed sufficiently and then the absorbance at 515 nm of the solution was determined immediately using the spectrophotometer; and

4. The concentration of free chlorine residual was calculated according to the regression equation, which was determined based on a 'standard curve' of 'absorbance' vs. 'concentration'. The standard curve used in the DPD method was obtained by

   a. Preparing a series of potassium permanganate (KMnO$_4$) standard solutions, which are equivalent to 0.5 to 4 mg L^{-1} in DPD reaction (0.891 mg

66

$KMnO_4$ L^{-1} produces a chlorine equivalent of 1.0 mg L^{-1} in the DPD reaction);

b. Transferring 25 mL from each of these solutions to 40 mL vials, adding a pouch of DPD Free (Total) Chlorine Reagent into each vial, and determining the absorbance; and

c. Writing down the absorbance and its corresponding equivalent chlorine concentration and plotting a curve with 'absorbance' on the x axis and 'chlorine equivalent concentration (mg L^{-1})' on the y axis.

Based on this curve, the concentration of free chlorine residual can be related to its absorbance by a linear relation. In the following measurements, the concentration of free (or total) chlorine residual can be calculated according to this relation. This method is useful when the chlorine concentration is in the range of 0.5 to 4 mg L^{-1}; the minimum detectable concentration is ~10 μg L^{-1}. When the concentration of free chlorine in water sample exceeds 4 mg L^{-1}, the sample should be diluted using CDF DI water or corresponding buffer solution before the measurement. Figure 3.3 shows the standard curve used in the DPD colorimetric method in this research for the chlorine concentration determination.
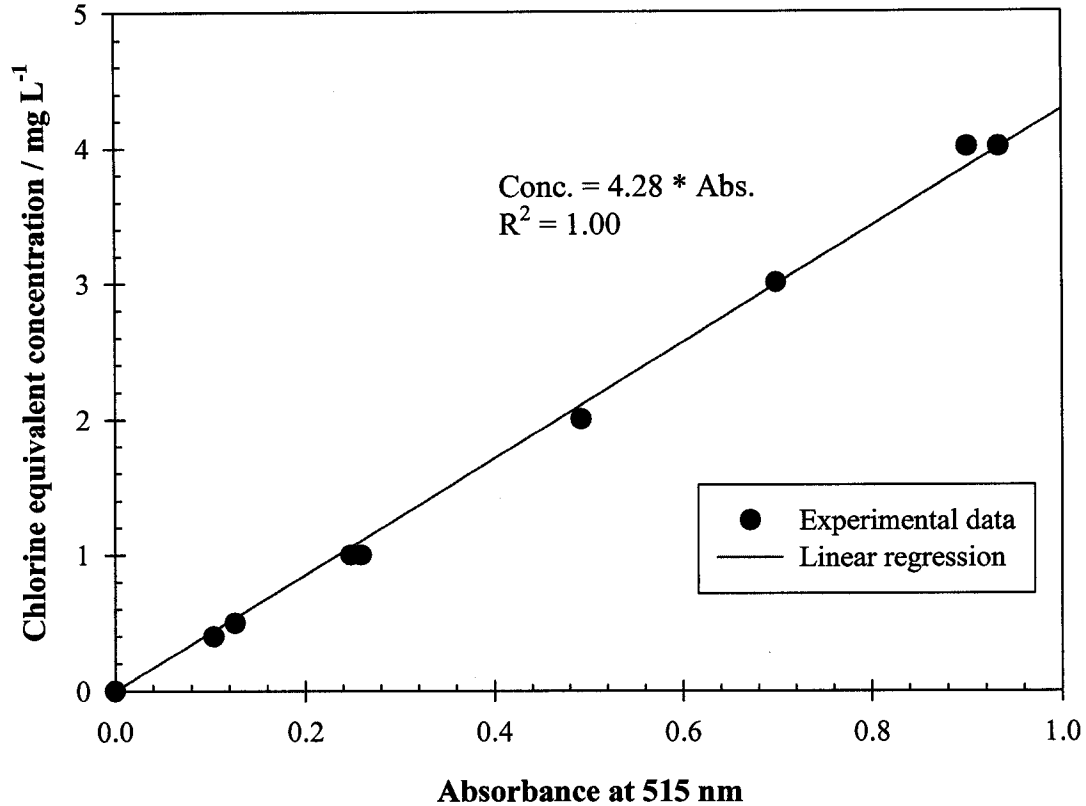
Figure 3.3 Standard curve for the chlorine concentration determination in DPD colorimetric method

If the chlorine concentration is higher than 50 mg L^{-1}, the absorbance of the water sample was used for the concentration determination. As discussed in the subsequent text, HOCl has an absorption peak at 236 nm, and OCl^- has an absorption peak at 292 nm. In addition, the molar absorption coefficient of HOCl at 236 nm and that of OCl^- at 292 nm can be determined experimentally. For a free chlorine sample, its absorbance at 236 or 292 nm can be measured using either a 10.0 mm or 50.0 mm quartz cuvette in the spectrophotometer. Therefore, the chlorine species concentration can be obtained based on the Beer-Lambert Law:

[3.7] $A(\lambda) = \sum_i \varepsilon(\lambda)_i c_i \ell$

68

Where, $A(\lambda)$ is the absorbance at wavelength λ, $\varepsilon(\lambda)$ is the molar absorption coefficient at the wavelength λ in M^{-1} cm^{-1}, c is the concentration in M and l is the light path length in cm.

3.2.6 Calculation of the quantum yield of free chlorine decomposed[9]

The quantum yield of free chlorine decomposed Φ is defined as the number of moles of free chlorine present in sample photodecomposed by one einstein[10] of UV photons absorbed. Therefore, the quantum yield can be determined based on

[3.8] $$\Phi = \frac{\text{moles of 'free chlorine' decomposed}}{\text{einsteins of UV photons absorbed at 254 nm}}$$

where "free chlorine" includes OCl^- and/or $HOCl$ present in samples. In the pH range of 5 to 10 and in the absence of free ammonia and amines, free chlorine exists primarily as an equilibrium mixture of OCl^- and $HOCl$.

As discussed in above, two sample aliquots were used in each measurement of this study. One was exposed to UV light and the other was put in dark as a control sample. The concentrations of free chlorine in these samples were determined by either of the methods described above; then, the free chlorine decomposed was determined according to the change of the free chlorine concentration in the sample exposed to UV irradiation corrected by control sample. In this study, the following equation was used for the calculation of the 'moles of free chlorine decomposed'

[3.9] $$\Delta M = (C_{bi}V_{bi} - C_{ai}V_{ai}) - (C_{bc}V_{bc} - C_{ac}V_{ac})\frac{V_{mi}}{V_{mc}}$$

---

[9] A calculation example is given in Appendix 3.1.
[10] One einstein is a mole (6.023×10^{23}) of photons.

69

where, ΔM is the moles of free chlorine decomposed due to the UV irradiation, C is the concentration (M) of free chlorine in each sample, V is the volume (L) of each sample, the subscripts of "i" and "c" are the "sample irradiated by UV light" and "control sample stored in dark", the subscripts of "b" and "a" are the "before" and "after" exposure to UV irradiation, and "m" means mean.

The "einsteins absorbed at 254 nm" can be determined from:

[3.10] $$\text{einsteins absorbed at 254 nm} = \frac{E \times \text{PF} \times A \times t \times (1-R) \times (1-10^{-A_{254}})}{U_{254}}$$

where, E is the irradiance (W cm^{-2}) measured at the center of sample position, PF is the Petri Factor defined as the average irradiance[11] over the surface of sample exposed to UV light divided by the irradiance at the center, A is the area of sample surface directly exposed to UV light (i.e., the cross-sectional area of the hole on the opaque cap covered on the sample beaker, cm^2), t is the exposure time (s), R is the reflection coefficient (0.025) on the sample surface, A_{254} is the mean absorbance of the sample at 253.7 nm during the exposure time and U_{254} is the energy of one einstein of UV photons at 253.7 nm (471,527.6 J einstein^{-1}).

---

[11] Here, the irradiance is measured at the position of the hole on the opaque cap covered on the beaker.

70

3.2.7 Fluence (UV dose)

The fluence (UV dose) H' was determined according to the protocols specified by Bolton and Linden (2003). Specifically, this involved converting the incident fluence rate (irradiance) E_0, as determined using the radiometer, to the average fluence rate E_{avg} utilizing the various correction factors specified in that protocol.

3.2.8 Experimental procedure for the quantum yield measurement

Prior to determining the quantum yield of free chlorine decomposed at certain pH, some preparative work, such as the preparation of CDF DI water, buffer solutions for the desired pH value and some CDF glassware (including volumetric flask, beaker, volumetric transfer pipette, and so on), were carried out. Then, the quantum yield of free chlorine was determined based on the following steps.

1. The water sample with a proper concentration of free chlorine should be prepared using the appropriate buffer solution according to the method described above.

2. The volumetric flask containing the free chlorine sample should be covered by aluminum foil and stored in ambient conditions for use in the following steps.

3. The collimated beam UV apparatus should be turned on to stabilize for about 15 minutes.

4. When the output of the UV lamp was stable, the Petri factor and the UV irradiance at the center of the sample position were determined. Subsequently, the weights of two empty CDF beakers (50 mL, Pyrex®, Fisher Scientific Co., Canada) with a small stir bar in each one were determined and then about 30 to 40 mL of the free chlorine sample was transferred to each beaker. One of them was used as the sample exposed to UV light and the other one was put in dark as a

71

control sample. In order to determine accurately the volume of sample in each beaker, the total weight of each beaker with free chlorine sample also needed to be determined before exposure to UV light or dark.

5. Put one sample in the appropriate position under the collimated beam apparatus, adjust the magnetic stirrer to a moderate mixing speed, turn on the pneumatic shutter to let the UV light irradiate the sample and at the same time, start the stopwatch to record the exposure time. Simultaneously, put the other sample on the same type of magnetic stirrer in the dark far from the collimated beam UV apparatus and mix at the same speed.

6. After the desired exposure time, the shutter was closed to block off the UV light and the sample was moved from the collimated beam UV apparatus to a balance to determine the amount of sample lost due to the evaporation during this period of time. The control sample was also weighed for the same purpose.

7. Finally, the free chlorine concentrations in these samples are determined and the quantum yield was calculated by the method described above.

3.3 Results and discussion

3.3.1 Buffer effects on the quantum yield of free chlorine at various pH values

Since the purpose of this study was to determine the quantum yield of free chlorine decomposed at different pH values, various buffer solutions were used for the pH adjustment in the free chlorine samples. Before adding these buffer solutions for the free chlorine samples, it was necessary to check if the buffer solutions to be used caused deviations for the measurement of quantum yield. In order to determine the effect of

72

buffer concentration, each buffer solution was made in at least three concentrations: half, normal and double of the concentration to be used in the experiments of quantum yield determination.

Figure 3.4 shows the effects of buffer solutions at various pH values (pH 5, 8, 9 and 10) on the quantum yield of free chlorine decomposed in DI water. It was clear that the quantum yield was essentially independent of the buffer concentration at each pH, and no matter how the concentration changed, it remained approximately constant. Thus, the buffer solutions used for pH 5, 8, 9 and 10 in this study were considered to have no significant effects on the measurement of quantum yield. However, as shown in Figure 3.5, the buffer solution (Na_2HPO_4/NaH_2PO_4) for pH 7 has a slight effect on the quantum yield which gradually reduced with increasing buffer concentration. According to the regression line and the 95% prediction level in Figure 3.5, the quantum yield of free chlorine at pH 7 was 1.5 ± 0.1 if the concentration of phosphate buffer was 0 mM. This is very close to the quantum yield obtained by the experiment with 10 mM buffer solution. That is to say, the effect of phosphate buffer was not very significant at the concentration of 10 mM. Accordingly, the 10 mM phosphate buffer was employed in this study for the determination of quantum yield of free chlorine at pH 7.

73
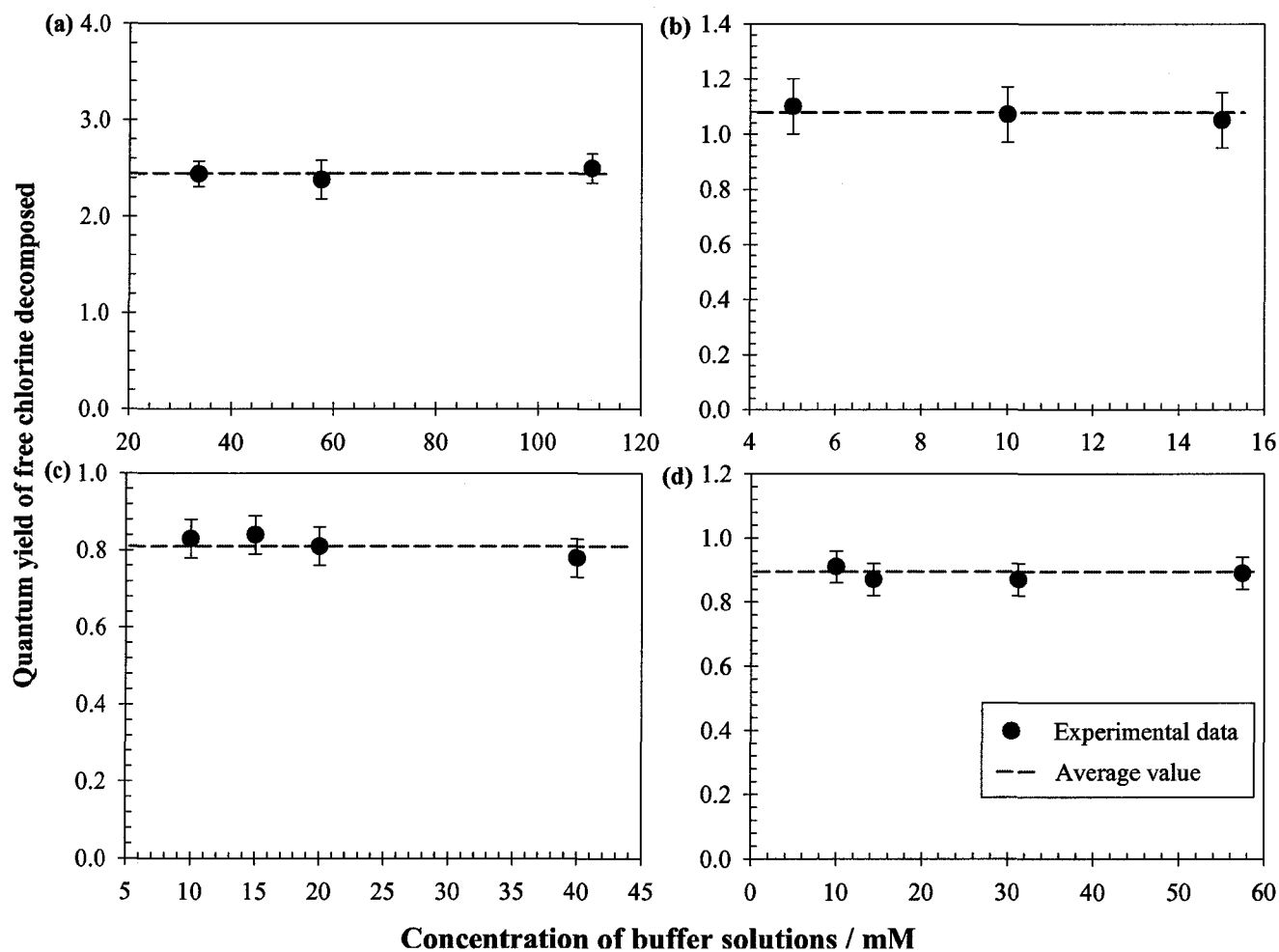
Figure 3.3 Effects of the concentration of buffer solution on the quantum yield: (a) the acetate buffer for pH 5 in 6.0 mM free chlorine sample, (b) the phosphate buffer for pH 8 in 6.0 mM free chlorine sample, (c) Sodium tetraborate buffer for pH 9 in 4.0 mM free chlorine sample and (d) bicarbonate buffer for pH 10 in 4.0 mM free chlorine sample. The experiments were performed in ambient condition ($21 \pm 2°C$).
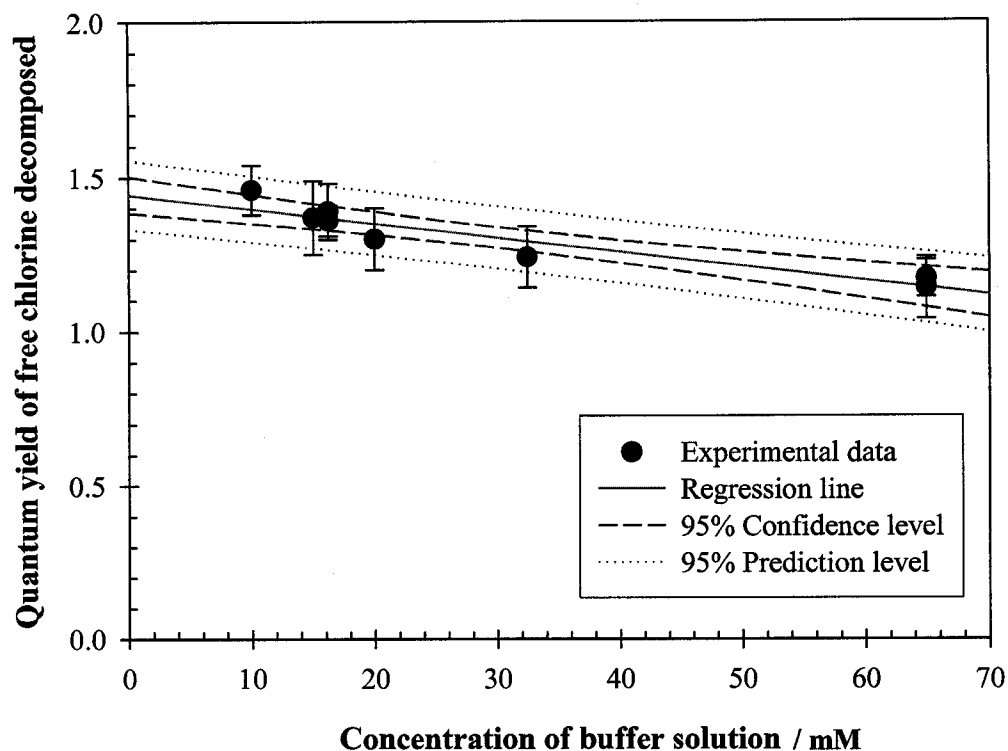
Figure 3.5 The concentration effect of phosphate buffer for pH 7 on the quantum yield of free chlorine (6.0 mM) decomposed in ambient condition (21 ± 2°C).

3.3.2 Absorption spectra and molar absorption coefficients of HOCl and OCl⁻

The absorption spectra and molar absorption coefficients of free chlorine are very important in this research. The reason is that the components of free chlorine mainly depend on pH. According to the equilibrium of reaction 3.1, for free chorine samples at pH 5 the dominant species is HOCl, whereas at pH 10, the dominant species is OCl⁻. Therefore, the amount of free chlorine decomposed by UV light at different pH values could be different due to the different free chlorine species and their different absorption spectra. The absorption spectra of HOCl and OCl⁻ are shown in Figure 3.6.
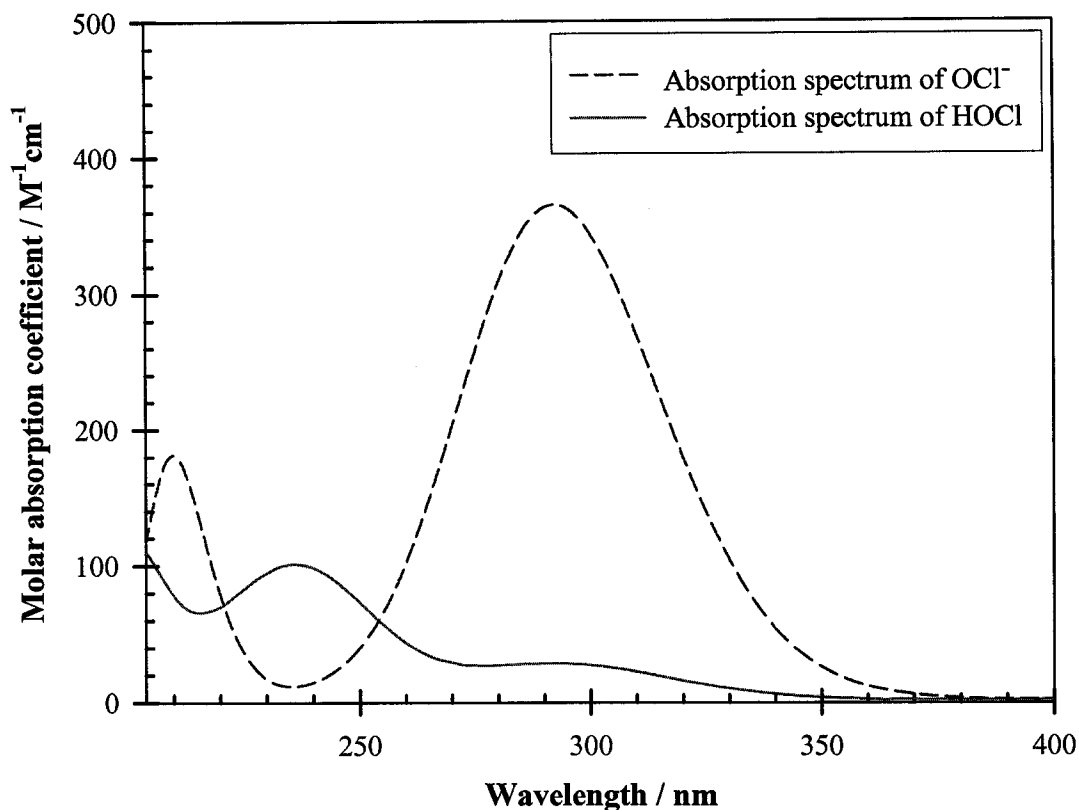
Figure 3.6 Absorbance spectra of HOCl and OCl⁻. The spectra of HOCl and OCl⁻ were measured at pH 5 and 10, respectively, at the ambient temperature (21 ± 2°C).

The absorption spectra show that there is an absorption peak at about 236 nm for HOCl; whereas for OCl⁻, the peak is at about 292 nm. Using more than 15 concentrations over the range of 3.5 to 1000 mg L^{-1}, the molar absorption coefficient obtained by regression at 235 nm for HOCl is 101 ± 2 M^{-1} cm^{-1}. In the same way, the molar absorption coefficient at 292 nm for OCl⁻ was determined to be 365 ± 8 M^{-1} cm^{-1}. The importance of these molar absorption coefficients is that when the concentration of free chlorine was more than 50 mg L^{-1} in this study, they were used for the measurement of free chlorine concentration using the method described above. In addition, the molar absorption coefficients of HOCl and OCl⁻ at 254 nm were also determined to be 59 ± 1

76

and 66 ± 1 M^{-1} cm^{-1}, respectively. These values were used for the calculation of fluence absorbed by free chlorine samples. Compared with the values listed in Table 3.2, the results obtained in this research are very consistent with data reported by Morris (1966), Chen (1967), and Thomsen et al. (2001). For the results obtained by Nowell and Hoigné (1992b), they are much higher than the data determined in this study and observed by others. This deviation might be caused by some errors present in their experimental system.

Table 3.2 Comparison of the molar absorption coefficients of HOCl and OCl⁻ obtained in this study and reported by other researchers (M^{-1} cm^{-1})

ε_{235}	ε_{292}	ε_{254}		Reference
HOCl	OCl⁻	OCl⁻	HOCl	
101 ± 2	365 ± 8	66 ± 1	59 ± 1	This study
100	350	58	62	Morris 1966
105	—	60	—	Thomsen et al. 2001
—	362	—	—	Chen 1967
—	368	155	121	Nowell and Hoigné 1992b
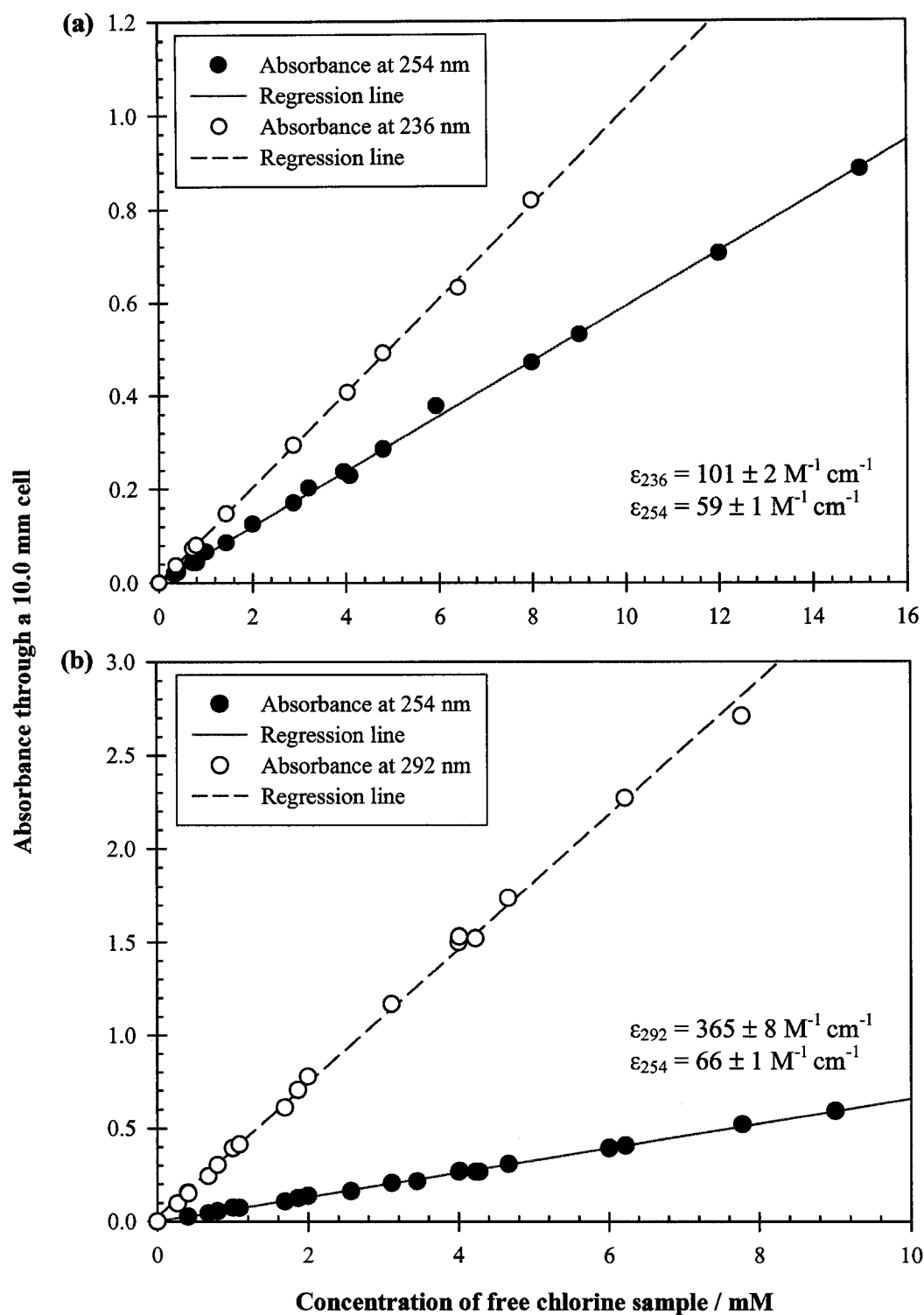
Figure 3.7 Molar absorption coefficients of HOCl and OCl⁻: (a) molar absorption coefficients of HOCl at 236 and 254 nm determined at pH 5 and ambient temperature (21 ± 2°C) and (b) molar absorption coefficients of OCl⁻ at 292 and 254 nm determined at pH 10 and ambient temperature (21 ± 2°C).

78

3.3.3 Quantum yield of free chlorine at different pH values

The quantum yields of free chlorine (HOCl and OCl⁻) at pH 5 and 10 were determined for different free chlorine samples under various concentrations. As shown in Figure 3.8, the quantum yield of HOCl is essentially constant at 1.0 ± 0.1 as long as the concentration is less than 70 mg L^{-1}; however, when the concentration varies from 71 to 1,350 mg L^{-1}, the quantum yield increases linearly with a slope of 0.0025 (mg Cl/L)$^{-1}$, such that at a concentration of 1,350 mg L^{-1}, the quantum yield has risen to 4.5 ± 0.2. In contrast, the quantum yield of OCl⁻ is virtually independent of concentration at 0.9 ± 0.1 when the concentration ranges from 3.5 to 640 mg L^{-1} (shown in Figure 3.9).

As reported by other researchers (Oliver and Carey 1977 and Buxton and Subhani, 1972a), the concentration dependence of the photolysis of HOCl can be explained by a chain reaction initiated by the reactions:

[3.11] $HOCl + h\nu \text{(UV photons)} \rightarrow \bullet OH + \bullet Cl$

[3.12] $\bullet OH + HOCl \rightarrow H_2O + \bullet OCl$
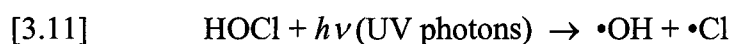
where the •Cl and/or •OCl species may participate in further reactions that deplete the HOCl[12]. For example, the •Cl atom may react with HOCl by

[3.13] $\bullet Cl + HOCl \rightarrow HCl + \bullet OCl$

Chain termination may involve the reactions

[3.14] $\bullet Cl + \bullet OCl + H_2O \rightarrow 2 \ HOCl$

[3.15] $2 \ \bullet OCl + H_2O \rightarrow HCl + HClO_2$

---
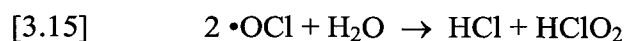
[12] No rate constant is available for reaction 3.12; however, it is likely that this reaction proceeds with a rate constant near diffusion controlled ($\sim 10^{10}$ M^{-1} s^{-1}).

The experimental results of this research indicate that the above reactions have a greater

effect on the quantum yield of HOCl at higher concentrations than at lower concentration.

At pH 10, •OH radicals can be generated by the reactions:

[3.16] $OCl^- + h\nu$ (UV photons) $\rightarrow$ $\cdot O^- + \cdot Cl$

[3.17] $\cdot O^- + H_2O \rightarrow \cdot OH + OH^-$
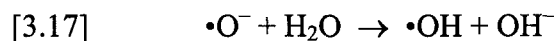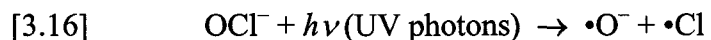
The •OH radical reacts with OCl^- by electron transfer with a rate constant of 8.8×10^9

$M^{-1} s^{-1}$ (Buxton and Subhani 1972b) to generate •OCl. However, at pH 10, it appears that

•Cl and/or •OCl species do not initiate any chain reactions, since the quantum yield is

observed to be independent of concentration at this pH.
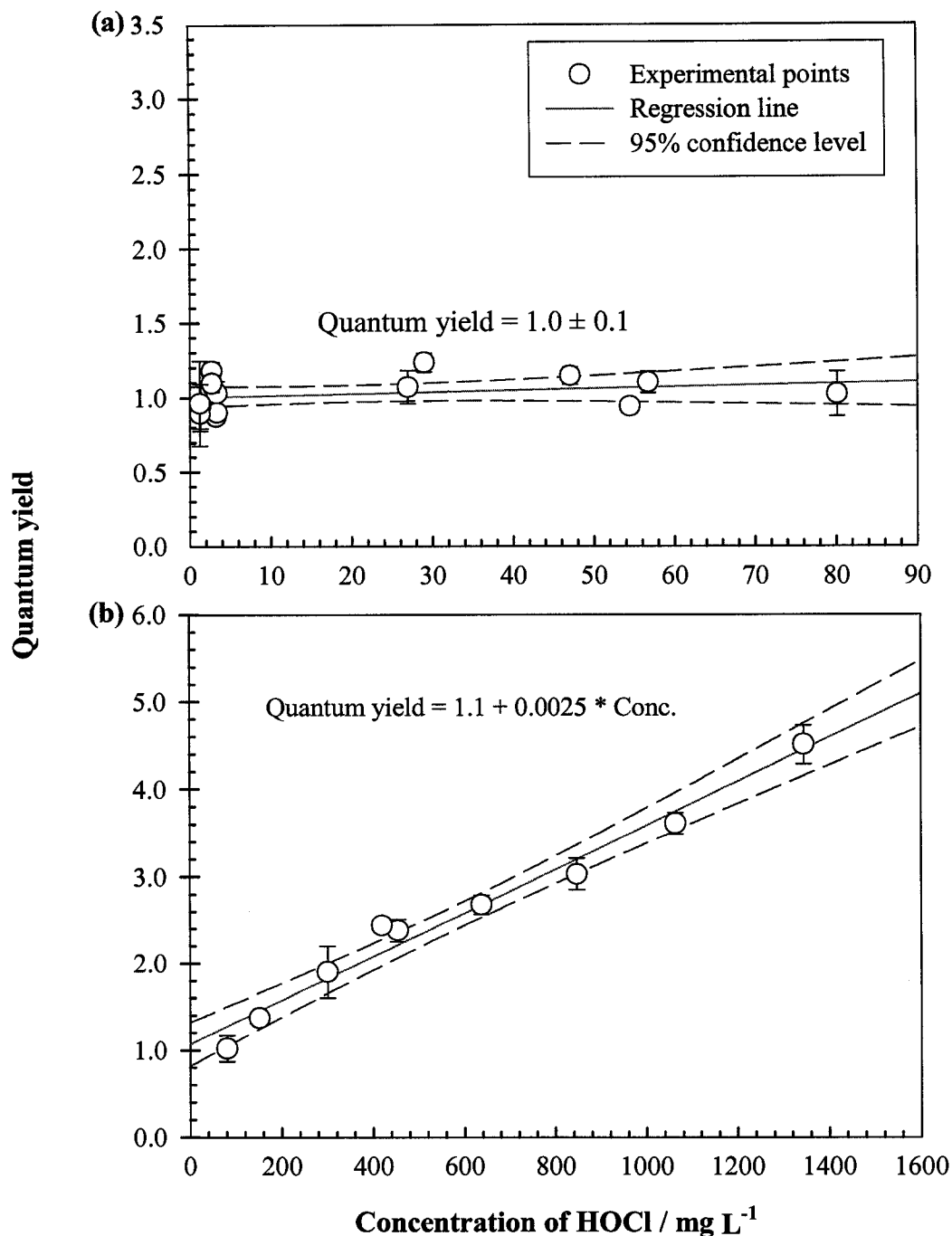
Figure 3.8 Quantum yields of free chlorine (HOCl) at pH 5 and ambient temperature (21 ± 2°C): (a) quantum yields determined when the concentration is lower than 70 mg L^{-1} and (b) quantum yields determined when the concentration is higher than 70 mg L^{-1}.

81
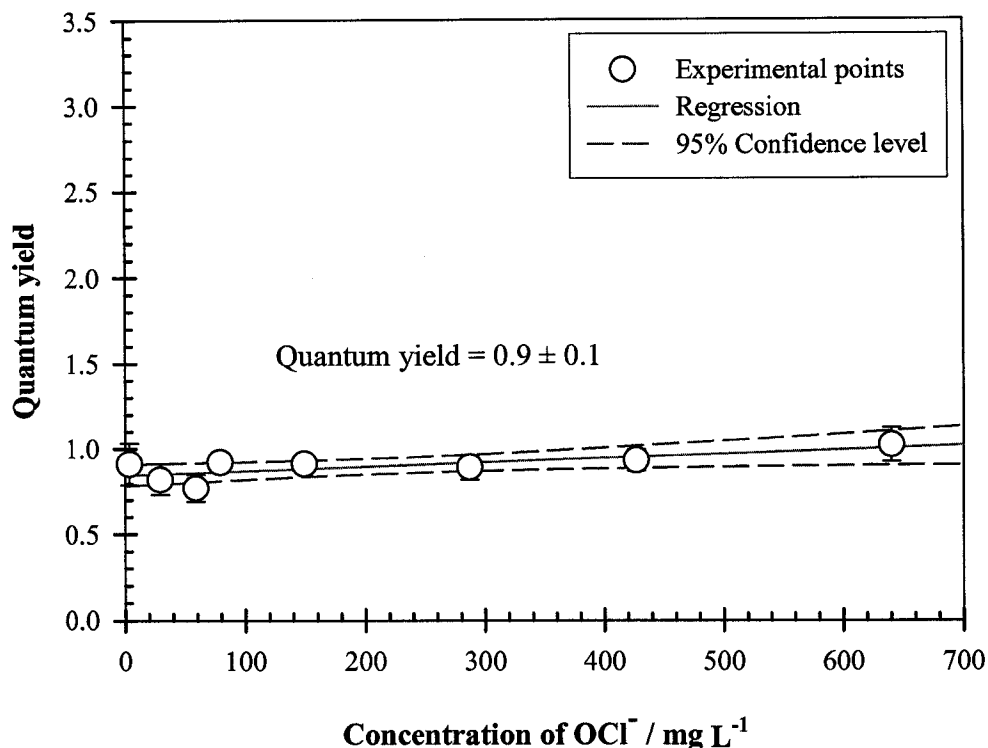
Figure 3.9 Quantum yields of free chlorine (OCI⁻) at pH 10 and ambient temperature (21 ± 2°C) when the concentration varies from 3.5 to 640 mg L⁻¹

3.3.4 A model for the quantum yield of free chlorine decomposed at 254 nm

According to the above discussion, free chlorine exists primarily as an equilibrium mixture of hypochlorous acid (HOCl) and its conjugate base (OCl⁻) with a pK_a of 7.5. In addition, based on the equilibrium of reaction 3.1, the fraction f of HOCl existing in free chlorine samples can be expressed as a function of pH as equation 3.2:

$$[3.2] \qquad f = \frac{[HOCl]}{[OCl^-]+[HOCl]} = \frac{1}{1+10^{pH-pK_a}}$$

From the absorption spectra of HOCl and OCl⁻ (Figure 3.4), the molar absorption coefficient of HOCl at 254 nm is different from that of OCl⁻. In addition, the quantum yields of HOCl and OCl⁻ and their tendency to change along with their concentrations are

82

different from each other. Assuming that the photolysis of HOCl and OCl⁻ are two independent processes and that the interactions between these two processes are negligible, the overall quantum yield of free chlorine (HOCl and OCl⁻) decomposed by UV light at 254 nm at a given pH value may be estimated by the following equation:

$$[3.18] \qquad \Phi_{overall} = \frac{f\varepsilon_{HOCl}}{f\varepsilon_{HOCl} + (1-f)\varepsilon_{OCl^-}}\Phi_{HOCl} + \frac{(1-f)\varepsilon_{OCl^-}}{f\varepsilon_{HOCl} + (1-f)\varepsilon_{OCl^-}}\Phi_{OCl^-}$$

where, ε_{HOCl} = molar absorption coefficient of HOCl at 254 nm;

ε_{OCl^-} = molar absorption coefficient of OCl⁻ at 254 nm;

f = the fraction of HOCl present in free chlorine samples;

Φ_{HOCl} = quantum yield of HOCl;

Φ_{OCl^-} = quantum yield of OCl⁻;

$\Phi_{overall}$ = overall quantum yield of aqueous chlorine at a given pH condition.

In the above equation, it needs to be emphasized that the quantum yield of HOCl is not a constant. As discussed in the above section, it is about 1.0 ± 0.1 when the concentration is less than 70 mg L⁻¹. Otherwise, it will be a function of its concentration as shown in Figure 3.8(b). Therefore, when Eq. 3.18 is used to estimate the quantum yield of free chlorine decomposed, the quantum yield of HOCl corresponding to its concentration should be employed. In addition, the parameters (molar absorption coefficient, quantum yield, etc.) were determined at 254 nm, so this model should only be used for the condition of low pressure UV lamps.

As discussed in the above section, the model (Eq. 3.18) was developed based on the assumption of no interactions between the photolysis processes of HOCl and OCl⁻. Because only a unique component, HOCl or OCl⁻, was present in free chlorine samples at

83

pH 5 or 10, the assumption of the model was met under these critical conditions and obviously, the model worked very well for the quantum yield prediction. However, at intermediate pH values (between pH 5 to 10), free chlorine sample always consists of both HOCl and OCl⁻. Therefore, several experiments were performed in order to examine if the model can be applied at different pH values. Figure 3.10 shows that the quantum yields calculated by the model at various pH values are consistent with those measured by the experiments. Hence, this model should be appropriate to estimate the overall photolysis quantum yield of free chlorine under various pH conditions. In addition, this figure also indicates that the assumptions of the model are essentially correct.

84
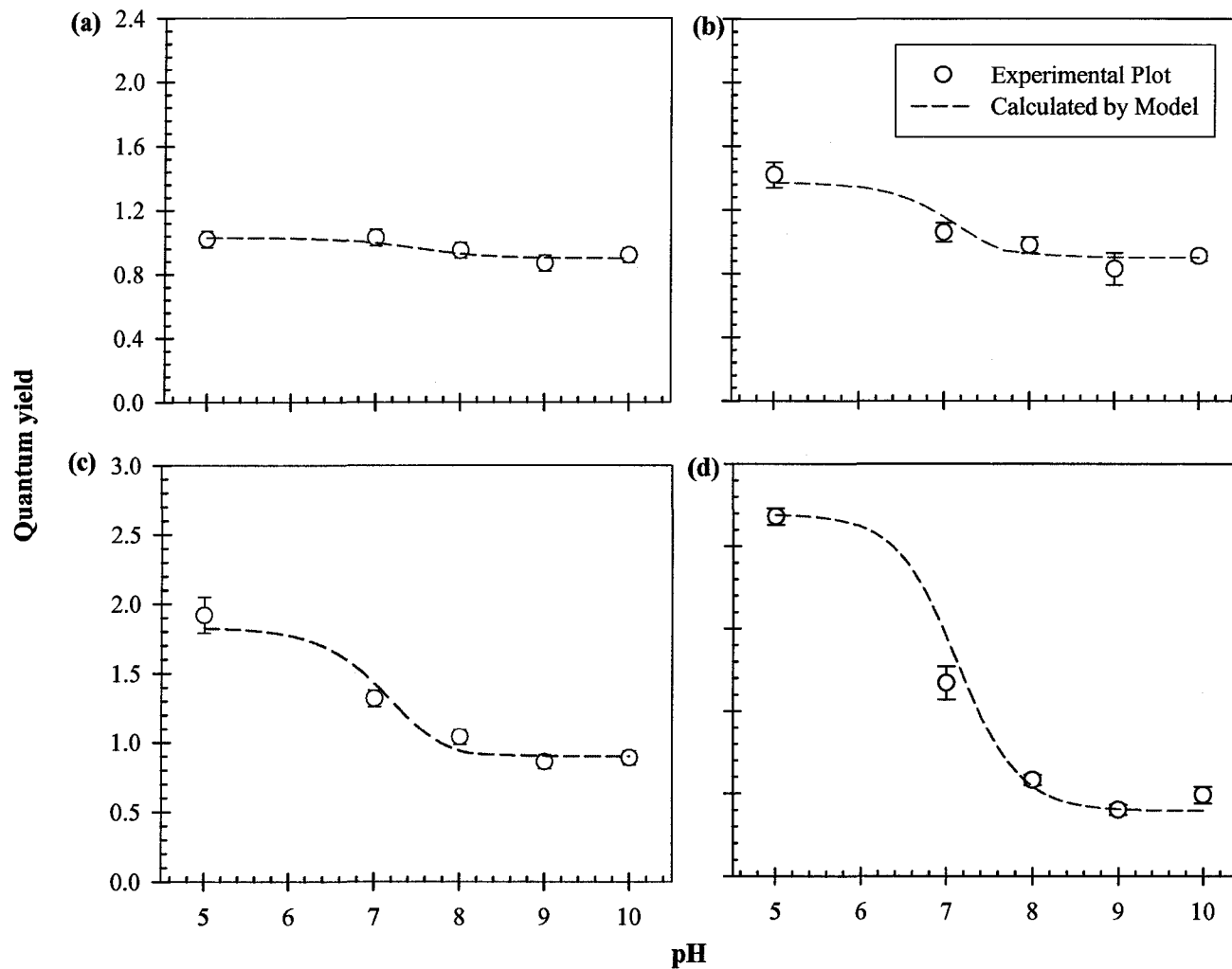
Figure 3.4 Comparison of the quantum yields of free chlorine measured by experimental method and calculated by the model at various pH and free chlorine concentrations: (a) 1.0 mM, (b) 2.0 mM, (c) 4.0 mM and (d) 9.0 mM (temperature 21 ± 2°C)

3.3.5 Effect of contaminants on the quantum yield

It should be stressed that the quantum yields discussed in the above paragraphs were determined in DI water. Actually, the drinking water quality varies greatly from place to place and because the strong oxidative radicals (e.g., •OH and •Cl) are produced in the photolysis of free chlorine, the materials dissolved in drinking water may have an important effect on the quantum yield. In this study, some organic compounds, such as methanol, 1,4-dioxane and *tert*-butanol, were added into the DI water to essentially investigate the effects of organic materials on the quantum yield of free chlorine.

Figure 3.11 shows the dependence of quantum yield of free chlorine on the concentration of methanol at pH 5. From this figure, the quantum yield gradually increases from about 2 up to approximately 50 when the concentration of methanol changes from 0 to 120 mM. There is an apparent linear correlation present between the concentration of methanol and the quantum yield of free chlorine. The photoproducts of free chlorine samples with methanol were qualitatively analyzed by the Nash method (Nash 1953) and formaldehyde (HCHO) was detected. Therefore, it can be inferred that the •CH$_2$OH radical is produced by the attack of hydroxyl radical (•OH), generated from the photodecomposition of HOCl, on the methanol. Then, the •CH$_2$OH radical initiates a chain reaction involving HOCl to cause the increase of the quantum yield at pH 5. This process may be expressed as the following reactions

[3.11] $\quad$ HOCl + hv (UV photons) → •OH + •Cl

[3.19] $\quad$ •OH + CH$_3$OH → •CH$_2$OH + H$_2$O

[3.20] $\quad$ •CH$_2$OH + HOCl → ClCH$_2$OH + •OH

[3.21] $\quad$ •CH$_2$OH + O$_2$ → •O$_2$CH$_2$OH → HCHO + HO$_2$
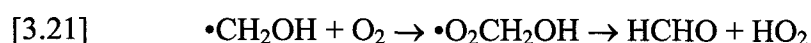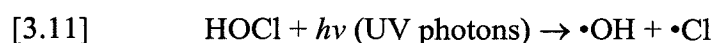
By contrast, the quantum yield of free chlorine (OCl⁻) obtained at pH 10 always is 1.2 ±

0.2, even when the methanol concentration is 20 mM and 50 mM, respectively.

Compared with the quantum yield (0.9 ± 0.1) obtained in DI water at pH 10, these results

indicate that methanol has little impact on the photodecomposition of OCl⁻.
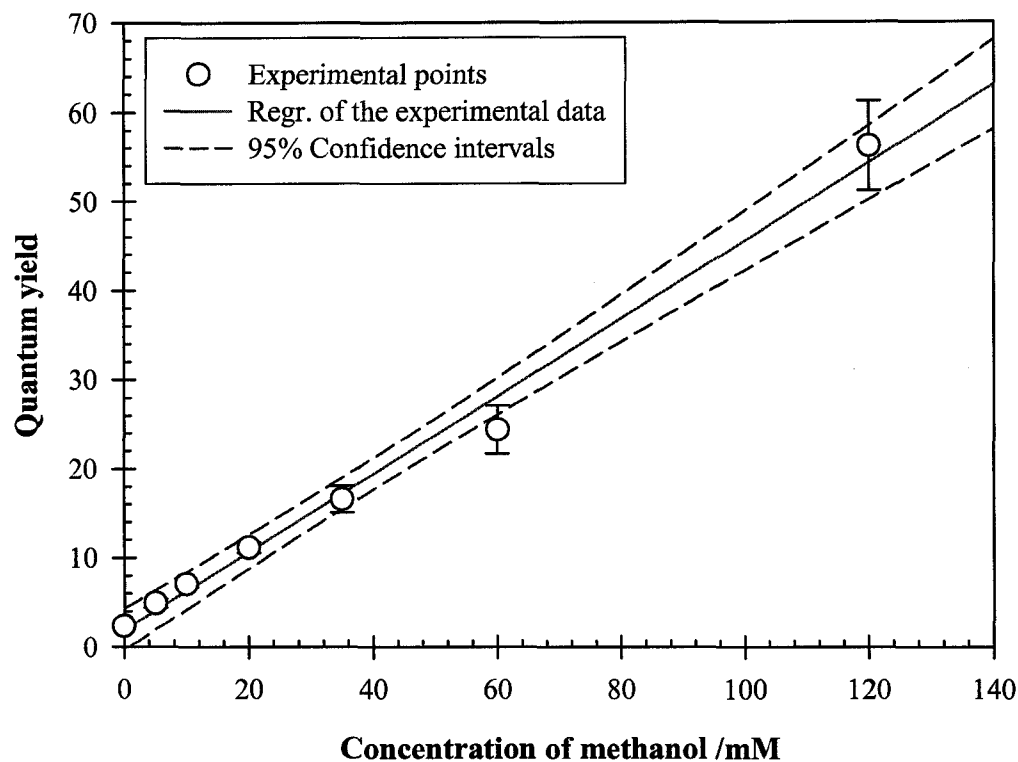
Figure 3.11 Dependence of quantum yield of free chlorine (6.0 mM) decomposed on the concentration of methanol at pH 5 and ambient temperature (21 ± 2°C)

The effects of three different organic compounds, *tert*-butanol, methanol and 1,4-

dioxane on the quantum yield of free chlorine (HOCl) decomposed at pH 5 were

examined. As shown in Figure 3.12, different organic compounds have different effects

on the quantum yield and the relative sensitivity of the quantum yield to these organic

chemicals is gradually increased from *tert*-butanol to 1,4-dioxane. For example, the

87

quantum yield of free chlorine decomposed at pH 5 is 2.4 ± 0.2 for the 6 mM free

chlorine sample without any organics in, but it increases to 4.1 ± 0.5 for the same sample

with 10 mM tert-butanol, and 7.0 ± 0.3 for 10 mM methanol and 11.2 ± 0.5 for 10 mM

1,4-dioxane. In the real operation of utilities, it is inevitable that some natural or artificial

organic compounds are dissolved in the raw water and the organics may be different from

one utility to another. From this study, it can be concluded that for the free chlorine

samples with same concentration prepared by the water obtained from different utilities,

the quantum yield of free chlorine decomposed could be different and more chlorine

could be decomposed at lower pH values.
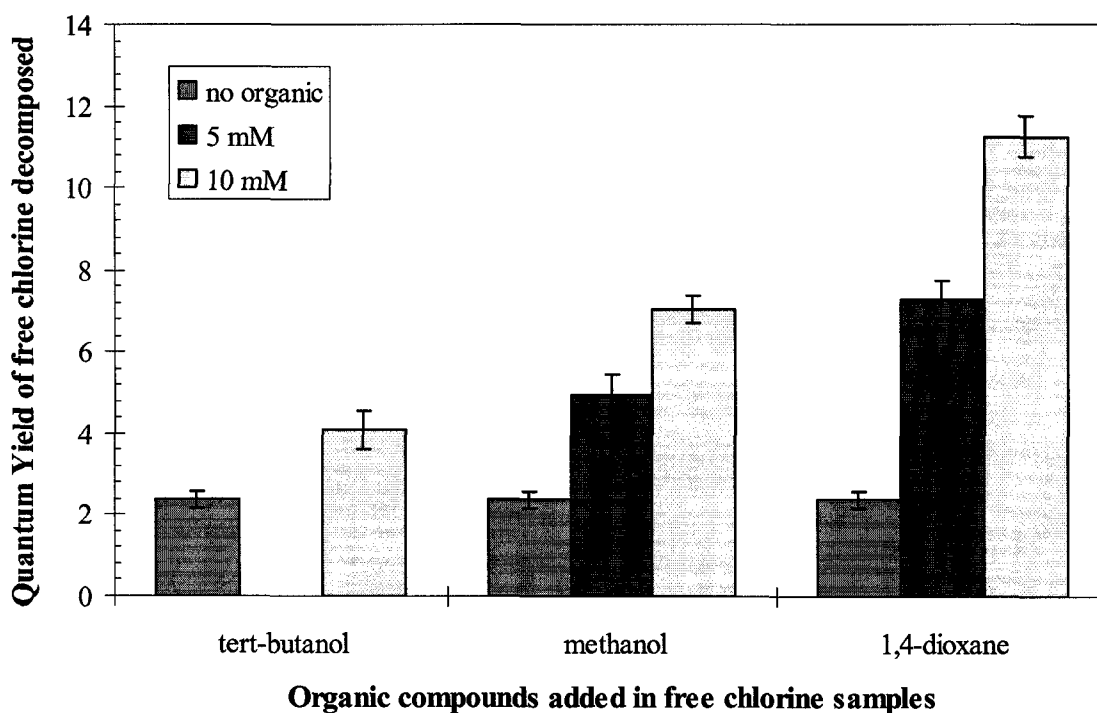
Figure 3.12 Comparison of the effects of three different organics on the quantum yield of free chlorine (6.0 mM) decomposed at pH 5 and ambient temperature (21 ± 2°C)

88

3.3.6 Dependence of the chlorine species decomposition on the fluence

When the concentration of free chlorine is not very high (less than 70 mg L^{-1}), the quantum yield of free chlorine decomposed can be assumed to be independent of its concentration. Therefore, the photodecomposition rate of free chlorine can be expressed by a first order kinetics expression

$$[3.22] \qquad \ln\frac{[C]_o}{[C]_t} = kt$$

where, $[C]_o$ and $[C]_t$ are the free chlorine concentration before and after exposure to UV light for a time of t min; k is the first-order constant in units of min^{-1}. Because the time-based first-order rate constant (k) can be affected by the experimental conditions (e.g., irradiance, absorbance, path length, etc.) and hence is difficult to be reproduced, Eq. 3.22 usually is modified to

$$[3.23] \qquad \ln\frac{[C]_o}{[C]_{H'}} = k'H'$$

where, $[C]_o$ and $[C]_{H'}$ are the chlorine species concentration before and after exposure to a UV fluence of H'; k' is the fluence-based first-order rate constant (Bolton and Stefan, 2003). Here k' only depends on the quantum yield and molar absorption coefficient of UV light absorbers (see Eq. 3.24). So, theoretically k' is a constant for a given UV light absorber and can be easily reproduced.

$$[3.24] \qquad k' = \frac{\Phi\varepsilon\ln(10)}{10U_\lambda}$$

where ε is the molar absorption coefficient ($M^{-1} cm^{-1}$) of UV light absorber and other terms are defined as above. According to Eq. 3.23, one can plot the logarithm (base e) of

89

the free chlorine reduction vs. fluence absorbed to obtain the fluence-based first-order

constant k'. Then, the quantum yield can be calculated from Eq. 3.24.
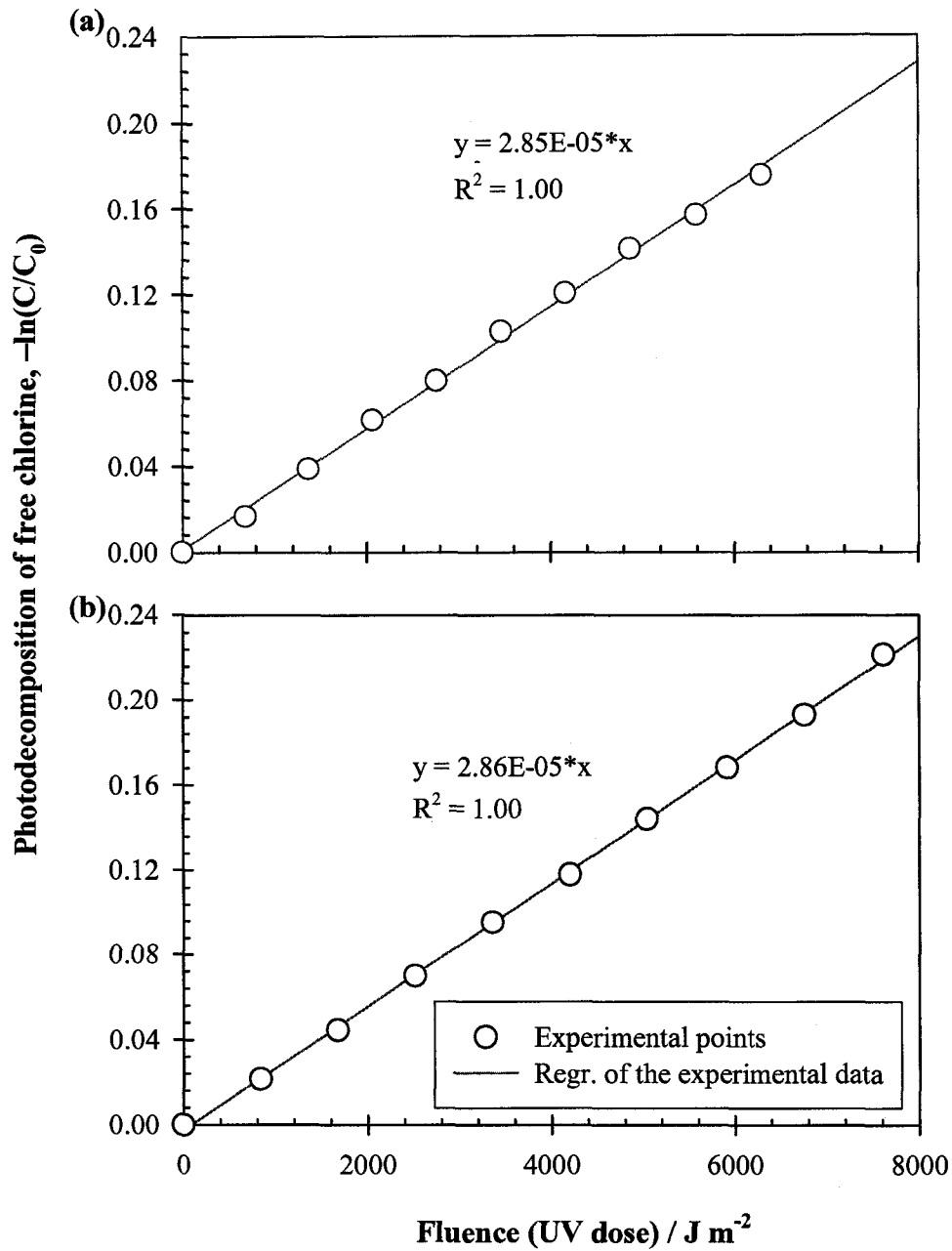
Figure 3.13 Log (naperian) reduction of free chlorine as a function of UV fluence (UV dose) in the ambient condition (21 ± 2°C): (a) 1.0 mM free chlorine samples at pH 5 and (b) 1.0 mM free chlorine samples at pH 10.

90

As an example, Figures 3.13 (a) and (b) show that the logarithmic (base e) reduction of free chlorine increases linearly with fluence and the fluence-based first-order rate constant k' is $(2.86 \pm 0.10) \times 10^5 \ m^2 \ J^{-1}$ in both cases, when the concentration of free chlorine is about 20 mg L^{-1}. Based on the fluence-based rate constant, the quantum yields estimated according to Eq. 3.24 were about 1.0. This result is very close to the value obtained by the method given in above. Figures 3.13 also indicates that only a slight amount (~1%) of free chlorine was decomposed when the concentration of free chlorine was about 20 mg L^{-1}, and the UV fluence was 400 J m^{-2}, a fluence that was often specified in UV disinfection regulations. Because DI water was used in this study, it was possible that a larger fraction of free chlorine could be destroyed in drinking water as discussed in above. Generally, the destruction of free chlorine depends not only on the fluence, but also on the concentration of free chlorine, water quality and the pH. Table 3.3 shows the variation of the free chlorine photodecomposition for various conditions.

Table 3.3 Photodecomposition of free chlorine at the fluence of 400 J m^{-2}

pH	Free chlorine concentration / mg L^{-1}	Organics in water matrix[13]	Percent of free chlorine reduced
5	71	DI water	1.1%
10	71	DI water	1.1%
5	213	DI water	2.8%
10	213	DI water	1.2%
10	213	50 mM methanol	1.3%
5	213	35 mM methanol	18%
5	213	8.4 mM 1,4-dioxane	11%

[13] The TOC concentration in DI water used here is in the range of 0 to 0.4 ppm.

91

3.4 Conclusions

The molar absorption coefficients of HOCl and OCl$^-$ at 254 nm obtained in this research were 59 ± 1 and 66 ± 1 M^{-1} cm^{-1}, respectively. These results are about half of those reported by Nowell and Hoigné (1992a), but are very consistent with other reported data (Morris, 1996; Chen, 1967; and, Thomsen et al., 2001).

In DI water, the pH and the concentration of free chlorine are important influencing factors for the photolysis of free chlorine. At low concentrations (lower than 70 mg L^{-1}), the quantum yields of HOCl and OCl$^-$ are approximately constant at 1.0 ± 0.1 and 0.9 ± 0.1, respectively, as obtained in this research. However, at higher concentrations (more than 71 mg L^{-1}) the quantum yield of free chlorine (HOCl) at pH 5 linearly increases with the concentration at a rate of 0.0025 (mg Cl/L)$^{-1}$. Compared with HOCl, it was found that the concentration has an insignificant effect on the quantum yield of OCl$^-$ over the investigated concentration range of 3.5 to 640 mg L^{-1} in this study. According to the experimental results, a mathematical model (Eq. 3.18) was established to allow an estimate of overall quantum yield of free chlorine photodecomposed by UV irradiation at 254 nm in DI water. Compared with the experimental results measured at various pH values and free chlorine concentrations, the quantum yields calculated by this model agree quite well with the measured quantum yields.

Three organic chemicals, *tert*-butanol, methanol and 1,4-dioxane, were used to study the effects of water quality on the quantum yields of free chlorine decomposed in various operating conditions. It was observed that the presence of organics in free chlorine sample can be a significant influencing factor on the quantum yield of HOCl, but not on the quantum yield of OCl$^-$. The addition of methanol at pH 5 can cause a

92

significant increase in the quantum yield of HOCl; whereas, at pH 10, the effect of methanol addition was minimal. The decomposition of free chlorine significantly depends on the pH, concentration of free chlorine, fluence and water quality. At fluence of 400 J m^{-2}, the free chlorine is decomposed slightly (~1%) in DI water when the concentration of free chlorine is not very high (~20 mg L^{-1}), but it could be distinctly consumed in the presence of some organics. For different organics, their effects on the quantum yield or decomposition of free chlorine were observed to be different. In practical operations, there always are some organic compounds in drinking waters, therefore, it can be concluded that the quantum yield of free chlorine in water from different sources can be different, due to the effect of water quality. In addition, the decomposition of free chlorine also depends on the pH and more chlorine could be degraded at lower pH values.

3.5 References

APHA, AWWA and WEF 1995a. Standard Methods for the Examination of Water and Wastewater (19th edition): 4500-Cl C. Iodometric method II. American Public Health Association, 1015 Fifteenth Street, NW, Washington, DC 20005.

APHA, AWWA and WEF 1995b. Standard Methods for the Examination of Water and Wastewater (19th edition): 4500-Cl G. DPD colorimetric method. American Public Health Association, 1015 Fifteenth Street, NW, Washington, DC 20005.

Bolton, J.R. and Linden, K.G. 2003. Standardization of methods for fluence (UV Dose) determination in bench-scale UV experiments. *J. Environ. Engng.*, **129(3)**: 209–216.

Bolton, J.R. and Stefan, M.I. 2002. Fundamental photochemical approach to the concepts of fluence (UV dose) and electrical energy efficiency in photochemical degradation reactions. *Res. Chem. Intermed.*, **28(7–9)**: 857–870.

Buxton, G.V. and Subhani, M.S. 1972a. Radiation chemistry and photochemistry of oxychlorine ions: II. Photodecomposition of aqueous solutions of hypochlorite ions. *J. Chem. Soc.: Faraday Trans. I*, **68(4)**: 958–969.

Buxton, G.V. and Subhani, M.S. 1972b. Radiation chemistry and photochemistry of oxychlorine ions: I. Radiolysis of aqueous solutions of hypochlorite and chlorite ions. *J. Chem. Soc.: Faraday Trans. I*, **68(4)**: 947–957.

Chen, T.H. 1967. Spectrophotometric determination of microquantities of chlorate, chlorite, hypochlorite and chloride in perchlorate. *Anal. Chem.*, **39(7)**: 804–813.

Morris, J.C. 1966. The acid ionization constant of HOCl from 5 to 35°. *J. Phys. Chem.*, **70(12)**: 3798–3805.

Nash, T. 1953. The colorimetric estimation of formaldehyde by means of the Hantzsch reaction. *Biochem. J.*, **55(3)**: 416–421.

Nowell, L.H. and Hoigné, J. 1992a. Photolysis of aqueous chlorine at sunlight and ultraviolet wavelengths: II. Hydroxyl radical production. *Wat. Res.*, **26(5)**: 593–598.

Nowell, L.H. and Hoigné, J. 1992b. Photolysis of aqueous chlorine at sunlight and ultraviolet wavelengths: I. Degradation rates. *Wat. Res.*, **26(5)**: 593–598.

Oliver, B.G. and Carey, J.H. 1977. Photochemical production of chlorinated organics in aqueous solutions containing chlorine. *Environ. Sci. Technol.*, **11(9)**: 893–895.

Thomsen, C.L., Madsen, D., Poulsen, J.A., Thogersen, J., Jensen, S.J.K. and Keiding, S.R. 2001. Femtosecond photolysis of aqueous HOCl. *J. Chem. Phys.*, **115(20)**: 9361–9369.

Appendix 3.1 An example for the quantum yield calculation

A 1.1 mM free chlorine sample at pH 10 will be taken as an example for the quantum yield calculation. The calculation is mainly according to the principles introduced in Section 3.2.6. Two aliquots of aqueous chlorine sample were used in the experiment: one was exposed to the UV irradiation, and the other one was put in dark as a control sample. Before the sample was exposed to UV light, the following parameters were determined:

Weight of the beaker (including stir bar) for UV exposed sample, W_{UV} = 48.26 g

Internal diameter of the beaker = 45.0 mm

Weight of the beaker (including stir bar) for control sample, W_{Ctr} = 29.35 g

Density of free chlorine sample = 987.85 g/L

Petri factor = 0.968

Reflection factor = 0.975

Energy per einstein of UV photons at 254 nm = 471527.63 J einstein^{-1}

Molar absorption coefficient of the sample at 292 nm = 365 M^{-1}cm^{-1}

Molar absorption coefficient of the sample at 254 nm = 66 M^{-1} cm^{-1}

According to the procedure described in Section 3.2.4, the absorbance and weight of these samples were measured every 10 min. The irradiance on the surface of sample was 0.183 mW cm^{-2}. The experimental results are shown in Table 3.4.

95

Table 3.4 Experimental results obtained in the determination of quantum yield of 1.1 mM free chlorine sample decomposed at pH 10

Run	Exposure time / min	Absorbance @ 292 nm		Total weight of the UV sample / g		Total weight of the CONTROL sample / g	
		Sample$_{UV}$	Sample$_{Ctr}$	Before	After	Before	After
0	0	1.9700	1.9700	78.51	78.51	75.97	75.97
1	10	1.9240	1.9673	78.51	78.45	75.97	75.93
2	10	1.8748	1.9638	78.36	78.32	73.79	73.75
3	10	1.8288	1.9668	77.90	77.85	71.57	71.53
4	10	1.7868	1.9725	77.76	77.70	69.27	69.23
5	10	1.7447	1.9727	77.59	77.54	66.19	66.14
6	10	1.7017	1.9770	77.44	77.39	63.83	63.78
7	10	1.6583	1.9760	77.31	77.25	61.35	61.31
8	10	1.6195	1.9797	77.17	77.11	58.27	58.23
9	10	1.5820	1.9897	76.99	76.94	55.54	55.49

In the above table:

1. The light path length of the absorbance at 292 nm was 50.0 mm;
2. Sample$_{UV}$ is the sample exposed to UV light;
3. Sample$_{Ctr}$ is the sample used as control sample;
4. Total weight of UV/CONTROL sample is the weight of free chlorine sample, the corresponding beaker and a stir bar;
5. "Before" and "After" mean the data obtained before and after the exposure time.

For the first 10-min exposure, the amount of free chlorine decomposed can be calculated in the following way:

1. The concentration of free chlorine sample before exposure:

$$C_{UV} = C_{Ctr} = 1000*1.9700/(365.03 \text{ M}^{-1} \text{ cm}^{-1}*5 \text{ cm}) = 1.079 \text{ mM}$$

2. The concentration of free chlorine samples after exposure:

$$C_{UV} = 1000*1.9240/(365.03 \text{ M}^{-1} \text{ cm}^{-1}*5 \text{ cm}) = 1.054 \text{ mM}$$

$$C_{Ctr} = 1000*1.9673/(365.03 \text{ M}^{-1} \text{ cm}^{-1}*5 \text{ cm}) = 1.078 \text{ mM}$$

96

3. The average volume of the free chlorine samples during the exposure time:

$$V_{UV} = (78.51 + 78.45 - 2*48.26) \text{ g}/(2*987.85 \text{ g L}^{-1}) = 30.6 \text{ mL}$$

$$V_{Ctr} = (75.97 + 75.93 - 2*29.35) \text{ g}/(2*987.85 \text{ g L}^{-1}) = 47.2 \text{ mL}$$

4. Moles of free chlorine in these samples before exposure:

$$M_{UV} = 1.079 \text{ mM}*(78.51 - 48.26) \text{ g}/987.85 \text{ g L}^{-1} = 3.305 \times 10^{-5}$$

$$M_{Ctr} = 1.079 \text{ mM}*(75.97 - 29.35) \text{ g}/987.85 \text{ g L}^{-1} = 5.094 \times 10^{-5}$$

5. Moles of free chlorine in these samples after exposure:

$$M_{UV} = 1.054 \text{ mM}*(78.45 - 48.26) \text{ g}/987.85 \text{ g L}^{-1} = 3.222*10^{-5}$$

$$M_{Ctr} = 1.078 \text{ mM}*(75.93 - 29.35) \text{ g}/987.85 \text{ g L}^{-1} = 5.083*10^{-5}$$

6. Moles of free chlorine decomposed because of irradiation:

$$M_{de} = (3.305 \times 10^{-5} - 3.222 \times 10^{-5}) - (5.094 \times 10^{-5} - 5.083 \times 10^{-5})*(30.6 \text{ mL}/47.2 \text{ mL})$$

$$= 7.629 \times 10^{-7}$$

Within the first 10-min irradiation, the amount of UV photons absorbed by free chlorine can be obtained as follows:

1. Absorption coefficient of irradiated sample at 254 nm:

Before exposure: $1.9700*(65.66 \text{ M}^{-1} \text{ cm}^{-1}/365.03 \text{ M}^{-1} \text{ cm}^{-1})/5 \text{ cm} = 0.071 \text{ cm}^{-1}$

After exposure: $1.9240*(65.66 \text{ M}^{-1} \text{ cm}^{-1}/365.03 \text{ M}^{-1} \text{ cm}^{-1})/5 \text{ cm} = 0.069 \text{ cm}^{-1}$

2. Area of cross section of UV beaker:

$$S = 3.14*(4.50/2)^2 = 15.90 \text{ cm}^2$$

3. Light path length of the irradiated sample:

$$L = 1000*[(78.45 - 48.26) \text{ g}/987.85 \text{ g L}^{-1}]/15.90 \text{ cm}^2 = 1.92 \text{ cm}$$

4. The fraction of UV light absorbed by free chlorine:

$$f = 1 - 10^{-1.92*(0.071+0.069)/2} = 0.266$$

5. Einsteins of UV photons absorbed:

0.183 mW/cm^2 *15.90 cm^2 *600 s*0.975*0.968*0.266/(1000*471527.63 J einstein^{-1})

$= 9.376 \times 10^{-7}$ einsteins of UV photons

Therefore, the quantum yield of aqueous chlorine decomposed with 254 nm UV light can

be calculated from:

$\Phi = 7.629 \times 10^{-7} / 9.376 \times 10^{-7} = 0.81$

In the same way, the quantum yields of 9 runs were calculated and the results

were listed in Table 3.5.

Table 3.5 Calculation results for the quantum yield of 1.1 mM free chlorine decomposed at pH 10

Run #	Moles of free chlorine decomposed	Regression fit[14]	Einsteins of UV photons absorbed	Quantum yield
0	0.00E+00	−1.03E–07	0.00E+00	
1	7.63E–07	7.61E–07	9.38E–07	**0.81**
2	1.54E–06	1.60E–06	1.85E–06	**0.83**
3	2.38E–06	2.42E–06	2.74E–06	**0.87**
4	3.21E–06	3.21E–06	3.60E–06	**0.89**
5	3.93E–06	3.99E–06	4.44E–06	**0.89**
6	4.73E–06	4.74E–06	5.25E–06	**0.90**
7	5.46E–06	5.48E–06	6.05E–06	**0.90**
8	6.19E–06	6.19E–06	6.83E–06	**0.91**
9	6.98E–06	6.89E–06	7.58E–06	**0.92**

A "regression" analysis (the "data analysis" tools of Microsoft Excel™) was conducted

using the data of "moles of chlorine decomposed" and "einsteins of UV photons

absorbed" in Table 3.5, and the summary of statistic analysis was given in Table 3.6.

---

[14] The data of regression fit were calculated according to the result of regression analysis:
Regression fit = Intercept + Einsteins of photons absorbed * X variable

98

Table 3.6 Summary output of the regression analysis

Regression Statistics	
Multiple R	0.999727
R Square	0.999454
Adjusted R Square	0.999386
Standard Error	6.01E–08
Observations	10

ANOVA

	df	SS	MS	F	Significance F
Regression	1	5.29E–11	5.29E–11	14647.25	2.43E–14
Residual	8	2.89E–14	3.61E–15		
Total	9	5.29E–11			

	Coefficients	Std. Error	t Stat	P-value	Lower 95%	Upper 95%
Intercept	–1E–07	3.62E–08	–2.86028	0.0211421	–1.9E–07	–2E–08
X Variable	0.930334	0.007687	121.0258	2.429E–14	0.912608	0.948061

99
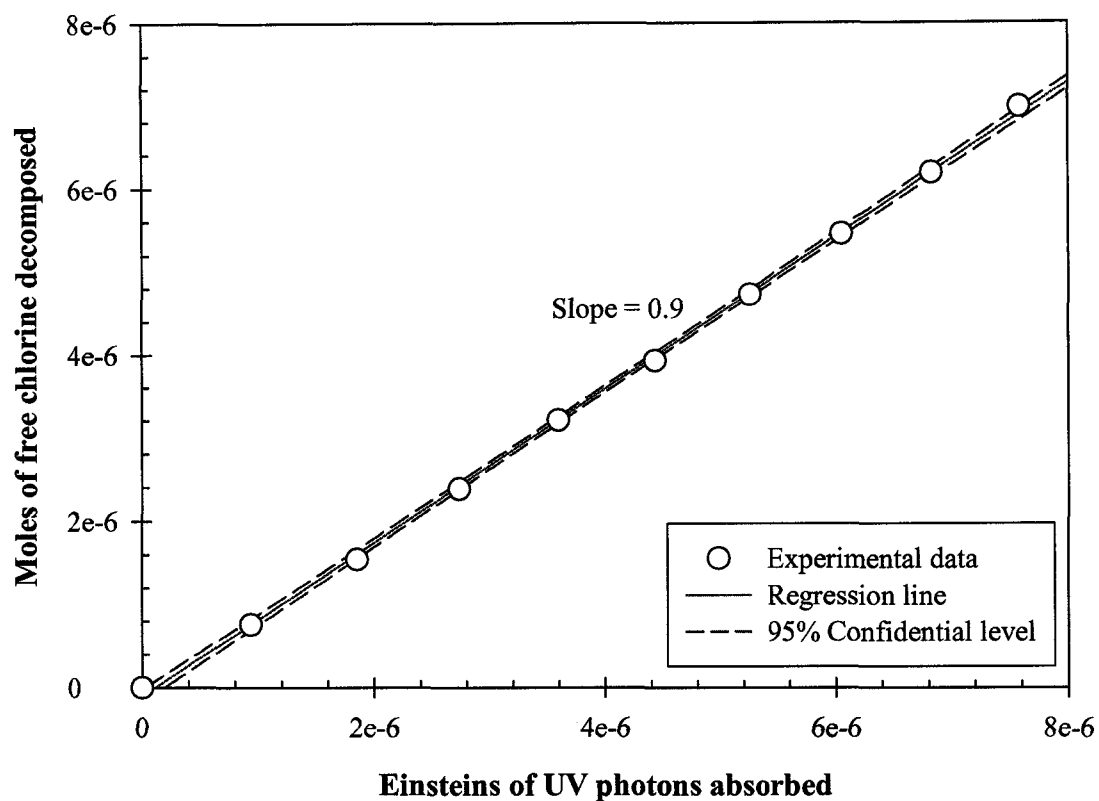
Figure 3.14 Experimental data and regression line for the determination of 1.1 mM free chlorine decomposed at pH 10 (21 ± 2°C)

Therefore, according to the above calculation and statistic analysis, the quantum

yield of 1.1 mM free chlorine at pH 10 is about 0.9.

CHAPTER 4 PHOTODECOMPOSITION OF AQUEOUS FREE

CHLORINE: INFLUENCING FACTORS AND END PRODUCTS

4.1 Introduction

As described in previous chapters, the general purpose of this research project is to develop a method using free chlorine for monitoring of the fluence delivery in UV reactors. A key step in this research is to determine the quantum yield of decomposition of free chlorine in various testing waters. The quantum yield of decomposition of free chlorine in DI water was studied in detail in the previous chapter, and, in particular, it was found that the quantum yield is affected by the presence of some organic compounds. Hence, an important purpose of this chapter is to investigate the quantum yield of decomposition of free chlorine in natural waters[15] and some other potentially significant influencing factors, such as the temperature and wavelength of UV light. There have been few studies about the effect of temperature on the quantum yield of decomposition of free chlorine (or the photodecomposition of free chlorine) in natural waters. Theoretically, the variation of temperature in a normal range should not cause a significant influence on the photochemical reactions. This means that the quantum yield of decomposition of free chlorine should be independent of the operating temperatures. For example, in a study relating to the water dechlorination by UV irradiation, Giles and Danell (1983) found that for water temperatures ranging from 7.5 to 20.6°C, there was no significant effect on the dechlorination efficiency. However, some chain-reactions may occur in the free chlorine

---

[15] The 'natural waters' used in this study was artificially prepared based on a recipe to simulate natural waters with general qualities, but were not 'true' natural waters.

system when some organic compounds are present. As discussed in the previous chapter, these chain-reactions are not photochemical reactions, and the equilibrium and rate of these reactions could be affected by temperature. Hence, it was necessary to carry out a study to analyze the dependence of quantum yield of free chlorine on temperature.

Due to the energy of UV photons and UV absorbance of free chlorine, the wavelength of UV light could also be an influencing factor on the quantum yield of free chlorine. Buxton and Subhani (1972) observed that the quantum yields for the disappearance of OCl^- at 365, 313 and 253.7 nm were 0.60 ± 0.02, 0.39 ± 0.01 and 0.85 ± 0.02, respectively. This obviously indicates that the quantum yield of free chlorine decomposed may be dependent on the wavelength of UV light. In this chapter, the dependence of quantum yield on the wavelength of UV light ranging from 200 to 300 nm, the most effective germicidal irradiation used in water disinfection, was investigated.

Another important objective of this chapter was to explore the degradation products in the photolysis of free chlorine. There are many studies associated with the disinfection by-products (DBPs) generated due to the interaction of UV irradiation and chlorination. For example, Zheng et al. (1999a and 1999b), Kashinkunti et al. (2004), Mackey et al. (2000) and Liu et al. (2006) investigated the effect of UV irradiation on the formation of chlorinated DBPs and did not observe significant changes on the formation of THMs, HAA9, carboxylic acids, aldehydes, and TOX at relatively low fluences. In these studies, some organic contaminants were usually involved with the formation of DBPs. In spite of that, more studies have focused on the products directly resulting from free chlorine in the photolysis process. Nowell and Hoigné (1992a and 1992b) determined the degradation rates and hydroxyl radical production for aqueous chlorine

102

photolyzed by sunlight and 254 nm UV light. Örmeci et al. (2005) investigated the degradation of free or combined chlorine by UV irradiation and the effect of residual chlorine on the delivery of UV dose in drinking water disinfection. Feng et al. (2006) determined the quantum yield for the photolysis of free chlorine under different conditions. However, they did not investigate the end-products of aqueous free chlorine in the photolysis reactions. Buxton and Subhani (1982) made a detailed analysis on the decomposition mechanism of the photolysis of hypochlorite ions (OCl⁻) at different wavelengths, but they did not investigate the photodecomposition of aqueous HOCl and the effects of organic compounds on the photolysis of free chlorine.

Therefore, this chapter primarily focuses on the influencing factors and end products of the photodecomposition of free chlorine. Specifically, the following investigations were undertaken:

1. An examination of the effect of some natural organic compounds (humic acid and alginic acid) on the quantum yield of the photolysis of free chlorine;

2. An examination of the effects of the TOC concentration and temperature as influencing factors. In this, a two-level factorial design experiment was carried out to analyze the effect of temperature on the quantum yield of the free chlorine decomposed;

3. The quantum yields of free chlorine exposed to various UV wavelengths (200 to 300 nm) was carried out;

4. The end products of free chlorine decomposed by UV irradiation at 254 nm were determined;

103

5. The effects of some operating conditions (e.g., pH and TOC concentration) on the formation of photodecomposition products of free chlorine were investigated; and

6. The mechanism of the photolysis of free chlorine with 254 nm UV light was explored.

4.2 Materials and methods

4.2.1 Regents and apparatus

Potassium chromate (Fisher, certified ACS), silver nitrate (Fisher, certified ACS), sodium chloride (BDH, analytical reagent), and sodium hydroxide solutions (Fisher, certified, 1N) were all used as received for the measurement of chloride ions by the argentometric method (APHA et al. 1995a). Potassium permanganate (BDH, analytical reagent) and DPD Free Chlorine Reagent for 25 mL samples (Hach® Lange GmbH, Anachemia Science Inc., Canada) were used as received for the free chlorine determination by the DPD method (APHA et al. 1995b). Sodium acetate trihydrate (Mallinckrodt, crystal, analytical reagent) and glacial acetic acid (Fisher, reagent ACS) were used for the preparation of the pH 5 buffer, and sodium tetraborate (Fisher, crystal, certified ACS) was used as received for the preparation of the pH 10 buffer. Sodium hydroxide (1 N) and sulfuric acid solutions (Fisher, certified, 1 N) were diluted with DI water to be used for the pH value adjustment. Sodium hypochlorite (Fisher, purified grade, 5.65 to 6% NaOCl) was refrigerated and diluted with DI water or some buffer solutions for the preparation of free chlorine samples in this study. In the determination of degradation products of free chlorine by the ion chromatography method, sodium bicarbonate (BDH, analytical reagent) and sodium carbonate (BDH, analytical reagent)

104

were used as received for the preparation of the eluent solution; sulfuric acid (Fisher, reagent ACS, 98%) was diluted to prepare the regenerating solution; and sodium chloride and potassium chlorate (BDH, analytical reagent) were used as received for the preparation of standard solutions. Humic acid (Acros Organics, sodium salt, 50 to 60% as humic acid) and alginic acid (Acros Organics, sodium salt) were used as received to adjust the TOC in water samples. The ferric sulfate (J.T. Baker Chemical Co., n-hydrate powder, 'Baker analyzed'[®] reagent), potassium oxalate (Fisher, crystals, certified ACS), 1,10-phenanthroline (Fisher, certified ACS), sodium acetate (Mallinckrodt, granular, analytical reagent) and hydroxylamine hydrochloride (Fisher, certified ACS) were used to determine the UV irradiance at various wavelengths (200 to 300 nm) by the method of ferrioxalate actinometer.

A Milli-Q water purification system (Millipore, Academic A10) was used for the production of high quality water, which was used in all analytical determinations and experiments in this study. A collimated beam apparatus (Calgon Carbon Corporation, Model Number 1 kW-1) with a 10 W low-pressure UV lamp (Atlantic Ultraviolet Corporation, Model G12T6L 15114) or a 1 kW medium-pressure UV lamp (Model QC-1000-45000071, HNG, Germany) was used to generate a nearly parallel beam of UV light. The irradiance of the UV light was measured by a radiometer (Gigaherhz Optik, Optometer P9710) with a UV-C detector (Gigaherhz Optik, UV-3718-2 SN 5517). The concentration of free chlorine was determined by the DPD method using a UV-vis recording spectrophotometer (Shimadzu, UV-2401PC) at 515 nm. The degradation products of free chlorine were measured using an ion chromatography apparatus (Dionex Corporation, Model: DX-300). An Accumet[®] Research A50 dual channel pH meter

105

(Fisher) was used for pH measurements. Other routine equipment, such as magnetic stirrers, an electronic balance and volumetric glassware, were also used in this study.

4.2.2 Preparation of synthetic water samples

A 'synthetic' drinking water was employed to simulate natural water. This was prepared according to the recipe described by Liu et al. (2002). Table 4.1 gives the primary components of the synthetic water. The pH of the synthetic water prepared according to Table 4.1 was about 8.6 and the TOC was at the range of 3.2 to 3.8 mg L^{-1}. Since the TOC was primarily attributed to humic acid and alginic acid in the synthetic water, the samples with various TOC levels, which would be used for the study of the effect of TOC concentration on the quantum yield of free chlorine decomposed, were made by decreasing or increasing the concentrations of these two TOC organics. When the free chlorine samples were prepared using the synthetic water, some free chlorine was consumed by the organic compounds comprising the TOC. The chlorine demand dose should depend on the TOC concentration. Accordingly, in order to reduce the interruption of TOC organics on the photodecomposition of free chlorine, the free chlorine samples made by the synthetic water in this study were usually stabilized for about 10 h before being used in the photolysis experiments.

Table 4.1 The components of the synthetic water (mg L^{-1})

Ca^{2+}	Mg^{2+}	Na^+	$(CO_3)_{TOT}$	NO_3^-	Cl^-	SO_4^{2-}	Humic acid	Alginic acid
29.1	10.0	36.2	90.0	3.0	40.0	55.0	2.56	5.32

106

4.2.3 Photodecomposition of free chlorine samples

In this study, for all of experiments involving the photodecomposition of free chlorine, two aliquots of free chlorine samples were used. One was exposed to UV light and the other was stored in dark as a control sample. The experimental procedure used for the UV exposure and irradiance measurement was same as that described in Section 3.2.4.

To determine the quantum yield of free chlorine decomposed at low temperature, an experimental system was employed, as shown in Figure 4.1. The sample exposed to UV light was put in a small cooler that contained the mixture of small pieces of ice and water to keep the temperature in the range 0 to 5°C. At the same time, the control sample was also put in the same kind of ice water. After the exposure time, the free chlorine decomposed by UV light was determined, and then the quantum yield of the photodecomposition of free chlorine was calculated according to the method given in the Section 3.2.6.

107
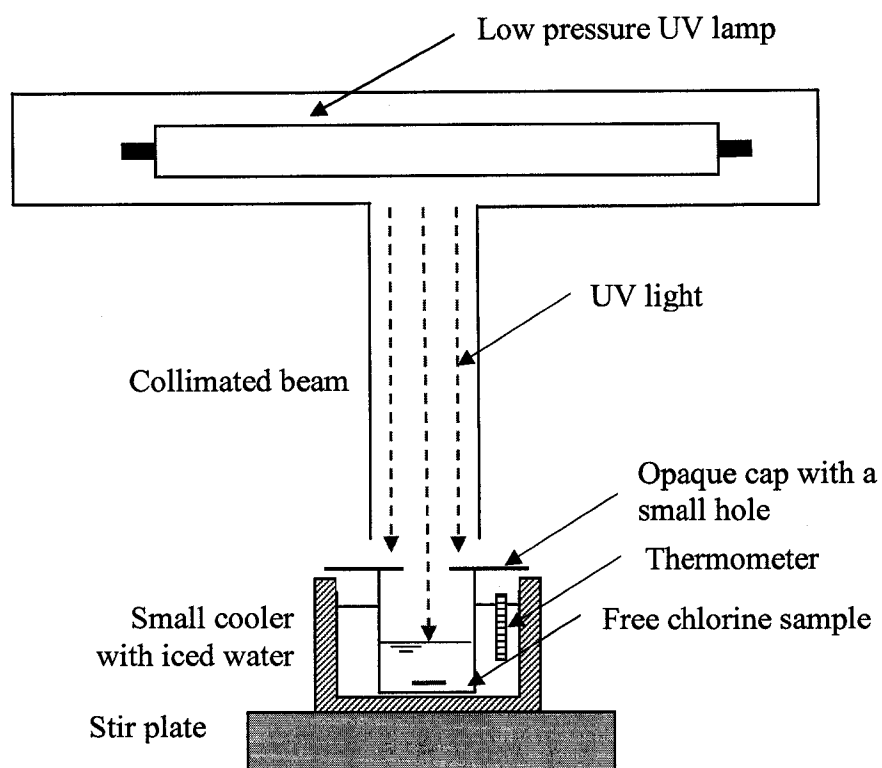
Figure 4.1 The schematic diagram of the experimental system used for the measurement of the quantum yield of free chlorine decomposed at low temperature

In the experiment to study the influence of the wavelength of the UV light on the quantum yield of the photolysis of free chlorine, the collimated beam UV apparatus with a 1 kW medium-pressure UV lamp (Model QC-1000-45000071, HNG, Germany) was used to generate the parallel UV light. A series of UV light filters (Andover Corporation Optical Filter, Melles Griot Canada, Inc.) were set under the UV lamp in the collimated beam to produce the UV light with intended wavelengths. The UV irradiance at the surface of free chlorine samples and the center of the UV beam was measured with a radiometer (International Light, Model IL1400A) equipped with a SED240 UV detector. Since this radiometer was calibrated at 254 nm, the measured UV irradiances at various

108

wavelengths were corrected by the factors determined based on the ferrioxalate actinometer method (Bolton 2006) to account for the sensor sensitivity of the radiometer.
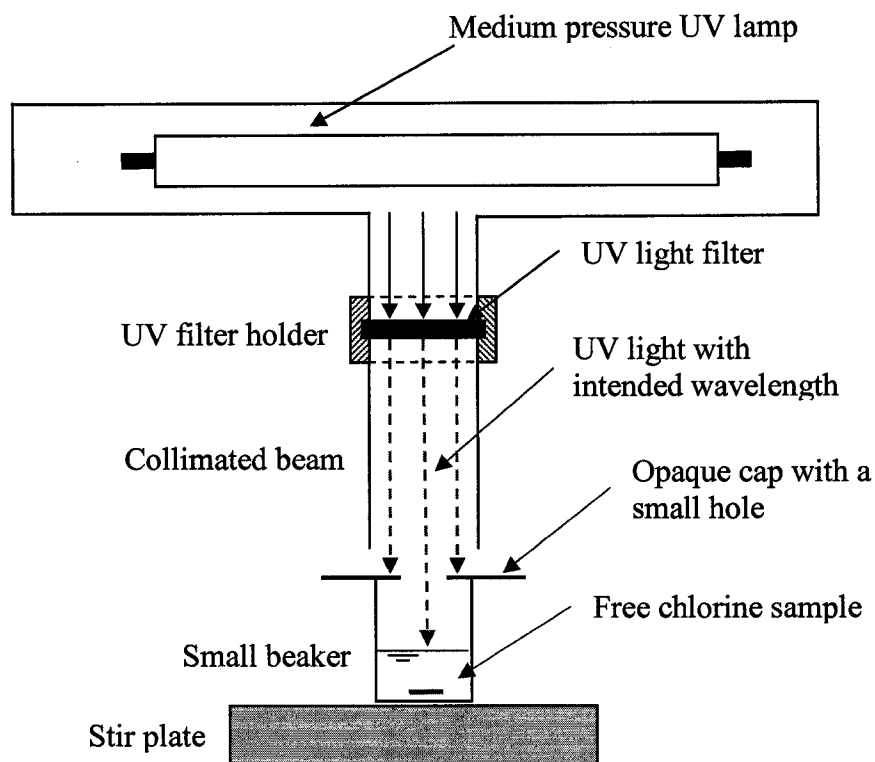
Figure 4.2 A medium-pressure UV lamp and UV light filters employed to generate the UV light with intended wavelength

4.2.4 Determination of free chlorine and its possible degradation products

In this study, the amounts of free chlorine disappearance and degradation products formation were always determined by making appropriate volume-weighted corrections for the control sample as shown in Eq. 4.1.

[4.1] $$\Delta_{UV} = \Delta_{Sample} - \Delta_{Control} \times \frac{\overline{V}_{Sample}}{\overline{V}_{Control}}$$

where, Δ is the change of the amount of free chlorine or degradation products after the exposure time (mg), $\overline{V}$ is the average volume before and after the exposure time (mL) and the subscript 'sample' and 'control' mean the sample exposed to UV light and the sample used as a control, respectively.

In addition, in order to analyze the mass balance of the free chlorine decomposed and end products generated, the units of free chlorine and its products were translated to mg Cl L^{-1}. For example, if the concentration of a free chlorine sample determined by DPD method is 3.0 mg Cl as Cl_2 L^{-1}, it does not indicate that the Cl atoms or ions in the sample were 3.0 mg L^{-1}. It means the "oxidizing power" of the free chlorine sample is equivalent to that of 3.0 mg Cl_2 L^{-1}. Because the available chlorine in HOCl or OCl$^-$ is twice that in Cl_2, the actual chlorine in the free chlorine sample should be half of the concentration expressed as "mg Cl as Cl_2 L^{-1}", that is, 1.5 mg L^{-1}. Another example is that the concentration of chlorate (ClO_3^-) in terms of "mg ClO_3^- L^{-1}" should be multiplied by a factor of 0.425, the ratio of the formula weight of Cl$^-$ (35.45) to that of ClO_3^- (83.45), to be exchanged to the unit of 'mg Cl L^{-1}'.

The concentration of free chlorine (HOCl and OCl$^-$) was determined by the DPD method (APHA et al. 1995b), which was briefly described in the Chapter 3. The argentometric method (APHA et al. 1995a) and ion chromatograph (IC) method were applied for the measurement of chloride ions (Cl$^-$) in this study. The chlorite (ClO_2^-) and chlorate (ClO_3^-) ions also were assessed by IC method. The detailed description of the argentometric method and IC method detection methods are given in Appendix 4.1.

110

4.3 Results and discussion

4.3.1 Influencing factors on the quantum yield of free chlorine decomposed

4.3.1.1 Natural organic compounds (humic acid and alginic acid)

As discussed in Chapter 3, it has been observed that some simple organic compounds, such as methanol, 1,4-dioxane and *tert*-butanol, have significant effects on the quantum yield of the photodecomposition of free chlorine. In this study, a 'synthetic' drinking water, with certain level of TOC, comprising contributions from humic acid and alginic acid, was utilized to simulate natural waters for the investigation of the correlation between the natural organic materials and quantum yield of decomposition of free chlorine.

A series of samples, in which the free chlorine concentration was kept at 3.0 ± 0.2 mg L^{-1} and the TOC varied from 0.4 to 6.8 ppm, were prepared and the quantum yields of free chlorine decomposed in these samples with 254 nm UV light were determined under the ambient conditions. The experimental results are given in Figure 4.3. As illustrated in this figure, the quantum yield of the photolysis of free chlorine gradually increased from about 1.1 to 4.9 when the TOC concentration varied from 0.4 to 6.8 ppm. The correlation was essentially linear between the increase of both the quantum yield and that of the TOC concentration. This reveals that the natural TOC materials also have a significant effect on the quantum yield of decomposition of free chlorine and for water samples from various sources, the quantum yield of decomposition of free chlorine in these waters could be different because of the variation of the TOC in these waters. This observation may arise from some chain-reactions initiated by the intermediate photolysis

111

products of free chlorine and the TOC materials. According to Oliver and Carey (1977), the increase of quantum yield may be explained by the following reactions:

$$[4.2] \qquad HOCl + h\nu \rightarrow \cdot OH + \cdot Cl$$

$$[4.3] \qquad \cdot OH \text{ (or } \cdot Cl) + RH \rightarrow \cdot R + H_2O \text{ (or } H^+ + Cl^-)$$

$$[4.4] \qquad \cdot R + HOCl \rightarrow RH + \cdot OCl$$

$$[4.5] \qquad \cdot R + \cdot R' \rightarrow \ldots \ldots \rightarrow \text{end products}$$
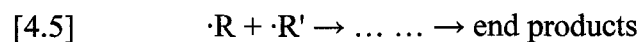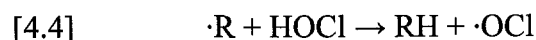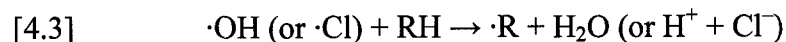
According to the above reactions, the hydroxyl ($\cdot$OH) and chlorine ($\cdot$Cl) radicals produced in the photolysis of free chlorine react with natural TOC materials (RH) and the intermediate product $\cdot$R can abstract a hydrogen atom from HOCl to consume more free chlorine in these reactions. This may be the cause of the increase of the quantum yield of free chlorine decomposed in the samples with natural TOC compounds. Another possible reason is that the TOC materials could be photolyzed by UV light to some small fragments, and these fragments may be easily oxidized by free chlorine (shown as Eqs. 4.6 and 4.7). So the extra amount of free chlorine consumed by these TOC fragments could lead to an increase of quantum yield of decomposition of free chlorine with the presence of TOC materials in water matrix. However, no matter what causes the increase of the quantum yield of decomposition of free chlorine, it should be remembered that the quantum yield of free chlorine in real operations will be different in different water matrices, and hence it should be determined before each run.

$$[4.6] \qquad RH + h\nu \rightarrow R'H + \text{other products}$$

$$[4.7] \qquad R'H + HOCl \rightarrow R'^+ + Cl^- + H_2O$$

112
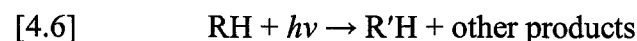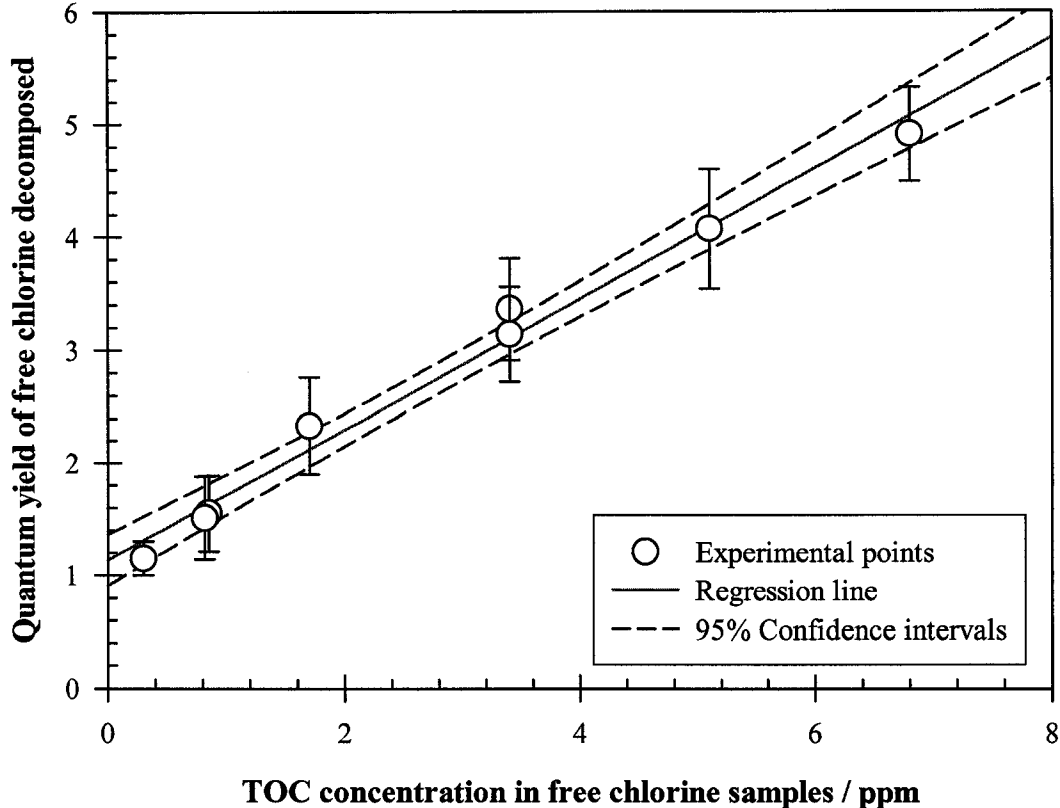
Figure 4.3 Dependence of the quantum yield of free chlorine decomposed on the natural TOC compounds (humic acid and alginic acid)

4.3.1.2 Temperature

Since the temperature of water matrix varies seasonally very much in most drinking water treatment utilities, it is necessary to determine the effect of temperature on the quantum yield of free chlorine. The water quality and temperature were selected as the two factors for a two-level factorial experiment. In the experiment, the initial concentration of free chlorine samples was 3.0 ± 0.2 mg L^{-1} in each run, and the pH was always kept at ~8.5. A low-pressure UV lamp was used for the UV light generation. Table 4.2 shows the experimental results of the dependence of quantum yield on temperature.

113

From Table 4.2, the quantum yield of the photolysis of free chlorine was always around 1.0 when the DI water (low level TOC) was used as the water matrix for the preparation of free chlorine samples. Obviously, the quantum yield was not significantly dependent on temperature for this condition. This may indicate that the free chlorine decomposed in this case is primarily caused by photochemical reactions, since the UV photons react directly with free chlorine, and the effect of a temperature change from 2 to 22°C on the photochemical reaction is negligible. However, when synthetic water with certain level of TOC compounds (humic acid and alginic acid) was used, the temperature had a significant effect on the quantum yield of free chlorine decomposed. In this study, it was observed that the quantum yield increased by almost a factor of two (1.7 ± 0.3 to 3.4 ± 0.5) when the temperature changed from about 3 to 22°C. As discussed in previous chapters, the TOC materials present in free chlorine samples can increase the quantum yield because of some possible chain-reactions (Eqs. 4.3 to 4.7) occurring between free chlorine and some intermediate photochemical products. By contrast with the results obtained using DI water as water matrix, the variation of the quantum yields of free chlorine decomposed in synthetic water for different temperatures implies that the reaction rate and/or equilibrium of these chain reactions (Eqs. 4.3 to 4.7) are probably influenced by the experimental temperature. At higher temperatures, the reaction rates of chain reactions should be faster, and the equilibrium constants may increase compared to those at lower temperatures. Therefore, a larger amount of free chlorine can be consumed at high temperatures compared to that consumed at low temperatures. This results in an increase of the quantum yield of free chlorine decomposed in synthetic water with an increase of temperature.

114

Table 4.2 Comparison of the quantum yields of free chlorine decomposed at various temperatures and in different water matrixes

Water Quality	Temperature	Quantum yield of free chlorine decomposed
Synthetic water (TOC = 3.4 ppm)	22 ± 2 °C	3.4 ± 0.5
DI water (TOC: 0 to 0.4 ppm)	22 ± 2 °C	1.0 ± 0.1
Synthetic Water (TOC = 3.4 ppm)	2 ± 2 °C	1.7 ± 0.3
DI water (TOC: 0 to 0.4 ppm)	2 ± 2 °C	1.0 ± 0.2

Based on the results obtained in this study, it can be concluded that the effect of temperature on the quantum yield of the photodegradation of free chlorine depends on the water quality. The purer the water sample (the lower the concentration of TOC in water sample), the smaller the effect of temperature will be. Therefore, this emphasizes again that the water quality is a very important influencing factor for the quantum yield of decomposition of free chlorine and that the temperature can change the quantum yield in practice because of the water quality.

4.3.1.3 Wavelength of UV light

As reported in some studies (Rahn et al. 2003, Li et al. 2005 and Shen et al. 2005), the photolysis of some chemicals is sensitive to the wavelength of UV light. For example, the quantum yield of the iodide-iodate chemical actinometer decreases linearly from 0.8 at 254 nm to 0.3 at 284 nm (Rahn et al. 2003). In addition, the quantum yield of aqueous OCl^- reported by Buxton and Subhani (1972) also appears to vary from 0.85 at 254 nm to 0.39 at 313 nm. Since the energy of photons is different at different wavelengths and the molar absorption coefficient of free chlorine also is different at different wavelengths, these factors could affect the sensitivity of aqueous free chlorine to the UV light at

115

different wavelengths. Since medium-pressure UV lamps, with a polychromatic output in the germicidal region, are usually used in the water or wastewater treatment utilities and the photodegradation of free chlorine also may be used for the validation of medium-pressure UV reactors, it is necessary to investigate the dependence of quantum yield of decomposition of free chlorine on the wavelength of UV light. In this study, free chlorine samples with a concentration of 3.0 ± 0.2 mg L^{-1} and a pH of 8.0 ± 0.3 were prepared in DI water. These samples were exposed to UV light at various wavelengths under ambient conditions. The quantum yield of decomposition of free chlorine at each wavelength was determined by different methods and discussed below (for more details about the quantum yield determination, see Appendix 4.2).

Figure 4.4 shows the quantum yields determined in this study when the UV irradiance was measured by a UV radiometer (International Light, Model IL 1400A) equipped with a UV detector (International Light, Model SED240) which was calibrated at 254 nm. In order to convert the irradiance value measured by the radiometer to the real value occurring at the measuring wavelength which was truly used in a measurement, the sensor factor, which was calculated based on the sensor spectral sensitivity relative to 254 nm at various wavelengths and the spectral irradiance measured at the wavelength, was used for the determination of the quantum yield of the photodegradation of free chlorine. As shown in Figure 4.4, the quantum yields determined by this method in this study are 0.96 ± 0.14 at 254 nm and 0.39 ± 0.07 at 300 nm. This observation indicates that the quantum yields obtained in this study have a very consistent tendency with the data reported by Buxton and Subhani (1972). However, in order to check the sensitivity of the UV detector to the UV light at various wavelengths, the ferrioxalate actinometer was also

116

used in this study for the measurement of the UV irradiance at each wavelength. Figure 4.5 shows the correction factors, which are defined as the ratio of the irradiance determined by ferrioxalate actinometer to the irradiance measured by the UV radiometer, obtained from 220 to 300 nm in this study. In this figure, the sensor factor and correction factor are very close at the wavelengths around 254 nm, but the difference between them gradually becomes significant when the wavelength of UV light is far from the 254 nm. When the wavelength is lower than 254 nm, the correction factor is a little higher than the sensor factor; otherwise, the sensor factor is significantly higher than the correction factor. This indicates that the irradiance determined by ferrioxalate actinometer is smaller than that calculated according to the measurement of the radiometer and its sensor factor when the wavelength is higher than 254 nm and vice versa. In addition, this also means that the quantum yield of the photodegradation of free chlorine at each different wavelength determined based on the irradiance corrected by ferrioxalate actinometer is different from that determined according to the irradiance determined by the radiometer and its sensor factor. The quantum yields of the photodegradation of free chlorine at various wavelengths were determined based on the irradiance corrected by the results of ferrioxalate actinometry experiments and are shown in Figure 4.6. This figure shows that the quantum yields determined in this way are very different from those determined in the other way shown in Figure 4.4. In Figure 4.6, it shows that the variation of the wavelength of UV light from 220 to 300 nm has no significant effect on the quantum yield of the photodecomposition of free chlorine. In this case, the quantum yield was always in the range of 0.90 ± 0.15 when the wavelength ranged from 220 to 300 nm.

117
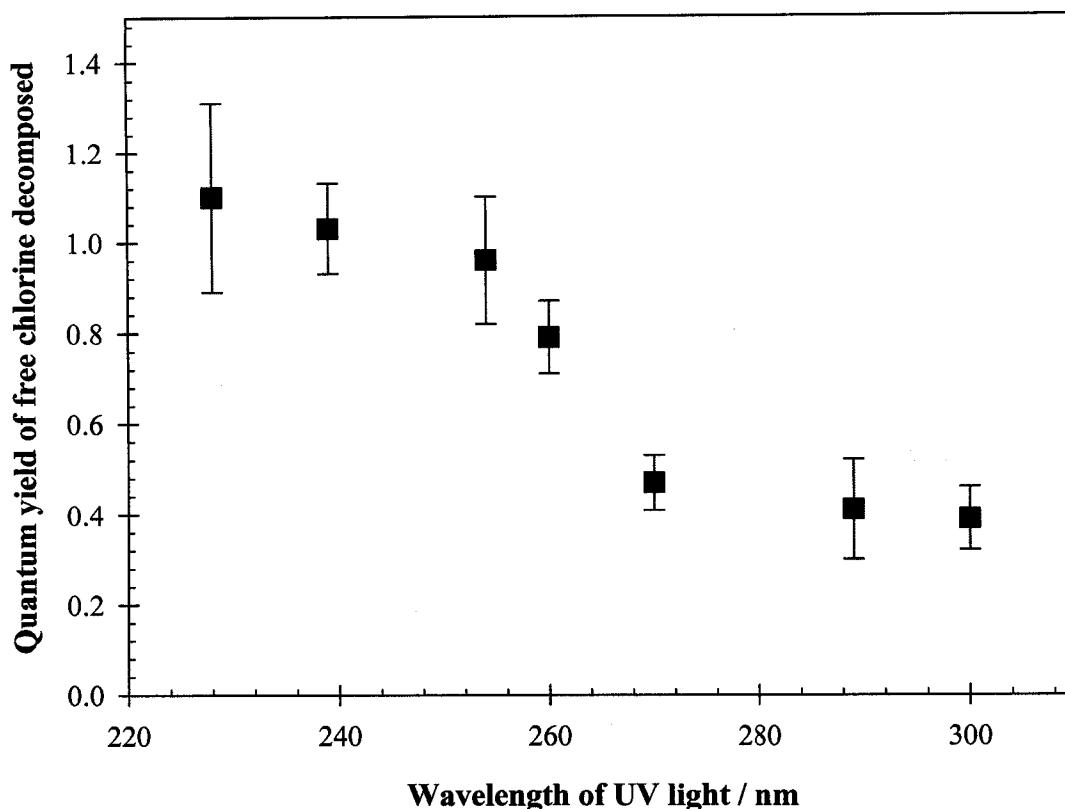
Figure 4.4 Dependence of the quantum yield of the photodegradation of free chlorine on the wavelength of UV light (quantum yields were determined according to the irradiance measured by the radiometer calibrated at 254 nm)

From Figures 4.4 and 4.6, one can clearly see the influence of the method for the measurement of UV irradiance on the quantum yields of free chlorine at various wavelengths. Figure 4.5 also reflects the difference of these two methods (radiometer and actinometer) for the measurement of the UV irradiance at different wavelengths. From the methodology point of view, the data obtained by ferrioxalate actinometer should be more reliable than those measured by radiometer. The reason is that the actinometer can accurately respond to the UV photons incident on the actinometry solution at each wavelength from 200 to 300 nm, but the detector of the radiometer is calibrated at 254 nm and it needs a sensor factor to correct the measurements when the radiometer is used at a wavelength other than 254 nm. When the wavelength is far from 254 nm, the

118

radiometer is not sensitive to this wavelength and a big error will arise in its reading. The sensor spectral sensitivity relative to 254 nm used for the calculation of sensor factor is provided by the radiometer manufacturer but was not determined in this study. In addition, the spectroradiometer used for the measurement of the spectrum of the UV light at certain wavelength was found very sensitive to the position of its detector. Therefore, the results obtained from the ferrioxalate actinometry measurement should be more reliable than those determined based on the measurement of the radiometer.
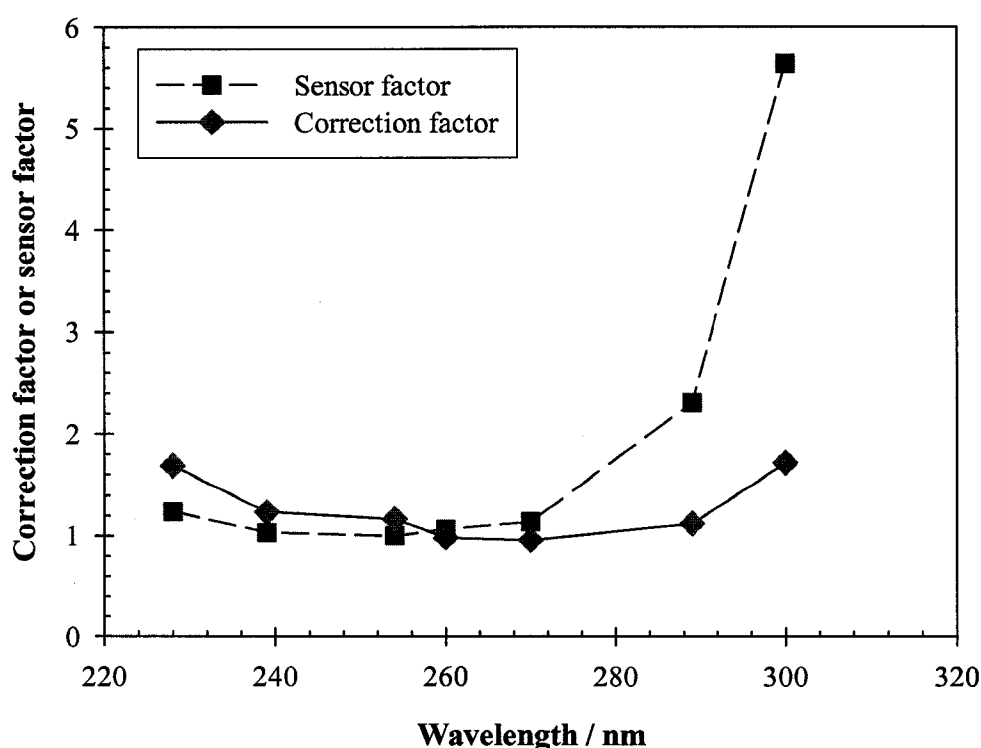
Figure 4.5 Comparison of the sensor factor and the correction factor (sensor factor is calculated based on the sensor spectral sensitivity relative to 254 nm and the spectrum measured by a spectroradiometer; and correction factor is the ratio of the irradiance determined by ferrioxalate actinometer and the irradiance measured by the radiometer)

From the photochemistry point of view, it also shows that the quantum yield of the photodegradation of free chlorine appears to be independent of the wavelength. For

119

example, the O–Cl bond energy[16] in the HOCl (H–O–Cl) molecule is 205 kJ mol^{-1}, and

the maximum wavelength of light that would be capable of dissociating this bond would

be 580 nm. However, from the absorption spectrum shown in Chapter 3, the photons of

light at the wavelengths higher than 360 nm will not be absorbed by free chlorine species.

This means that the O–Cl bond can certainly be dissociated by UV photons at

wavelengths from 200 to 300 nm. When the UV photons are absorbed by a free chlorine

molecule, the 'electronic state' of the molecule can be changed from the ground state to

the excited state. Because there should be only one 'lowest' excited state for the free

chlorine molecules, the quantum yield of the photodegradation of free chlorine should be

independent of the wavelength of UV light.

---

[16] The bond energy was obtained from http://chemistry.about.com/library/weekly/blbondenergies.htm
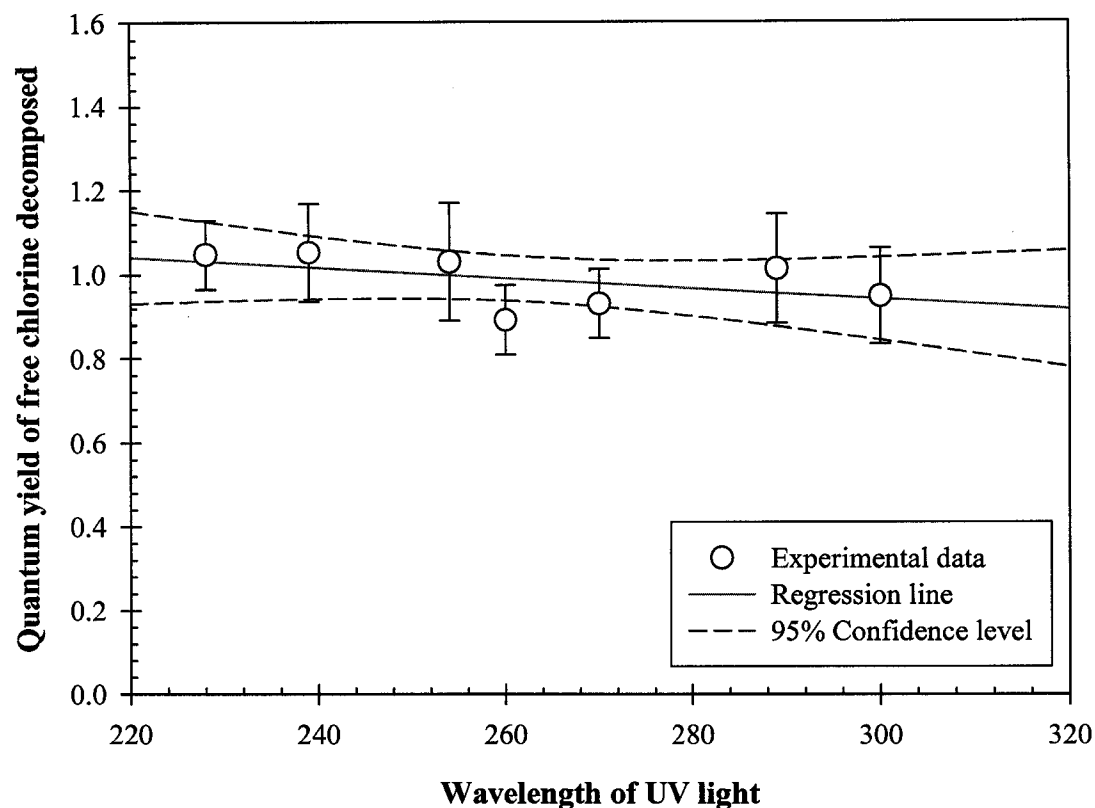
Figure 4.6 Dependence of the quantum yield of the photodegradation of free chlorine on the wavelength of UV light (the quantum yields were determined based on the irradiance measured by the Ferrioxalate actinometer)

4.3.2 End products of the photolysis of free chlorine

4.3.2.1 Chromatographs of free chlorine and the possible photodecomposition products

Figure 4.7 shows the chromatographs of chloride (Cl^-), chlorite (ClO_2^-), and chlorate (ClO_3^-) ions in DI water. As shown in this figure, the retention times for Cl^-, ClO_2^-, and ClO_3^- respectively are 3.4, 3.0 and 4.5 minutes. Also, the chromatograph of free chlorine sample at pH 8.5 is displayed Figure 4.8 and in this figure, two peaks at 3.4 and 4.5 minutes, respectively, were detected. As it was mentioned above, these peaks at the retention time of 3.4 and 4.5 minutes could be caused by chloride and chlorate ions present in samples. However, the free chlorine sample used in this run was prepared by

121

simply adding an appropriate amount of the stock concentrated sodium hypochlorite solution into DI water, and it could have some background chloride ions in the solution, but no chlorate exists in the original free chlorine sample. Therefore, it can be deduced that the peak at 4.5 minutes in Figure 4.8 should be caused by free chlorine species. If this assumption is correct, the peak caused by free chlorine should shrink when the free chlorine sample is exposed to UV light for a while, and at the same time, the peaks caused by the end products of the photodegradation of free chlorine should appear and increase.
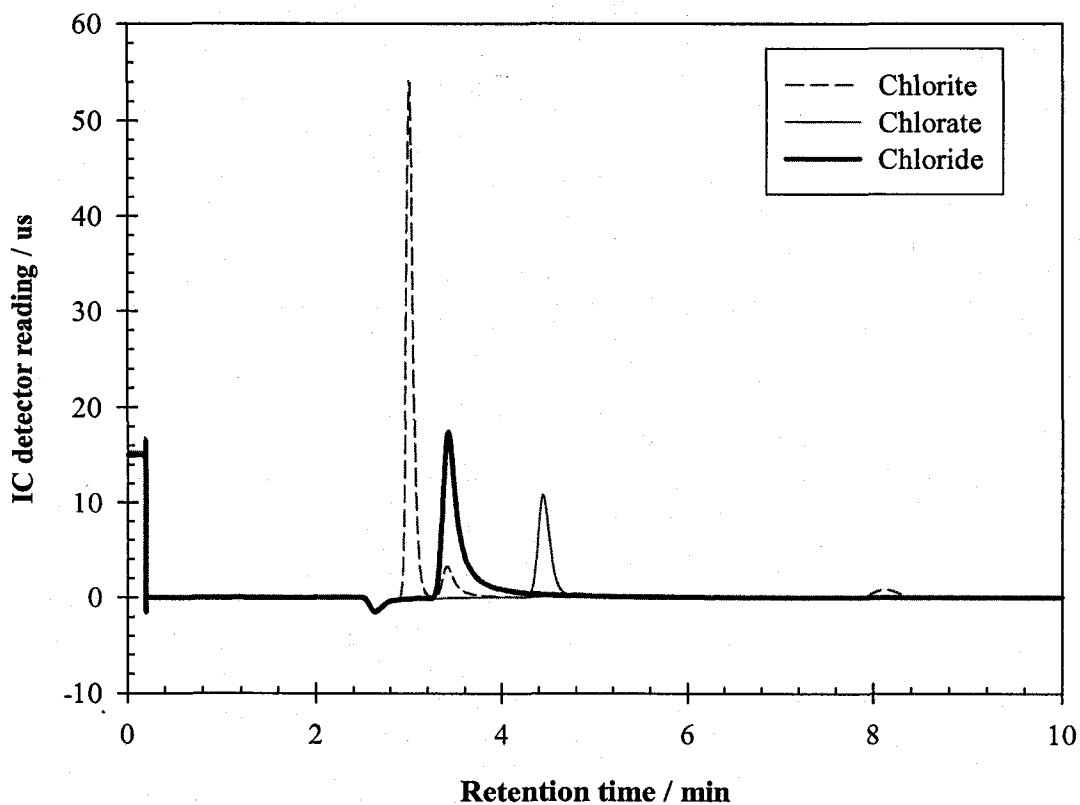
Figure 4.7 Chromatographs of the Chlorite (ClO_2^-), chloride (Cl^-), and chlorate (ClO_3^-) ions in DI water (the purity of sodium chlorite used for the preparation of standard chlorite solution is 80% and there are some Cl^- and SO_4^{2-} impurities in this solution. That is why there are two small peaks at around 3.4 and 8.2 minutes in the chromatograph of chlorite shown in this figure.)

122
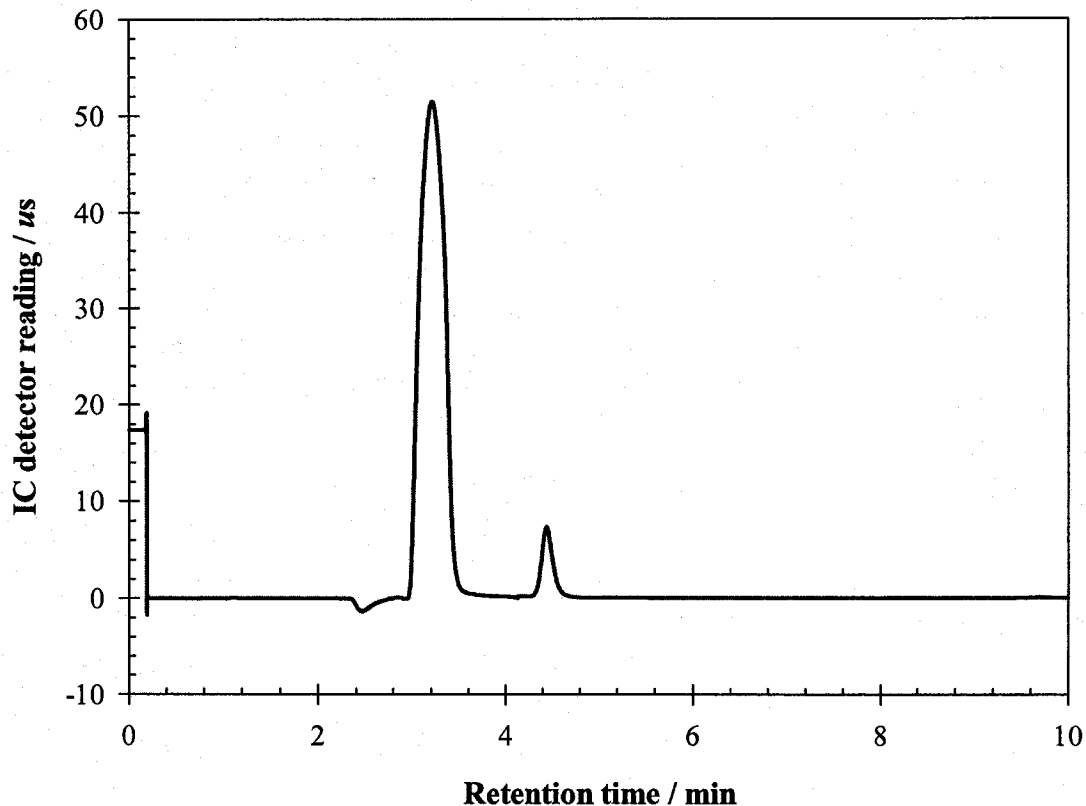
Figure 4.8 Chromatograph of the free chlorine in DI water at pH 8.5

Figure 4.9 shows the change of the chromatograph when free chlorine sample (pH 8.5) was exposed to UV light for a period of time. From this figure, it can be clearly observed that the peaks at 3.4 and 4.5 minutes have an obvious increase when the free chlorine sample was exposed to UV light for 1.5 or 3 h, and no peak was detected at the retention time of 3.0 minutes. A possible explanation for this observation is that chloride and chlorate ions were generated when the free chlorine sample was exposed to UV light. The increase of the chloride ions causes the expansion of the peak at 3.4 minutes and for the same reason, the increase of the chlorate ions fills the shrinkage of the peak at 4.5 minutes which was caused by the degradation of free chlorine. From the IC standard curves of free chlorine and chlorate ions (shown in Figure 4.10), it can be found that the

123

increase of the peak area at 4.5 minutes caused by 1 mg L^{-1} of chlorate ions is much larger than that caused by 1 mg L^{-1} of free chlorine. That is why the peak at the retention time of 4.5 minutes in Figure 4.9 also has an obvious increase after a period of UV exposure. However, the problem is still there that the peak caused by free chlorine species at 4.5 minutes overlaps that of the chlorate ions and one cannot quantitatively determine the chlorate ions based only on Figure 4.9.
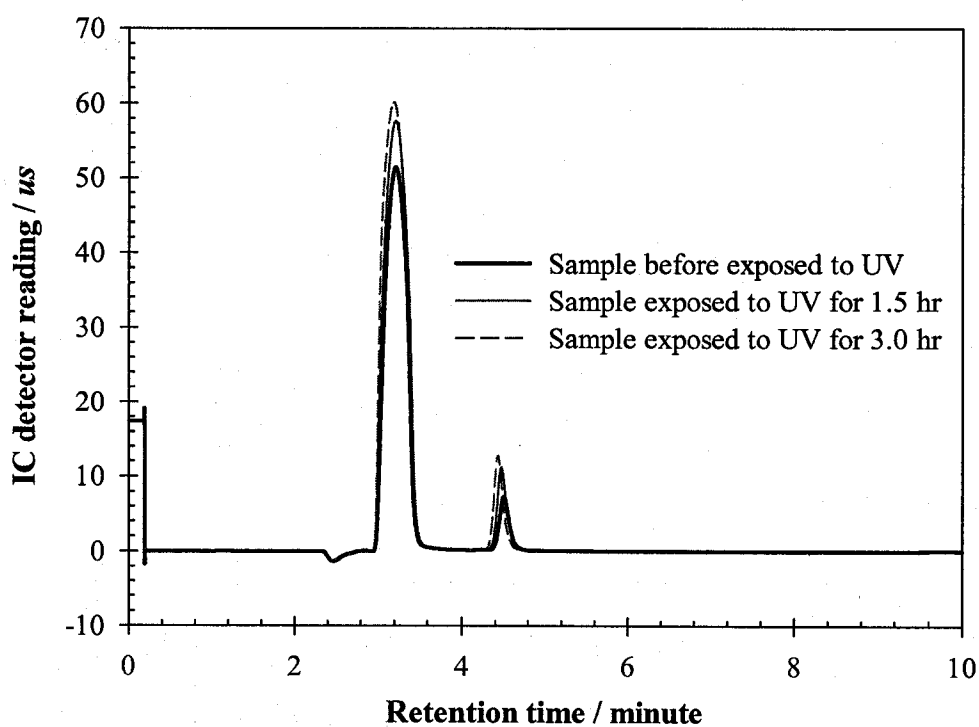
Figure 4.9 Chromatographs of free chlorine solution (32.11 mg Cl L^{-1}) exposed to UV light for different periods at pH 8.5

124
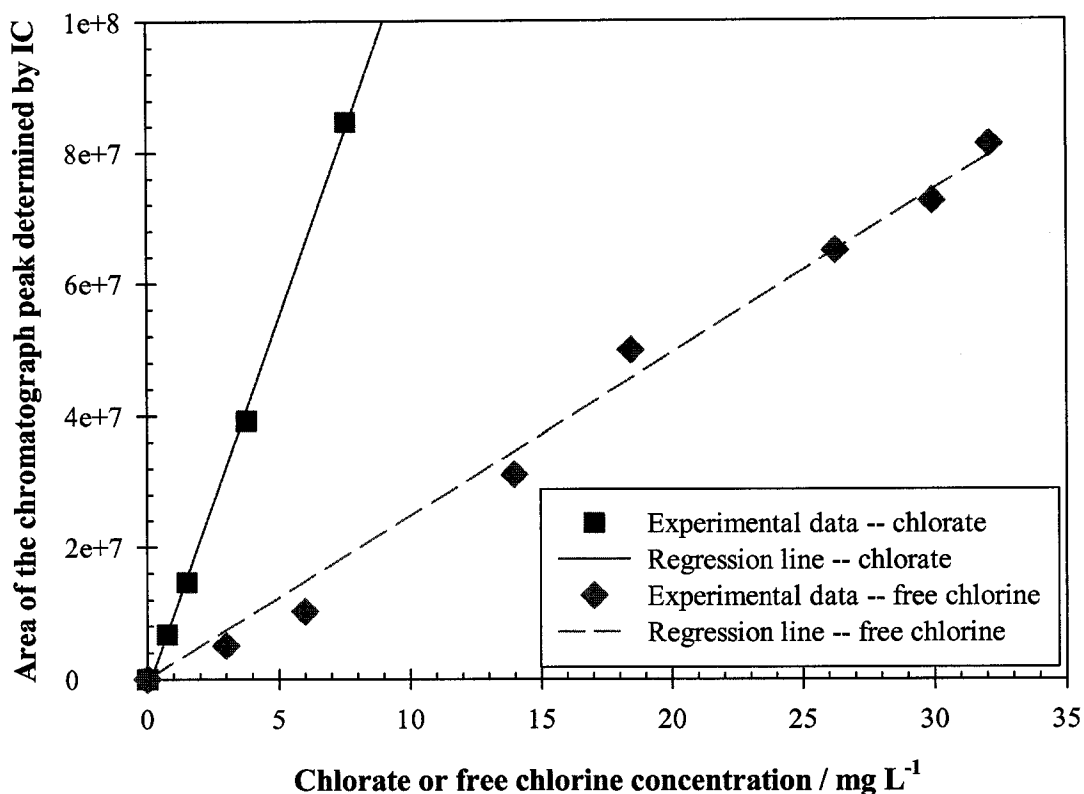
Figure 4.10 Comparison of the standard curves of chlorate ions and free chlorine for IC method (the retention time of both free chlorine and chlorate ions was found to be ~4.5 minutes in the IC method in this study, but from this figure the slope of regression line of chlorate ions is greatly steeper than that of the free chlorine. This means that the increase of the chromatograph peak area caused by 1 mg L^{-1} of chlorate is obviously greater than that caused by 1 mg L^{-1} of free chlorine.)

In order to separate the effect of free chlorine on the determination of chlorate ions from the chromatograph peak at 4.5 minutes, a standard curve was performed to assess the relation between the concentration of free chlorine and the area of chromatograph peak at 4.5 minutes. A series of freshly prepared free chlorine samples, in which the concentration ranges from 0 to 32 mg Cl L^{-1}, was used and the area of the peak at 4.5 minutes for each concentration was determined by IC. Since the concentration of free chlorine remaining in the sample after exposure to UV light can be determined by the

125

DPD method, the concentration of chlorate can be calculated according to the following equation:

$$[4.8] \qquad C_{\text{ClO}_3^-} = \frac{A_{\text{ClO}_3^-}}{k_{\text{ClO}_3^-}} = \frac{A_{\text{total}} - k_{\text{free Cl}} C_{\text{free Cl}}}{k_{\text{ClO}_3^-}}$$

where, $C_{\text{ClO}_3^-}$ is the concentration of chlorate, mg ClO_3^- L^{-1}; $A_{\text{ClO}_3^-}$ is the area of the chromatograph peak caused by chlorate ions at 4.5 minutes; $k_{\text{ClO}_3^-}$ is the slope of standard curve used for the ClO_3^- determination by the IC method, (mg OCl_3^-)$^{-1}$ L; A_{total} is total area of the peak at 4.5 minutes caused by the sample after exposure to UV light; $k_{\text{free Cl}}$ is the slope of standard curve determined by standard free chlorine solutions, (mg free Cl)$^{-1}$ L; and $C_{\text{free Cl}}$ is the concentration of free chlorine remaining in the UV irradiated sample, mg Cl L^{-1}.

It should be pointed out that in the above analysis for the calculation of the chlorate concentration, it is assumed that there is no interaction between free chlorine and chlorate for the formation of the chromatograph peak at 4.5 minutes. A series of solutions were prepared by mixing the standard free chlorine solution and chlorate solutions according to different proportions and the area of peak at 4.5 minutes was determined by IC. Since the concentrations of free chlorine and chlorate in the mixed solution can be calculated according to the make-up proportions, the area of peak at 4.5 minutes also can be calculated based on the standard curve of each component (free chlorine or chlorate). Figure 4.11 shows the relation of calculated area to the measured area of the peak at 4.5 minutes caused by the mixture solutions. As shown in this figure, the slope of the line is very close to 1 and this indicates that the assumption of the above calculation process is

126

correct and hence the chlorate concentration can be determined using the above process

(Eq. 5).
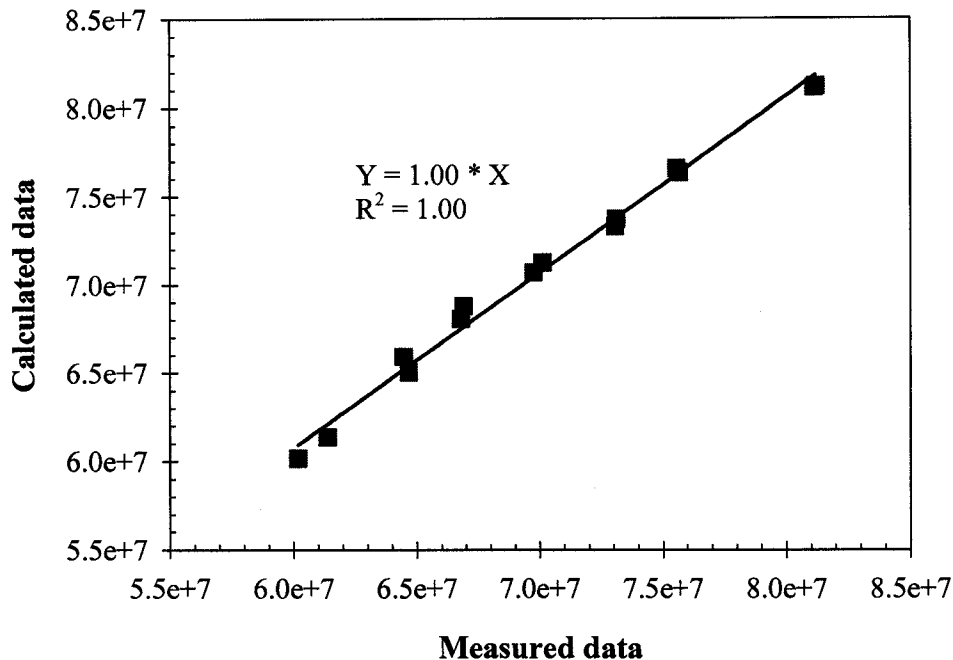
Figure 4.11 Comparison of the calculated and measured area of the chromatograph peak at 4.5 minutes caused by the mixture of standard free chlorine and chlorate solutions

4.3.2.2 Mass balance of the degradation products

A ~1000 mL free chlorine sample was freshly prepared in DI water (no buffer solution added) and stored in a bottle covered by aluminum foil under ambient conditions. The pH of this solution was 8.5 ± 0.2. A ~50 mL aliquot of this solution was used in each run for exposure to UV light for the intended period of time. Then, the disappearance of free chlorine and the formation of the degradation products were determined with the correction of the control sample. Figure 4.12 shows the time profiles of free chlorine decay and formation of its degradation products during the photolysis process.

127

From Figure 4.12, one can observe that the chloride and chlorate increase with the decomposition of free chlorine. The chloride and chlorate reached their maximum concentration at the same time when the free chlorine was completely decomposed at the end of experiment. The contour of mass balance illustrates that the initial concentration of free chlorine was 16.1 mg Cl L^{-1}, and there was no chloride or chlorate before exposure to UV light. When the sample was exposed to UV light for a period of time, free chlorine was degraded and chloride and chlorate were generated as shown in Figure 4.12. However, the total chlorine (Cl) concentration, the sum of free chlorine, chloride and chlorate present in the sample, still was around 16.1 mg Cl L^{-1} no matter how long time the sample was exposed. That is, there is a good agreement on the total chlorine (Cl) concentration in the initial and photodegraded samples, which suggests that the major products present in the system were properly identified and quantified. This means that chloride and chlorate are the primary degradation products in the photolysis of free chlorine, and no significant amount of chlorite or perchlorate were generated in this study. This result is very consistent with that reported by Buxton and Subhani (1972). They also found that only chloride and chlorate were produced when aqueous hypochlorite ions (OCl⁻) were photolyzed at 254 and 313 nm.

128
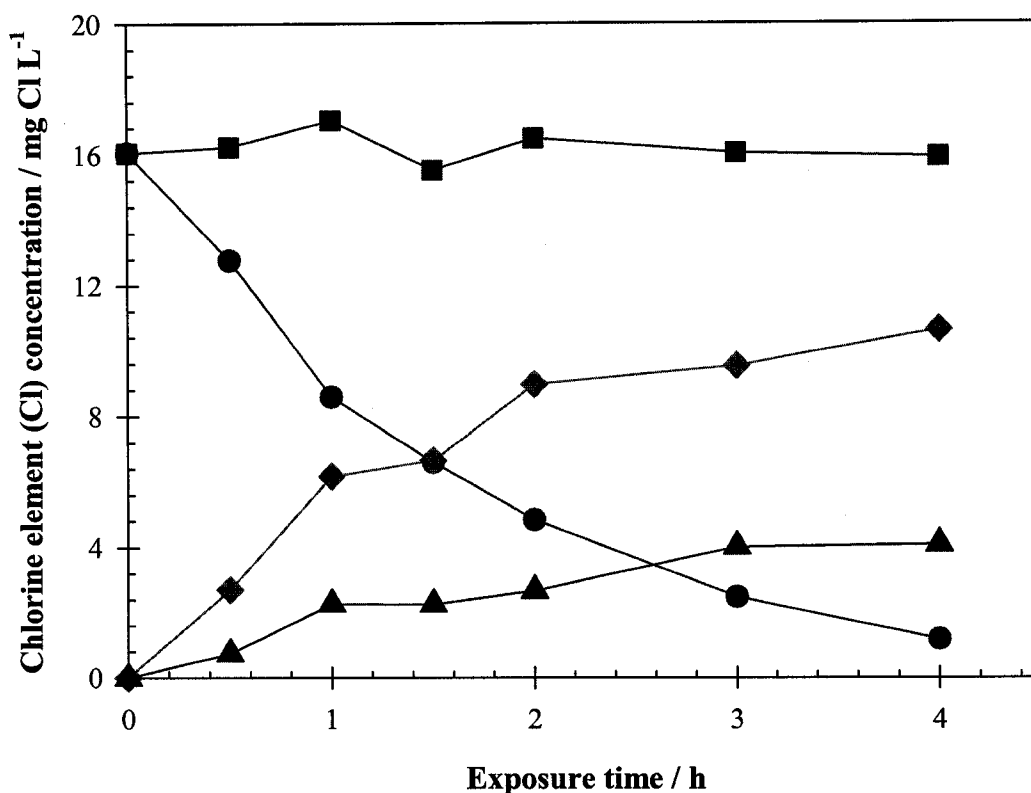
Figure 4.12 Time profiles of free chlorine and its photodecomposition products and the chlorine element (Cl) mass balance in the photolysis of free chlorine at pH 8.5 (● free chlorine, ▲ chlorate ions, ♦ chloride ions, and ■ total concentration of Cl

Similar to the experimental process at pH 8.5, freshly prepared free chlorine samples buffered in pH 5 acetate solution were exposed to UV light and the products generated in the photodecomposition of free chlorine were determined. Figure 4.13 presents the time profiles of free chlorine and the mass balance of its degradation products at pH 5. This figure also shows that at pH 5, the free chlorine was gradually decomposed with a corresponding increase of chloride and chlorate ions, but the total chlorine (Cl) concentration remained approximately constant at any time.

129
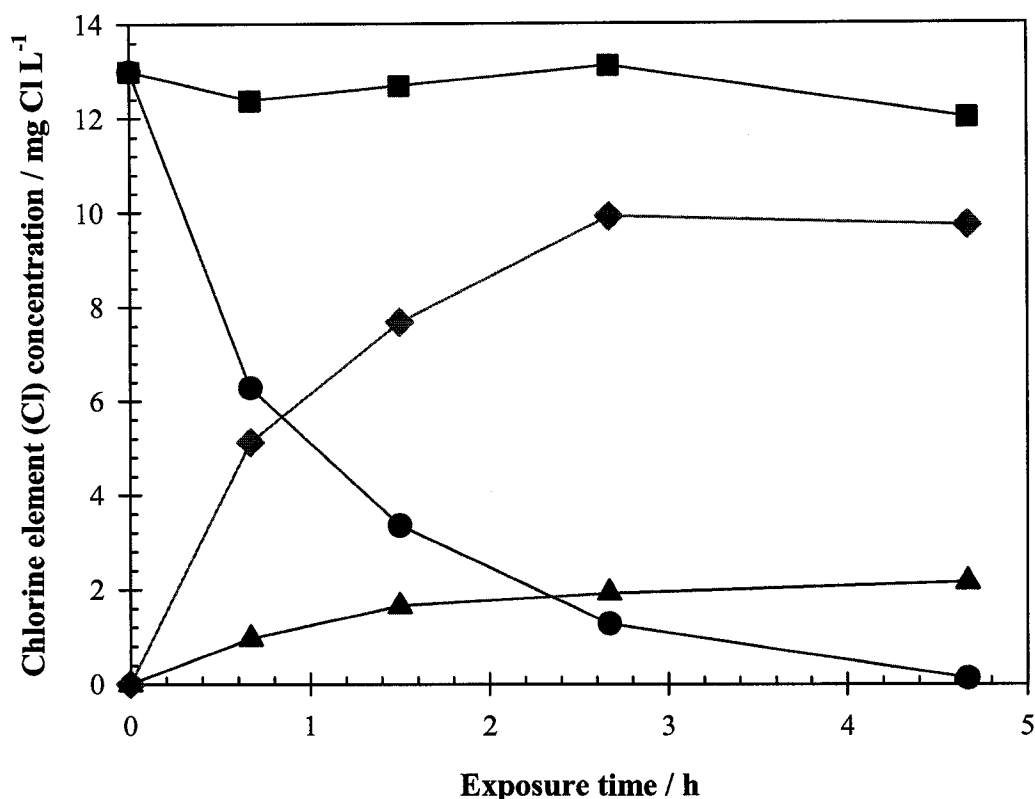
Figure 4.13 Time profiles of free chlorine and its photodecomposition products and the chlorine element (Cl) mass balance in the photolysis of free chlorine at pH 5 (● free chlorine, ▲ chlorate ions, ♦ chloride ions, and ■ total concentration)

Comparing Figures 4.12 and 4.13, one can conclude that both chloride and chlorate are produced in the photolysis of free chlorine at pH 5 and 8.5, and that the degradation products are independent of pH. However, the relative amounts (the ratio of chloride or chlorate to total chlorine present in the sample solution) for these two degradation products are not same at different pH values. It is obvious that the relative production of chloride at pH 5 is higher than that at pH 8.5; or in contrast, the chlorate produced at pH 5 is lower than that at pH 8.5. Except for experimental errors, a possible reason for this observation is the difference of the nature of the free chlorine components under the different pH conditions.

130

4.3.2.4 Effect of pH on the photodecomposition of free chlorine

Freshly prepared free chlorine samples at pH 5 (acetate buffer), 8.5 (no buffer added) and 10 (bicarbonate buffer) were exposed, respectively, to UV light for long enough time periods to be completely decomposed under ambient conditions, and the photodecomposition products in these samples were determined. In order to make a clear comparison, the amounts of these degradation products were expressed in terms of a relative quantity, namely, the ratio of a degradation product to the total chlorine (Cl) present in the sample. In addition, in order to account for the effect of experimental system errors, a control sample, which was put in dark and operated under similar conditions as that of the sample exposed to UV light, was also performed. The relative quantity of control sample was calculated using the amount of free chlorine remaining in the sample after the exposure time divided by the amount of free chlorine before the exposure time. This reflects the percentage of recovery when the free chlorine was not irradiated by UV light in the exposure time interval. Figure 4.14 compares the relative amount of control sample and each degradation species produced in the photolysis of free chlorine for various pH values.

First, Figure 4.14 shows that the recovery of the control sample is always around 100%, which means that most of free chlorine was still in the control sample and that the amount of free chlorine degraded in the control sample was very small over the exposure time. On the other hand, this also indicates that the loss of free chlorine because of evaporation, contaminants in experimental glassware or something else during the irradiation process does not have a significant effect on the experimental results. As shown in Figure 4.14, about 70 to 80% of free chlorine was decomposed to chloride and

131

about 20 to 30% of free chlorine became chlorate. When the pH increased from 5 to 10, there was a slight decrease in the production of chloride and, at the same time, the production of chlorate increased slightly. As discussed in the above section, a possible reason could be the difference of the free chlorine species at the different pH values. As has been indicated earlier, the predominant species in free chlorine is HOCl at pH 5, but is OCl$^-$ at pH 10. The experimental results illustrated in Figure 4.14 imply that the photodecomposition processes of free chlorine at different pH values could be different. However, it also needs to be emphasized that although there is a decreasing (or increasing) tendency for chloride (or chlorate) with the increase of pH, the amounts (percentage) of chloride (chlorate) ions have no distinct difference at different pH values when the errors are considered.

In Figure 4.14, the sum of percentages of chloride and chlorate is always about 100% at each pH, and this provides a very good agreement with the recovery ratio of control sample. This reveals that when the free chlorine is completely decomposed by low pressure UV light, the predominant degradation products are chloride and chlorate ions, no matter what component (HOCl, OCl$^-$, or both) is in the free chlorine solution.

132
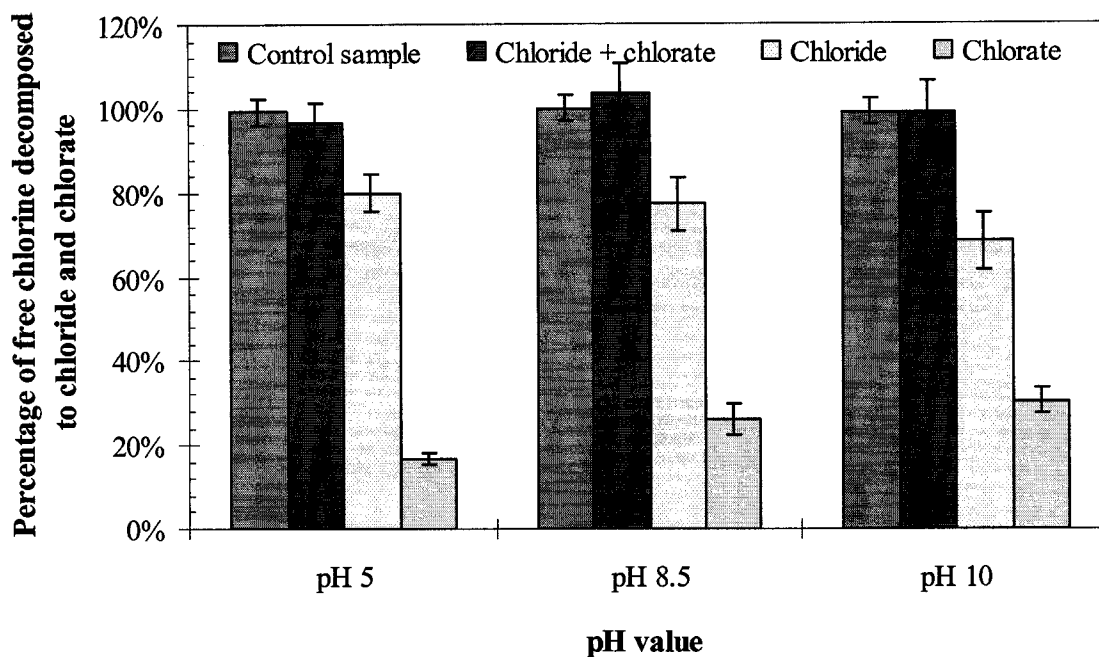
Figure 4.14 Mass balance of the degradation products when free chlorine solutions were exposed at various pH values to low pressure UV lamp for a long enough time to be completely decomposed.

4.3.2.5 Effect of free chlorine concentration on the degradation products

In Chapter 3, it was found that the concentration of free chlorine has a significant effect on the quantum yield. Accordingly, it is also necessary to check the effect of free chlorine concentration on the yields of photodecomposition products. In the above sections, it has been determined that the degradation products are chloride and chlorate ions. Therefore, in the following experiment, only chloride was used as the target product to investigate the dependence of the yields of degradation products on the concentrations of free chlorine. Free chlorine samples, with concentrations ranging from 3 to 55 mg L^{-1} were examined and the percentage of chloride generated was calculated according to

[4.8] $\text{chloride, } \% = \dfrac{M_{Cl^-}}{M_{HOCl}} * 100$

133

where, M_{Cl^-} is the amount (mg Cl L^{-1}) of chloride ions generated during the photolysis of free chlorine samples and M_{HOCl} is the amount (mg Cl L^{-1}) of free chlorine degraded by UV light. Figure 4.15 shows the relative amount of chloride generated in the photodecomposition of free chlorine.

As shown in Figure 4.15, the percentage of free chlorine decomposed to chloride is always around 80% and is independent of the concentration of free chlorine. The only exception is that the production of chloride is about 70% at a concentration of 3 mg Cl L^{-1}. This deviation is probably caused by the errors of measurement in the experimental process because the amounts of free chlorine decomposed and chloride generated are very small when the initial free chlorine concentration is very low. So, a small error for the chloride or free chlorine measurement could result in a large deviation for the relative result.
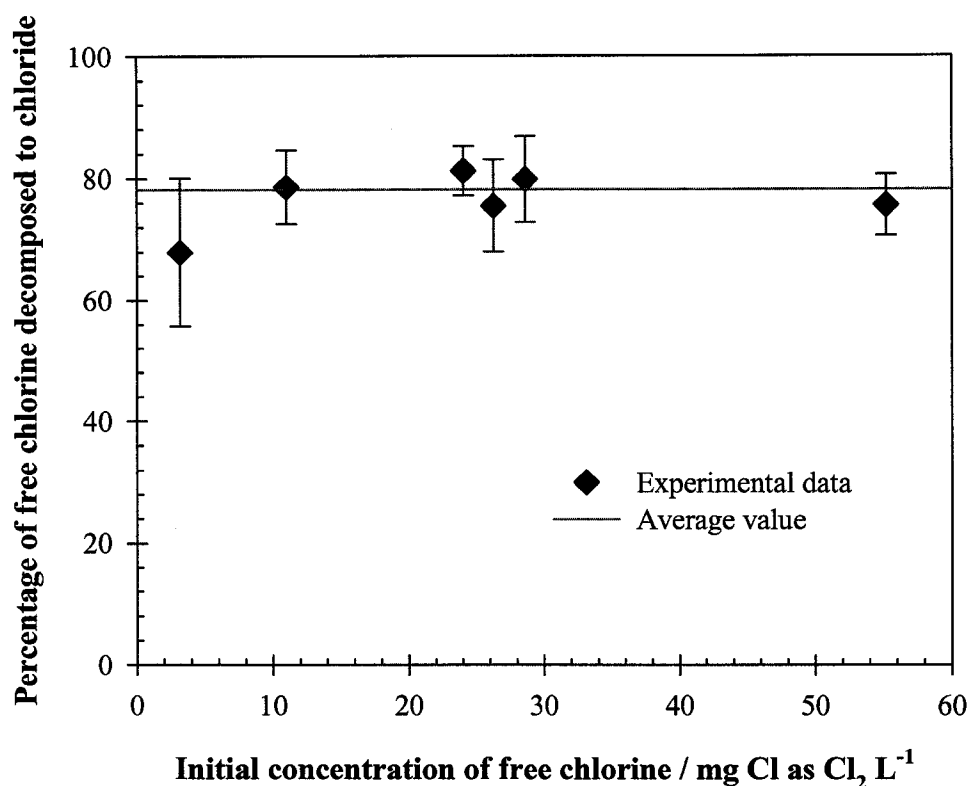
Figure 4.15 Dependence of the relative yield of chloride on the free chlorine concentration (pH = 5.2 ± 0.2)

4.3.2.6 Effect of TOC on the Production of Chloride

The results obtained in above experiments were determined for free chlorine samples prepared using DI water. However, in practice, there always are some natural organic materials in the influent of water treatment utilities. Because free chlorine, UV light, and the radicals generated in the photolysis of free chlorine could react with these organic materials present in water, the degradation of free chlorine could be very complex. In this study, a series of free chlorine samples with different TOC levels were prepared and chloride was used as the target degradation product to trace the photodecomposition of free chlorine in these samples.

135

Figure 4.16 shows the effect of TOC concentration on the percentage of chloride

formation in the photolysis of free chlorine with 254 nm UV light. As was observed in

the above experiments, about 80% of free chlorine was decomposed to chloride at around

pH 5 when DI water was used for the preparation of free chlorine sample in which the

TOC level was not very significant. However, if the synthetic water with certain levels of

TOC was used for the free chlorine sample preparation, the percentage of free chlorine

degraded to chloride mildly increased with an increase of the TOC concentration. Figure

4.16 demonstrates that the percentage smoothly goes up from about 80% to 90% when

the TOC concentration ranges from 0 to 6.8 ppm. Although the accuracy of the

experimental results could be affected by the experimental errors, it still can be clearly

observed that the TOC level has an influence on the relative amount of chloride generated

in the photolysis of free chlorine, based on a statistical analysis of the experimental

results. Except for experimental errors, a possible reason for the increase of chloride ratio

is that the organics or the organic fragments generated in the photodecomposition of

organics present in free chlorine sample could be oxidized by free chlorine or the radicals

($\cdot$OH and $\cdot$Cl) to generate chloride ions.

[4.2] $\quad$ $HOCl + UV_{254\ nm} \rightarrow \cdot OH + \cdot Cl$

[4.9] $\quad$ $\cdot OH + \cdot Cl + HOCl \rightarrow \ldots\ldots \rightarrow Cl^- + ClO_3^-$

[4.10] $\quad$ $\cdot OH\ (or\ \cdot Cl) + organics/organic\ fragments \rightarrow oxidized\ organic + H_2O/Cl^-$

[4.11] $\quad$ $HOCl + organic\ fragments \rightarrow oxidized\ organic + H_2O + Cl^-$
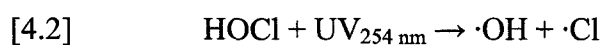
According to the above reactions, Reaction 4.2 occurs when HOCl is exposed to UV light

and then, if there are no radical scavengers present in the sample, the photolysis products,

hydroxyl and chloride radicals, react with HOCl to generate the final degradation

136

products, chloride and chlorate ions. However, if there are some organics or organic fragments, which are generated in the photolysis of organics and easily oxidized by free chlorine, Reactions 4.10 and 4.11 may occur in the system and only chloride ions are generated in these reactions. Therefore, in this study, this may be the reason why the production of chloride was observed to have a slight increase with an increase in the TOC level.
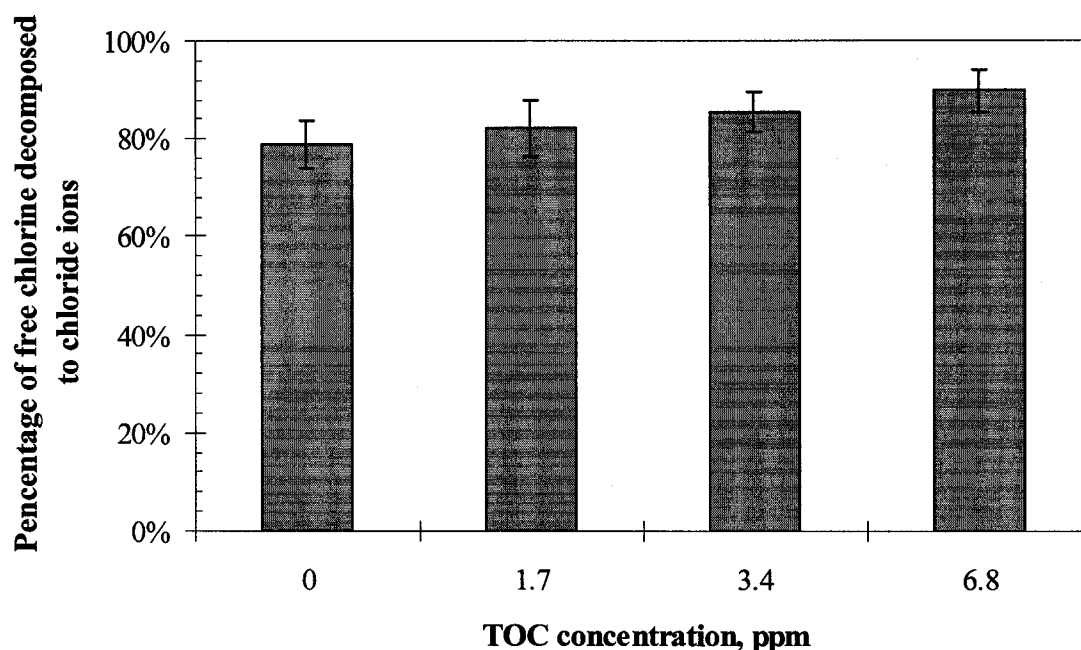
Figure 4.16 Effect of TOC concentration on the relative yield of chloride of the photodecomposition of free chlorine (pH = 5.2 ± 0.2)

4.3.3 Process of free chlorine degradation with 254 nm UV light

This section will only undertake a preliminary and simple exploration into the mechanisms of the photodecomposition of free chlorine in DI water. Since the presence of organics will make the reaction system quite complex, it is hard to trace the real degradation process of free chlorine. In addition, because free chlorine present in

137

drinking water primarily consists of HOCl and OCl⁻, the degradation mechanism of these two free chlorine species will be discussed separately in the following.

Buxton and Subhani (1972) made a detailed investigation on the photodecomposition mechanism of aqueous hypochlorite ions (OCl⁻). In their study, they observed that the aqueous OCl⁻ was decomposed to chloride, chlorate and oxygen with the quantum yields of $\Phi_{OCl^-} = 0.85$, $\Phi_{Cl^-} = 0.70$, $\Phi_{ClO_3^-} = 0.15$, and $\Phi_{O_2} = 0.20$ at 254 nm. Based on their observations, they proposed the following photodecomposition mechanism of OCl⁻:

- the photolysis of OCl⁻:

[4.12] $ClO^- + UV_{254\,nm} \rightarrow \cdot Cl + O^-$ or $O(^1D) + Cl^-$

- the reactions of ·Cl:

[4.13] $\cdot Cl + ClO^- \rightarrow Cl^- + \cdot OCl$

[4.14] $2 \cdot OCl \leftrightarrow Cl_2O_2$

[4.15] $2\,Cl_2O_2 + 2\,H_2O \rightarrow 2\,Cl^- + ClO^- + ClO_3^- + 4\,H^+ + O_2$

- the degradation of O⁻:

[4.16] $O^- + ClO^- \rightarrow \cdot OCl + O^{2-}$ $(H^+ + O^- + ClO^- \rightarrow \cdot OCl + OH^-)$

[4.17] $O^- + H_2O \leftrightarrow \cdot OH + OH^-$
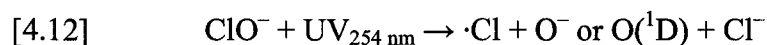
[4.18] $\cdot OH + ClO^- \rightarrow OH^- + \cdot OCl$

- the degradation of or $O(^1D)$:

[4.19] $O(^1D) + H_2O \rightarrow H_2O_2$

[4.20] $H_2O_2 + ClO^- \rightarrow H_2O + Cl^- + O_2$
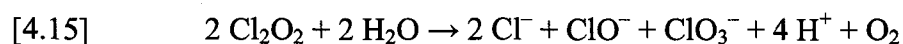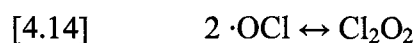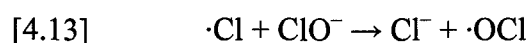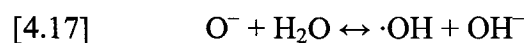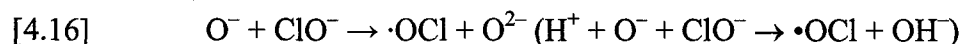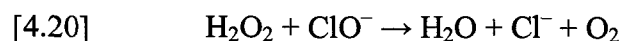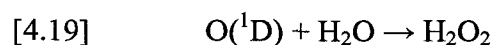
According to the analysis of Buxton and Subhani (1972), the final degradation products in the photolysis of aqueous hypochlorite ions are oxygen, chloride and chlorate. Their

138

conclusion is confirmed by the observation of chloride and chlorate in the free chlorine samples photolyzed by UV light obtained in this study. In the free chlorine solution degraded by 254 nm UV light in our experiment, only chloride and chlorate were detected and about 70 to 80% and 20 to 30% of chlorine element (Cl) were transformed from free chlorine to chloride and chlorate, respectively. These results are very consistent with those reported by Buxton and Subhani (1972).

However, for the hypochlorous acid (HOCl), the degradation process could be different. When hypochlorous acid (HOCl) is exposed to UV light, it is photolyzed to hydroxyl and chloride radicals in the following way

[4.21] $HOCl + UV_{254\,nm} \rightarrow \cdot OH + \cdot Cl$
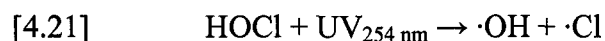
Reaction 4.21 has been proven by many studies (Oliver and Carey, 1977; Molina et al., 1980; and Butler and Phillips, 1983). In addition, as discussed in Chapter 3, it also was indirectly confirmed in an experiment in this research in which formaldehyde (HCHO) was detected when aqueous HOCl was irradiated by 254 nm UV light in the presence of methanol (CH_3OH). Then, the hydroxyl and chloride radicals produced in the photolysis of HOCl are expected to abstract a hydrogen atom from HOCl to generate $\cdot OCl$, since the electron affinity of $\cdot OH$ or $\cdot Cl$ exceeds that of $\cdot OCl$, according to the following reactions:

[4.22] $\cdot OH + HOCl \rightarrow H_2O + \cdot OCl$

[4.23] $\cdot Cl + HOCl \rightarrow \cdot OCl + H^+ + Cl^-$
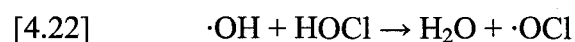
In the products of Reactions 4.22 and 4.23, only the $\cdot OCl$ is unstable and will be involved in further reactions. The subsequent reactions of $\cdot OCl$ had been established by Buxton and Subhani (1972) and reported as Reactions 4.14 and 4.15. The end-products of the photodecomposition of aqueous HOCl are ClO_3^-, Cl^-, and O_2.

139

4.4 Conclusions

In order to make a detailed investigation on the quantum yield of the photolysis of free chlorine, some potential influencing factors on the quantum yield were studied in this study. In Chapter 3, it was found that some simple organics, such as methanol, 1,4-dioxane and *tert*-butanol, can significantly increase the quantum yield. In this study, natural organic compounds (humic acid and alginic acid) were used as the TOC sources and the effect of TOC on the quantum yield was examined. When the natural TOC concentration ranged from 0 to 6.8 ppm, it was observed that the quantum yield of free chlorine (3.0 ± 0.2 mg L^{-1}) increased from about 1.1 to 4.9 under ambient conditions. Therefore, it is obvious that the natural TOC (or organic compounds) has a significant effect on the quantum yield of the photodegradtion of free chlorine. However, the effect of temperature on the quantum yield is not so clear. When the free chlorine sample was prepared in DI water (where the TOC concentration is less than 0.4 ppm), no significant change of the quantum yield was observed when the experimental temperature varied from about 2 to 22°C. However, the situation, as demonstrated in this study, was completely different when synthetic drinking water samples were used for the preparation of the free chlorine samples. For a free chlorine concentration of 3.0 ± 0.2 mg L^{-1} with a TOC level of 3.4 ppm, the quantum yield was observed to decrease from about 3.4 at 22°C to 1.7 at 2°C. Therefore, it can be concluded that the experimental temperature has a significant effect on the quantum yield of the photolysis of free chlorine in the presence

140

of organic compounds[17]; otherwise, the effect is negligible. The wavelength of UV light also was investigated, but, in this study, no distinct effect on the quantum yield was noted.

The degradation products of the photodecomposition of free chlorine were investigated. In the free chlorine samples irradiated by 254 nm UV light, chloride (Cl^-) and chlorate (ClO_3^-) ions were detected. The time profiles of the photodecomposition of free chlorine were examined at pH 5 and 8.5. As the exposure time increased, the free chlorine was increasingly decomposed and the chloride and chlorate concentrations gradually increased. The mass balance of total chlorine (Cl) indicates that the chloride and chlorate ions are the major end-products in the photolysis of free chlorine. In this study, no detectable amounts of chlorite (ClO_2^-) and perchlorate (ClO_4^-) were observed. Some potential influencing factors on the degradation products of free chlorine were examined. Concentrations of free chlorine ranging from 3 to 55 mg Cl as Cl_2 L^{-1} were investigated, and, in this study, no dependence of the end-products on the concentration of free chlorine was observed. When the pH was varied from 5 to 10, the relative amount of chloride decreased from about 80 to 70% and that of chlorate correspondingly increased from about 20 to 30%. This could arise from different photodecomposition mechanisms for HOCl as compared to those of OCl^-. In addition, the TOC present in samples can also cause an increase the production of chloride in the photodecomposition of free chlorine. In addition, according to the photodecomposition mechanism of aqueous OCl^- reported by Buxton and Subhani (1972), this study made a simple exploration into the mechanism of the photolysis of HOCl.

---

[17] There may be an exception for some organic compounds (e.g. acetate) which normally do not affect the photolysis of free chlorine.

4.5 References

APHA, AWWA, and WEF, 1995a. Standard Methods for the Examination of Water and Wastewater (19th edition): 4500-Cl⁻ B. Argentometric method. American Public Health Association, 1015 Fifteenth Street, NW, Washington, DC 2005.

APHA, AWWA, and WEF, 1995b. Standard Methods for the Examination of Water and Wastewater (19th edition): 4500-Cl G. DPD colorimetric method. American Public Health Association, 1015 Fifteenth Street, NW, Washington, DC 2005.
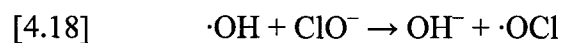
Bolton, J.R. 2006. Protocol for the measurement of irradiance using the ferrioxalate actinometer. Bolton Photosciences Inc., 628 Cheriton Cres. NW Edmonton, AB, Canada T6R 2M5.

Buxton, G.V. and Subhani, M.S. 1972. Radiation chemistry and photochemistry of oxychlorine ions: II. Photodecomposition of aqueous solutions of hypochlorite ions. *J. Chem. Soc.: Faraday Trans. I*, **68(4)**: 958–969.

Feng, Y., Smith, D.W. and Bolton, J.R. 2006. Photolysis of free chlorine (HOCl and OCl⁻) with 254 nm ultraviolet light. *J. Environ. Engng. Sci.* (in press).

Giles, M.A. and Danell, R. 1983. Water dechlorination by activated carbon, ultraviolet radiation and sodium sulphite. *Wat. Res.*, **17(6)**: 667–676.

Kashinkuti, R.D., Linden, K.G., Shin, G.A., Metz, D.H., Sobsey, M.D., Moran, M.C., Samuelson, A.M. 2004. Investigating multibarrier inactivation for Cincinnati - UV, by-products, and biostability. *J. AWWA*, **96(6)**: 114–127.

Li, H, Betterton, E.A., Arnold, R.G., Ela, W.P., Barbaris, B., and Grachane, C. 2005. Convenient new chemical actinometer based on aqueous acetone, 2-propanol, and carbon tetrachloride. *Environ. Sci. Technol.*, **39(7)**: 2262–2266.

Liu, W., Andrews, S.A., Bolton, J.R., Linden, K.G., Sharpless, C. and Stefan, M.I. 2002. Comparison of disinfection byproduct (DBP) formation from different UV technologies at bench scale. *Wat. Sci. Technol.: Wat. Supply*, **2(5–6)**: 515–521.

Mackey, E.D., Hargy, T.M., Wright, H.B., Malley, J.P. and Cushing, R.S. 2002. Comparing Cryptosporidium and MS2 bioassays – implications for UV reactor validation. *J. AWWA.*, **94(2)**: 62–69.

Nowell, L.H. and Hoigné, J. 1992a. Photolysis of aqueous chlorine at sunlight and ultraviolet wavelengths—I. Degradations rates. *Wat. Res.*, **26(5)**: 593–598.

Nowell, L.H. and Hoigné, J. 1992b. Photolysis of aqueous chlorine at sunlight and ultraviolet wavelengths—II. Hydroxyl radical production. *Wat. Res.*, **26(5)**: 599–605.

Oliver, B.G. and Carey, J.H. 1977. Photochemical production of chlorinated organics in aqueous solutions containing chlorine. *Environ. Sci. Technol.*, **11(9)**: 893–895.

Örmeci, B., Ducoste, J.J. and Linden, K.G. 2005. UV disinfection of chlorinated water: impact on chlorine concentration and UV dose delivery. *J. Wat. Supply: Res. Technol.—AQUA*, **54(3)**: 189–199.

Rahn, R.O., Stefan, M.I., Bolton, J.R., Goren, E., Shaw, P.S. and Lykke, K.R. 2003. Quantum yield of the iodide – iodate chemical actinometer: dependence on wavelength and concentration. *Photochem. Photobiol.*, **78(2)**: 146 ‑ 152.

Shen, C., Fang, S., Bergstrom, D.E. and Blatchley, E.R. 2005. (E)-5-[2-(Methoxycarbonyl)ethenyl]-cytidine as a chemical actinometer for germicidal UV radiation. *Environ. Sci. Technol.*, **39(10)**: 3826–3832.

Zheng, M., Andrews, S.A. and Bolton, J.R. 1999a. Impacts of medium-pressure UV and UV/H_2O_2 on THM and HAA formation in pre-UV chlorination drinking water. Proc.

Water Quality Technology Conference, Tampa FL, American Water Works Association, Denver, CO.

Zheng, M., Andrews, S.A. and Bolton, J.R. 1999b. Impacts of medium-pressure UV and UV/H_2O_2 treatments on disinfection byproduct formation. Proc, AWWA Annu Conf., Chicago, IL, American Water Works Association, Denver, CO.

144

Appendix 4.1 Methods for the detection of the photodegradation of free chlorine

A4.1.1 Ion chromatograph (IC)

In this study, a Dionex DX-300 Gradient Chromatography System with a Dionex Anion Self Regenerating Suppressor, a Dionex IonPac® AS9-SC (4 × 250 mm) analytical column and a Dionex IonPac® AG9-SC 4 × 50 mm guard column were used for the measurement of chloride (Cl^-), chlorite (ClO_2^-), and chlorate (ClO_3^-) ions. The 25 mN H_2SO_4 solution was used as the regenerant solution. The eluent solution was 1.8 mM Na_2CO_3/1.7 mM $NaHCO_3$ solution at a flow rate of 1 mL min^{-1}. Samples were filtered by 0.20 μm filter prior to injection to protect the analytical column from damage. During the measurement, the IC system conditions were: pressure 850 psi, background conductivity 16.5 μS, sample loop 10 μL, injection volume 200 μL. Under these conditions, the chromatograph peaks of Cl^-, ClO_2^-, and ClO_3^- ions occur at the retention time of 3.0, 3.4, and 4.5 min. The experimental procedure used for the IC measurement is briefly introduced as follows:

1. **Eluent solution and regeneration solution preparation:**

Eluent solution: dissolve 0.5712 g sodium bicarbonate ($NaHCO_3$) and 0.7632 g sodium carbonate (Na_2CO_3) in DI water, dilute this solution to 4 L with DI water, filter it by a 0.20 μm filter, and then rinse and fill the mobile phase reservoir (#1) of the IC system with the prepared eluent solution.

Regenerant solution: transfer 2.80 mL concentrated sulfuric acid (H_2SO_4, 98%) to DI water, dilute this solution to 4 L with DI water, filter the diluted H_2SO_4 solution by a

145

0.20 μm filter, and then rinse and fill the regeneration solution container of the IC system with the prepared regeneration solution.

2. Stock standard solutions preparation.

The stock standard solutions (1000 mg L^{-1}) for chloride (Cl^-), chlorite (ClO_2^-), and chlorate (ClO_3^-) measurement were prepared according to the following table:

Table 4.3 Chloride, chlorite and chlorate standard stock solution for IC method

Ion	Reagent	Weight after drying at 105°C	Stability at 4°C
Chloride (Cl^-)	NaCl	1.6485 g	1 month
Chlorite (ClO_2^-)	$NaClO_2$	1.3410 g	1 to 2 weeks
Chlorate (ClO_3^-)	$NaClO_3$	1.2753 g	1 month

The IC standard curves used for the calculation of the concentration of the target ions in samples were determined by standard solutions which were diluted from these stock solutions.

3. Sample preparation.

The samples taken from the photodegradation of free chlorine experiments were analyzed as soon as possible in this study. Before injected into the IC system, the samples were filtered by a 0.20 μm filter. When the concentration of chloride or chlorate ions could be very high ($Cl^- > 40$ mg L^{-1} or $ClO_3^- > 10$ mg L^{-1}), the filtered samples also were diluted by DI water (filtered by 0.20 μm filter).

4. Turn on the IC system.

Turn the gas cylinders, computer, and IC system sequentially. The pressure of helium gas should be set at 209 kpa and nitrogen gas should be at 558 kpa. Then, set the IC system to appropriate status and stabilize the system for about 20 minutes.

146

5. Sample measurement.

In the beginning of each measurement, inject 0.20 μm filtered DI water to the system for 2 to 3 times to clean the system and then, inject samples to the IC system to start the measurement. After the use of the IC system, the filtered DI water was employed for 2 to 3 times to clean the system again.

6. Export the experimental results and turn off the system.

A4.1.2 Argentometric method

The argentometric method (APHA et al., 1995) was selected for the chloride ions determination when the water quality was not suitable for IC measurement. In this method, a standard silver nitrate solution (0.0141 N) was prepared as titrant by dissolving 2.395 g silver nitrate ($AgNO_3$) in DI water and diluting to 1000 mL. The standard titrant was standardized by standard sodium chloride (NaCl) solution (0.0141 N), which was prepared by dissolving 824.0 mg NaCl (dried at 140°C) in DI water and diluting to 1000 mL. The potassium chromate (K_2CrO_4) solution treated by $AgNO_3$ was used as the titration indicator. With the addition of about 1 mL of K_2CrO_4 titration indicator, samples were directly titrated by $AgNO_3$ titrant in the pH range 7 to 10. Sulfuric acid (H_2SO_4) and sodium hydroxide (NaOH) solution were used to adjust the sample pH if it was not in this range. The titration was completed when the sample solution became pinkish yellow.

Appendix 4.2 Determination of the quantum yield of the photodegradation of free chlorine at wavelengths other than 254 nm

The experimental method and the calculation process used for the determination of the photodegradation of free chlorine at the UV light other than 254 nm are very similar to those employed at 254 nm described in Chapter 3. The only difference between these two cases is the method utilized for the UV irradiance measurement. In the experiments with 254 nm UV light, the UV irradiance was measured directly by a radiometer in which the UV detector was calibrated at 254 nm and its sensitivity varies with the wavelength. However, when the wavelength of the UV light used in experiments was not 254 nm, the irradiance still was measured by the radiometer. A sensor factor should be applied to correct the reading of the radiometer. In addition, in order to check the reliability of the irradiance measured by the radiometer (corrected by sensor factor), the ferrioxalate actinometer was also used for the determination of the irradiance at the UV light other than 254 nm. The determination of the sensor factor and the ferrioxalate actinometry method are introduced below.

A4.2.1 Sensor factor

In an experiment for the determination of the quantum yield of free chlorine exposed to UV light other than 254 nm, the sensor factor was determined in this study according to the following steps:

1. Determination of the spectral irradiance.

Sensor factor is the sensitivity at 254 nm divided by the weighted average sensitivity of the radiometer detector over the considered UV light wavelength band. In

this research, the monochromatic UV light (other than 254 nm) at each wavelength was produced by a medium-pressure (MP) UV lamp and a corresponding UV filter. It should be noted that the so-called monochromatic light here is not absolutely monochromatic. As shown in Figure 4.17, the wavelength band of 270 nm UV light generated by the MP lamp and a 270 nm UV filter actually ranges from 260 to 280 nm. The radiometer used to measure the UV irradiance was calibrated at 254 nm and its sensitivity varies with wavelength. In order to determine the real UV irradiance incidents at the studied wavelength, the sensor factor should be determined to correct the measurement of the radiometer. For the determination of sensor factor, the first step needs to determine the spectral irradiance of the studied UV wavelength band. In this research, the spectral irradiance was measured by a spectrometer (USB 4000-UV-Vis spectrometer, Ocean Optics Inc., Dunedin, FL). In each measurement, the spectrometer should be set a blank reference under the background light (natural light or illuminating light) of the laboratory where the experiment is performed. Then, the detector needs to be fixed vertically under the UV light on the same position where the detector of the radiometer is put on for the irradiance measurement. At last, open the software of OOIIrrad2beta (Ocean Optics Inc., Dunedin, FL), turn on the pneumatic shatter of UV generation system to let UV light irradiate to the detector, measure the spectral irradiance and save the determined data.

sensitivity of the detector at the wavelength λ nm. In this research, the sensor factors were calculated by a MS Excel™ spreadsheet. Here, the calculation of the sensor factor at 270 nm is given as an example to show the calculation process.

As shown in Figure 4.17, the wavelength of the UV light generated by the MP lamp and the 270 nm UV filter ranges from about 245 to 295 nm. When the wavelength is higher than 295 or lower than 245, the spectral irradiance is almost zero. Table 4.3 gives the results measured by the spectrometer in this condition.

Table 4.4 The spectral irradiance of the wavelength band generated by the MP lamp and a 270 nm UV filter

λ / nm	Irrad.	λ / nm	Irrad.	λ / nm	Irrad.	λ / nm	Irrad.	λ / nm	Irrad.
244.91	0.00	255.89	0.37	266.84	2.92	277.76	1.11	288.65	0.05
245.29	0.01	256.27	0.43	267.22	2.90	278.14	0.98	289.02	0.05
245.66	0.01	256.64	0.50	267.59	2.88	278.51	0.93	289.40	0.05
246.04	0.02	257.02	0.59	267.97	2.85	278.89	0.92	289.77	0.05
246.42	0.04	257.40	0.68	268.35	2.85	279.26	0.92	290.15	0.05
246.80	0.06	257.78	0.77	268.72	2.82	279.64	0.93	290.52	0.05
247.18	0.08	258.16	0.86	269.10	2.80	280.02	0.94	290.90	0.05
247.56	0.09	258.53	0.95	269.48	2.78	280.39	0.95	291.27	0.04
247.94	0.11	258.91	1.03	269.85	2.75	280.77	0.93	291.65	0.03
248.32	0.11	259.29	1.10	270.23	2.73	281.14	0.91	292.02	0.02
248.70	0.12	259.67	1.16	270.61	2.71	281.52	0.87	292.40	0.02
249.08	0.12	260.05	1.21	270.99	2.67	281.89	0.81	292.77	0.01
249.45	0.12	260.42	1.26	271.36	2.55	282.27	0.73	293.15	0.01
249.83	0.12	260.80	1.30	271.74	2.43	282.64	0.60	293.52	0.01
250.21	0.12	261.18	1.35	272.11	2.30	283.02	0.45	293.89	0.00
250.59	0.12	261.56	1.42	272.49	2.17	283.40	0.33	294.27	0.00
250.97	0.12	261.93	1.52	272.87	2.07	283.77	0.23	294.64	0.01
251.35	0.12	262.31	1.67	273.24	2.00	284.15	0.16	295.02	0.01
251.73	0.14	262.69	1.84	273.62	1.99	284.52	0.10	295.39	0.01
252.10	0.16	263.07	2.01	274.00	1.98	284.90	0.08	295.77	0.01
252.48	0.17	263.44	2.16	274.37	1.94	285.27	0.06	296.14	0.02
252.86	0.17	263.82	2.32	274.75	1.87	285.65	0.05	296.51	0.02
253.24	0.18	264.20	2.44	275.13	1.78	286.02	0.04	296.89	0.02
253.62	0.19	264.58	2.58	275.50	1.73	286.40	0.04	297.26	0.02
254.00	0.20	264.95	2.70	275.88	1.66	286.77	0.04	297.64	0.02
254.38	0.22	265.33	2.81	276.26	1.59	287.15	0.04	298.01	0.02
254.75	0.25	265.71	2.90	276.63	1.51	287.52	0.04	298.38	0.02
255.13	0.28	266.08	2.95	277.01	1.41	287.90	0.05	298.76	0.02
255.51	0.32	266.46	2.95	277.38	1.27	288.27	0.05	299.13	0.01

151
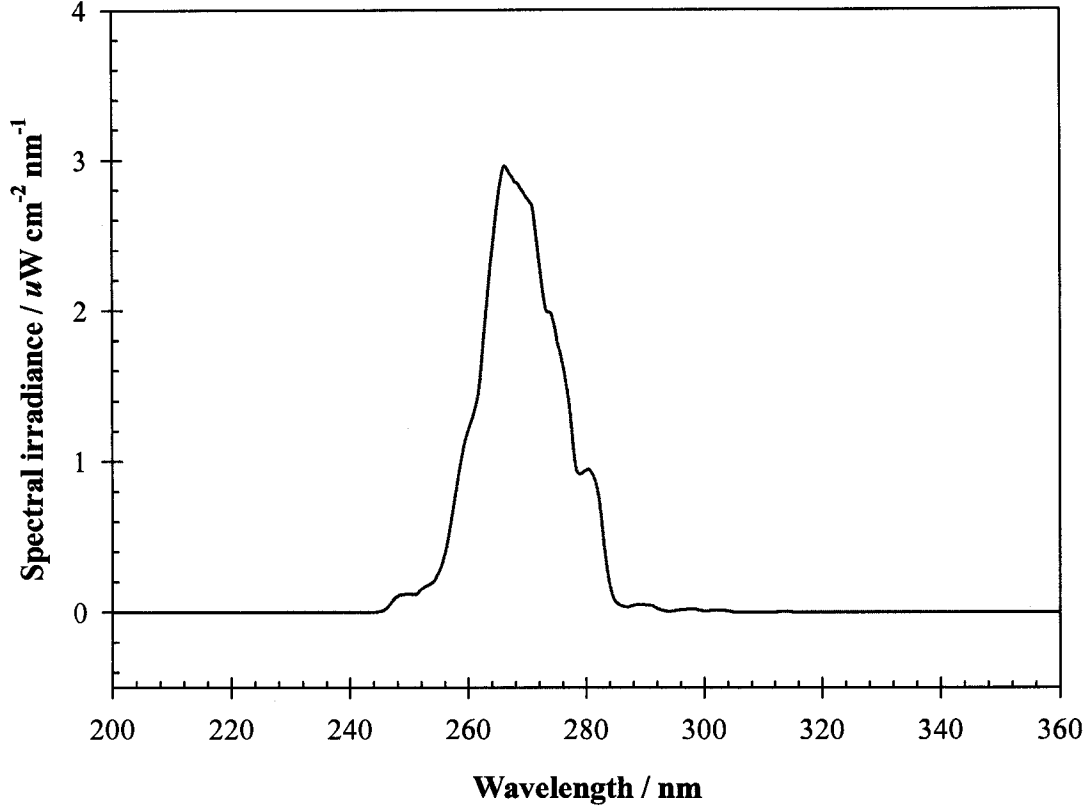
Figure 4.17 Spectral irradiance of UV light generated by the MP lamp and a 270 nm UV filter

2. Calculation of the sensor factor.

Sensor factor is calculated based on the following equation:

$$[4.24] \qquad \text{Sensor factor} = \frac{s_{254}}{\bar{s}}; \qquad \bar{s} = \frac{\sum_i N_i(\lambda)s_i(\lambda)}{\sum_i N_i(\lambda)}$$

where, s_{254} is the sensitivity of the detector of radiometer at 254 nm, $\bar{s}$ is the weighted average sensitivity of radiometer detector over the considered wavelength band, $N_i(\lambda)$ is the relative photon flow in a given wavelength band (e.g., 5 nm), and $s_i(\lambda)$ is the

150

The spectral sensitivity of the detector can be obtained from the radiometer manufacturer and the spectral sensitivity relative to 254 nm also can be calculated based on the spectral sensitivity. Table 4.4 shows the spectral sensitivity relative to 254 nm of the detector from 245 to 299 nm.

Table 4.5 The sensor spectral sensitivity relative to 254 nm for the wavelength ranging from 244.91 to 299.13 nm

λ / nm	Rel. sens.	λ / nm	Rel. sens.	λ / nm	Rel. sens.	λ / nm	Rel. sens.	λ / nm	Rel. sens.
244.91	0.99	255.89	0.99	266.84	0.91	277.76	0.76	288.65	0.47
245.29	1.00	256.27	0.99	267.22	0.91	278.14	0.76	289.02	0.46
245.66	1.00	256.64	0.99	267.59	0.90	278.51	0.75	289.40	0.45
246.04	1.00	257.02	0.99	267.97	0.89	278.89	0.74	289.77	0.44
246.42	1.00	257.40	0.98	268.35	0.89	279.26	0.73	290.15	0.43
246.80	1.01	257.78	0.98	268.72	0.89	279.64	0.72	290.52	0.42
247.18	1.01	258.16	0.98	269.10	0.88	280.02	0.71	290.90	0.42
247.56	1.02	258.53	0.97	269.48	0.88	280.39	0.70	291.27	0.41
247.94	1.02	258.91	0.97	269.85	0.88	280.77	0.69	291.65	0.40
248.32	1.03	259.29	0.97	270.23	0.87	281.14	0.68	292.02	0.39
248.70	1.03	259.67	0.96	270.61	0.87	281.52	0.67	292.40	0.38
249.08	1.04	260.05	0.96	270.99	0.86	281.89	0.66	292.77	0.37
249.45	1.04	260.42	0.96	271.36	0.86	282.27	0.65	293.15	0.36
249.83	1.04	260.80	0.96	271.74	0.85	282.64	0.64	293.52	0.35
250.21	1.04	261.18	0.96	272.11	0.85	283.02	0.64	293.89	0.34
250.59	1.04	261.56	0.96	272.49	0.85	283.40	0.63	294.27	0.34
250.97	1.03	261.93	0.95	272.87	0.84	283.77	0.62	294.64	0.33
251.35	1.03	262.31	0.95	273.24	0.84	284.15	0.61	295.02	0.32
251.73	1.02	262.69	0.95	273.62	0.84	284.52	0.60	295.39	0.31
252.10	1.02	263.07	0.95	274.00	0.84	284.90	0.59	295.77	0.30
252.48	1.02	263.44	0.95	274.37	0.82	285.27	0.58	296.14	0.29
252.86	1.01	263.82	0.95	274.75	0.81	285.65	0.57	296.51	0.28
253.24	1.01	264.20	0.95	275.13	0.80	286.02	0.56	296.89	0.28
253.62	1.00	264.58	0.94	275.50	0.78	286.40	0.54	297.26	0.27
254.00	1.00	264.95	0.94	275.88	0.76	286.77	0.53	297.64	0.26
254.38	1.00	265.33	0.94	276.26	0.76	287.15	0.52	298.01	0.25
254.75	1.00	265.71	0.93	276.63	0.76	287.52	0.51	298.38	0.24
255.13	1.00	266.08	0.93	277.01	0.76	287.90	0.49	298.76	0.23
255.51	1.00	266.46	0.92	277.38	0.76	288.27	0.48	299.13	0.22

Then based on Eq. 4.24, the relative flux at the wavelength λ nm, $N_i(\lambda)$, can be calculated. For example, from 244.91 to 245.29 nm, the spectral irradiance can be treated as a constant (here, it is 0.0046 μW cm^{-2} nm^{-1}) and the nominal wavelength is (244.91 + 245.29)/2 = 245.10 nm. So, the relative flux at this point is 0.0046 * 245.10 = 1.1275 μW cm^{-2}. In the same way, the relative flux from 244.91 to 299.13 nm can be calculated and the total relative flux, $\sum_i N_i(\lambda)$, also can be determined. For this example, the total relative flux is 35109 uW cm^{-2}. The sensitivity flux, $N_i(\lambda)s_i(\lambda)$, can also be calculated easily based on the relative flux and the sensor spectral sensitivity relative to 254 nm at the corresponding wavelength. For example, from 244.91 to 245.29 nm, the sensitivity flux is 1.1275 μW cm^{-2} * 0.99 = 1.1162 μW cm^{-2}. In the same way, the sensitivity flux from 244.91 to 299.13 nm can be calculated and the total sensitivity flux, $\sum_i N_i(\lambda)s_i(\lambda)$, also can be determined. For this example, the total sensitivity flux is 30523 uW cm^{-2}. According to Eq. 4.24, the weighted average sensitivity at 270 nm can be obtained:

$$\bar{s} = 30523/35109 = 0.869$$

Because the relative sensitivity of the radiometer to 254 nm UV light is 1, the sensor factor at 270 nm can be determined as:

Sensor factor = 1/0.869 = 1.15

A4.2.2 Ferrioxalate actinometer

The potassium ferrioxalate actinometer is one of the most widely used standard actinometer, which is based on the photo-reduction of iron, according to the following equation:

153

$$Fe(C_2O_4)_3{}^{3-} + h\nu \longrightarrow Fe^{2+} + 2.5\,C_2O_4{}^{2-} + CO_2$$

The quantum yield of Fe^{2+} production is essentially independent of wavelength in the range $220 - 320$ nm at 1.25. In this research, the experiments using ferrioxalate actinometer to determine the UV irradiance at various wavelengths followed the protocol provided by Dr. Bolton (Bolton Photosciences Inc., Edmonton, AB). Because ferrioxalate absorbs strongly in the range from 200 to 600 nm, the experiments were performed in a "dark room" with a red "safety" photographic lamp.

CHAPTER 5 APPLICATION OF THE PHOTODEGRADATION OF FREE CHLORINE AS A NEW METHOD FOR THE VALIDATION AND ONLINE MONITORING OF UV REACTORS IN DRINKING WATER TREATMENT

5.1 Introduction

Ultraviolet (UV) disinfection has been widely accepted throughout the world as an effective technology for the protection of public health against most pathogens and some chemical contaminants in drinking water treatment. A key component in the design and operation of UV reactors is to verify if they can deliver the targeted fluence (UV dose) to achieve the design disinfection levels under various operating conditions. Biodosimetry, the use of microbiological response as an indicator of the UV irradiation, is a widely used method for the validation of UV reactors. This is the most reliable method available at present for the full-scale validation of UV reactors and is often specified as an important validation method by some regulatory bodies (USEPA 2003, DVGW 1997 and ÖNORM 2003).

However, in practice, biodosimetry is not an all-powerful method for the measurement of fluence delivery. As reviewed in Chapter 2, it has some distinct limitations or disadvantages. For example, the reliability of this method has not been extensively tested for UV reactors with large flow rates (more than 90 ML d^{-1}) (Mamane-Gravetz and Linden 2004), and the sensitivity of biodosimeter challenge microorganism and the fluence distribution in UV reactors may affect the accuracy of the validation

155

results (Cabaj et al. 1996, Wright and Lawryshyn 2000 and Mackey et al. 2002). Therefore, some other methods have been suggested for the validation of UV reactors. For example, some have proposed using indigenous microbes to replace the laboratory cultured surrogates in biodosimetry (Blatchley and Hunt 1994, Nieminski et al. 2000 and Mamane-Gravetz and Linden 2004); others have applied mathematic models, validated by biodosimetry, for the monitoring of UV reactor performance (Severin et al. 1983, Blatchley et al. 1998, Bolton 2000, Lawryshyn and Cairns 2003, Fenner and Komvuschara 2005); still others have advised employing some chemical actinometers for the determination of fluences delivered in UV reactors (Harris et al. 1987, Linden et al. 1998, Stefan et al. 2001 and Rahn et al. 2006). Although these proposed methods provide some improvements in certain aspects, there still are some limitations, as described in Chapter 2.

According to the investigation of the quantum yield of the photodegradation of free chlorine (Chapter 3) and the influencing factors and photo-products (Chapter 4), the photodegradation of free chlorine (hereinafter called the PFC method) may be employed as a convenient and new method for the determination of UV reactor performance. In this method, for the validation of a given UV reactor, one need only determine the quantum yield for the photodegradation of free chlorine in a given water matrix and the amount of free chlorine degraded when the water matrix flows through the UV reactor. The fluences delivered in the validated UV reactor can then be obtained by a very simple calculation process, which is introduced below. Since the quantum yield for the photodegradation of free chlorine can be determined easily and quickly, this new PFC method should be much easier to perform and validation results should be obtained much faster than in the case

156

for biodosimetry methods. In addition, since the multi-barrier disinfection process of prechlorination followed by UV treatment is often used in water utilities, and no serious harmful by-products are produced in the photodegradation of free chlorine, the PFC validation method should be much cleaner than those using chemical actinometers, such as uridine, ferrioxalate and iodide/iodate, as proposed by previous researchers. Finally, this new approach could provide an idea to develop an 'online' continuous method for the determination of fluence (UV dose) in operating UV reactors.

Therefore, following the investigation of the quantum yield of photodegradation of free chlorine in previous chapters, the objective of this chapter is to study the possibility of using the photodegradation of free chlorine (the PFC method) to determine the fluences delivered in UV reactors. The research scope is mainly to

1. Use a 'standard' biodosimetry method using *Bacillus subtilis* spores as the challenge microorganism (hereinafter called the BD method) as a control to determine the reduction equivalent fluence (REF). This requires determining the survival curve (fluence-response curve) of the *Bacillus subtilis* spores used for the BD method;

2. Validate the experimental UV reactor using the BD method under various operating conditions;

3. Validate the same UV reactor using the PFC method for the same corresponding operating conditions as for the runs using the BD method; and

4. Compare the validation results obtained by these two methods and carry out an analysis regarding the effects of the operating conditions (e.g., UV transmittance, flow rate, and water quality) on the proposed new PFC validation method.

157

5.2 Materials and methods

5.2.1 Specification of the UV reactor used in the validation experiment

Figure 5.1 shows visually the UV reactor that was used in the validation experiments. This UV reactor was obtained from Wyckomar Inc. (Guelph, ON Canada) and Table 5.1 lists its specifications. In the validation study, the fluences delivered in this UV reactor under different operating conditions were determined by the free chlorine method and biodosimetry method. The experimental results were compared with each other and the reliability of the proposed validation method was evaluated.
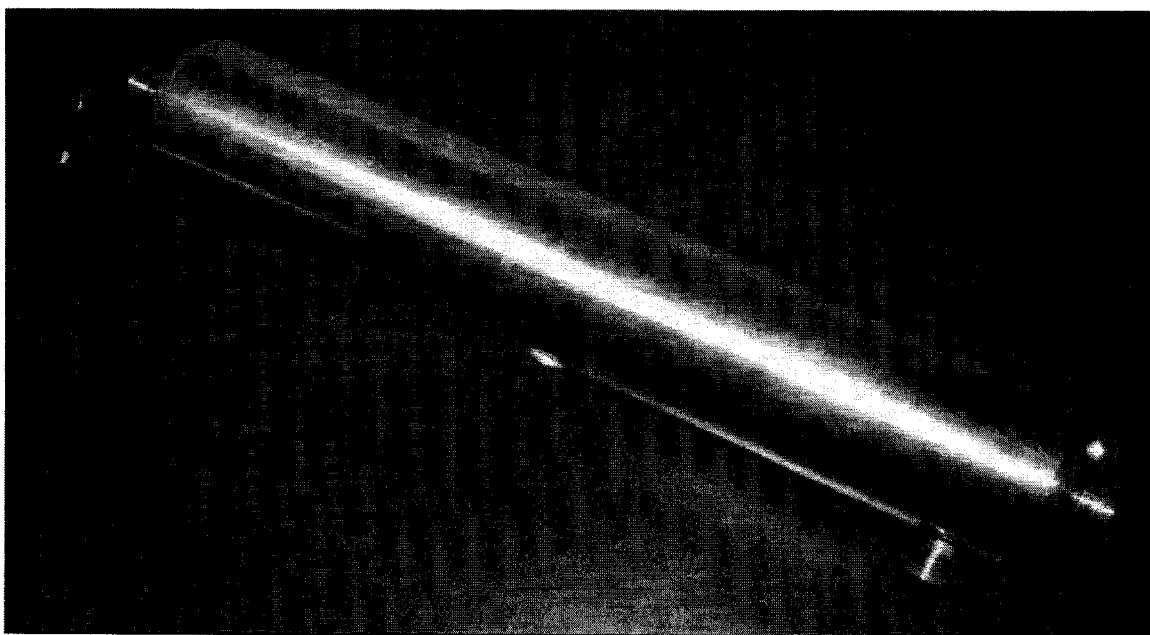
Figure 5.1 View of the UV reactor (provided by Wyckomar Inc.) used in the validation experiment

158

Table 5.1 Specifications of the UV reactor used in the validation experiment

Reactor size:	
Reactor length	480 mm
Reactor internal diameter	90 mm
Lamp length	360 mm
Lamp sleeve radius	12.7 mm
UV lamp:	
Number of lamps:	1
Model:	M1-G1-15
Power:[18]	1.84 W
Electrical:	
Ballast part number	BE1200-1
Input	120 V @ 60 Hz
Lamp current	800 mA

5.2.2 Preparation of water samples

In this research, the validation experiments were conducted using two different water matrices (W1 and W2) with different qualities. The W1 water was obtained from the local distilled water producing system. Its quality was better than tap water, but not as good as DI water. The pH of the W1 water was ~7.2 and the TOC varied from 0.8 to 1.2 mg/L. The W2 water was a synthetically prepared drinking water according to the recipe of Liu et al. (2002), as given in Table 5.2. The pH of the synthetic water was ~8.6 and the TOC was at the range of 3.2 to 3.8 mg/L.

---

[18] In order to get an appropriate fluence rate in this experiment, a paper filter was used to cover the UV lamp to reduce the irradiance of the UV lamp. The power listed here is the value after the UV lamp was covered.

159

Table 5.2 The components of synthetic drinking water (W2)

	Ca^{2+}	Mg^{2+}	Na^+	$(CO_3)_{TOT}$	NO_3^-	Cl^-	SO_4^{2-}	Humic acid	Alginic acid
mg/L	29.1	10.0	36.2	90.0	3.0	40.0	55.0	2.56	5.32

When the PFC method was used for the validation experiments, the water matrix with free chlorine was prepared as follows:

1. Collect ~150 L of W1 or W2 water in a 200 L reservoir.

2. Transfer an appropriate aliquot of fresh sodium hypochlorite solution (5.65 to 6%, Fisher Scientific Co.) to the reservoir and mix thoroughly (the concentration of free chlorine in the reservoir should be about 3.2 mg L^{-1}).

3. Add a UV absorber into the water matrix if necessary.

4. Adjust the pH of the water matrix in the range of 7.0 to 7.5 by adding 0.1 N sulfuric acid or 0.1 N sodium hydroxide solutions (Fisher Scientific Co.).

5. Put a lid on the reservoir and let the water stand for about 15 h to allow the water matrix to stabilize.

In the PFC method, the UV absorber used for the adjustment of UV transmittance of the test water should be selected carefully. It is required to cut down the UV light effectively and also should not be photodegraded by UV light or be oxidized by free chlorine. The ferric ion (Fe^{3+}) was observed to absorb the UV light significantly and its molar absorption coefficient is about 4,700 M^{-1} cm^{-1} (Bolton et al. 2001). In addition, ferric ions are in the steady reduced state and it cannot be oxidized by free chlorine or photodegraded by UV light. Therefore, in this study the ferric sulfate solution was used as the UV absorber to test the effect of UV transmittance on the validation results

160

determined by the decomposition of free chlorine. Some ferric oxide precipitate can be generated when a high concentration of ferric sulfate (low UV transmittance) is in the water matrix. Therefore, during the experimental process, the water matrix was always given sufficient mixing to keep the water quality homogenous.

In the validation experiments using the BD method, the water matrices were prepared in the almost same way as those used in the PFC method. However, in this case chlorine was not added to the water, and in order to avoid any possible adverse effect of ferric ions on the metabolism of *B. subtilis*, coffee (instant coffee, powder, Maxwell House™, bought from a grocery store) was used to adjust the UV transmittance of the test water. The coffee solution was prepared by adding 25 g of instant coffee into a 1000 mL Erlenmeyer flask with 500 mL DI water, and putting it on a laboratory stirrer/hot plate (Corning®, Model: PC-420, Fisher Scientific Co.). While stirring, the coffee solution was heated to boiling for about 5 minutes and then cooled down to ambient temperature (~22°C). After the coffee solution was prepared in this manner, the Erlenmeyer flask was covered with aluminum foil and stored in a refrigerator at 4°C prior to experimental use. In each run, an appropriate aliquot of the stock coffee solution was added into the water matrix to achieve the intended UV transmittance.

During the BD validation process, the challenge microorganisms (10^5 to 10^7 CFU mL^{-1}) were not added directly into the water matrix but were maintained in a separate container; they were subsequently injected [using a peristaltic pump (Model No. 7553-71, Masterflex®, Cole-Parmer Instrument Company, Concord, ON Canada)] into the water matrix just before flowing through the validated UV reactor.

161

5.2.3 Determination of the quantum yield of photodegradation of free chlorine

In this study, the quantum yield of photodegradation free chlorine was determined using a collimated beam apparatus with a 10 W low-pressure UV lamp, as described in Section 3.2.4, and the quantum yield was calculated using the method given in Section 3.2.6. The DPD method, used for the measurement of the free chlorine concentration, was described in Section 3.2.5.

5.2.4 Fluence (UV dose) measurement by the photodegradation of free chlorine

As studied in the Chapter 3, when the concentration of free chlorine is not very high, the photodegradation of free chlorine can be described as a first-order reaction:

$$[5.1] \qquad \ln\frac{[C]_0}{[C]_{H'}} = k_1' H'$$

where, $[C]_0$ and $[C]_{H'}$ are the free chlorine concentrations (mg L^{-1}) before and after exposure to the UV light, respectively, at the fluence of H' (J m^{-2}) and k_1' is the fluence-based first-order rate constant (m^2 J^{-1}). Here the value of k_1' depends on the quantum yield and molar absorption coefficient of free chlorine samples can be calculated according to (Bolton and Stefan, 2003):

$$[5.2] \qquad k_1' = \frac{\Phi \varepsilon \ln(10)}{10 U_\lambda}$$

where, Φ is the quantum yield of photodegradation of the free chlorine in the water sample, ε is the molar absorption coefficient (M^{-1} cm^{-1}) of free chlorine and U_λ is the molar photon energy (J $einstein^{-1}$) at wavelength λ.

162

Since the quantum yield Φ and molar absorption coefficient ε of the free chlorine can be determined in advance and U_λ is a constant for a given UV wavelength, the fluence-based first-order rate constant (k_1') can be calculated according to Eq. 5.2. In addition, when the test water with free chlorine flows through the validated UV reactor, the natural log of the free chlorine photodegradation ratio, $\ln\{[C]_0/[C]_{H'}\}$, also can also be determined easily. Therefore, the fluence (UV dose) delivered in the validated UV reactor can be obtained by modifying Eq. 5.1 to

$$[5.3] \qquad H' = \frac{1}{k_1'} \ln \frac{[C]_0}{[C]_{H'}}$$

5.2.5 Production and enumeration of *Bacillus subtilis* spores

In this study, *Bacillus subtilis* spores (ATCC 6633, American Type Culture Collection, Manassas, VA.) were used as the challenge microorganism for the BD tests. This is a strain of a non-pathogenic microorganism that has been used extensively for the validation of UV reactors (DVGW 1997, USEPA 2003 and Sommer *et al.* 1998). Stock solutions of *B. subtilis* were propagated by the Schaeffer's media method (Munakata and Rupert 1972, Sommer et al. 1995, DVGW 1997, and Leighton and Doi 1971) with some modifications. All experimental steps involving exposing *B. subtilis* spores to air were performed in a microorganism cabinet (Model 1284, Class II A/B3 Biological Safety Cabinet, Forma Scientific Co., Marietta OH) in order to avoid the accidental contamination. In addition, all glassware used to contain or transfer the *B. subtilis* solution was autoclaved at 121°C for 15 minutes; pre-sterilized plastic Petri dishes and volumetric pipettes were used for the microorganism growth.

Initially, the *B. subtilis* pre-culture was prepared by scratching an isolated *B. subtilis* colony from a streaked plate and inoculating the isolate to sterilized pre-culture media, which consisted of 8 g L^{-1} nutrient broth (BBL Nutrient Broth, Benton Dickinson Microbiology Systems, Cockeysville, MD), 0.25 g L^{-1} MgSO$_4$·7H$_2$O (analytical reagent, Fisher Scientific Co.), and 1.00 g L^{-1} KCl (analytical reagent, Fisher Scientific Co.). The mixture of pre-culture media and *B. subtilis* was incubated at 37°C on a shaker table (Innova™ 4080, New Brunswick Instruments Co. Inc., Edison, NJ) at 180 rpm for ~12 h. The culture should be in the log phase growth when used to inoculate spore production media. Subsequently, the *B. subtilis* spores were produced from the pre-cultures in the modified Shaeffer's Media, which was prepared by adding 1 mL/1000 mL of a filter-sterilized (0.22 μm, Millipore, Billerica, MA) solution of 1 mM FeSO$_4$, 10 mM MnCl$_2$, and 1 M CaCl$_2$ to sterile nutrient broth (sterilized at 121°C for 15 minutes). The mixture of growth media with the *B. subtilis* pre-culture was incubated at 37°C on a shaker table at 200 rpm for 72 h. Once completing the sporulation, the *B. subtilis* spores were harvested by centrifugation (Sorvall® RC-5B Refrigerated Superspeed Centrifuge, Mandel Scientific Company Ltd.) at 7500 RCF for 20 min at 4°C. The supernatant was decanted, the pellets were re-suspended in sterilized DI water and then centrifuged again. This process was repeated at least three times until the supernatant became clear and the pellets were mainly white in appearance. Once this process was completed, the pellets were re-suspended again in sterilized DI water and pasteurized in a water bath at 80°C for 30 minutes with intermittent swirling of the solution. The stock solution of *B. subtilis* was finally re-suspended in a 50% ethanol solution, homogenized (PowerGen 700, Fisher Scientific, Pittsburgh, PA) and stored at 4°C. The concentration of spores in the stock

164

solutions used for this study was ~1.0 × 10^9 CFU mL^{-1}. The presence of spores in the stock solution was verified using Schaeffer – Fulton staining and phase-contrast microscopic examination.

The *B. subtilis* spores in the stock solution and in experimental water samples were enumerated by the 'pour plate' method, namely

1. A decimal dilution series of the stock or sample was prepared. A serial dilution began with a 1 mL aliquot of the sample into a 9 mL dilution blank (sterile DI water) to yield 10 mL of a 10^{-1} diluted sample.

2. The solution was vortex mixed (Genie 2 Fisher Vortex, Fisher Scientific Co.) for about 1 minute, and 1 mL of the diluted sample was transferred to second 9 mL dilution blank to yield 10 mL of a 10^{-2} diluted sample, and so on through the dilution series.

3. To prepare a plate, a 1 mL aliquot of the desired decimal diluted sample was transferred to a sterilized Petri dish (100 mm × 15 mm, Fisherbrand®, Fisher Scientific Co.); then ~15 mL of 1.6% sterilized molten nutrient agar (Difo Laboratories, Detroit, MI) was poured into the dish. The contents of the dish were gently but thoroughly mixed by tilting the plate back-and-forth and side-to-side ten to twenty times. Finally, the solidified agar plates were incubated at 37°C for 48 to 72 h, and the colony forming units (CFU) were counted. All plating and enumerations were carried out in triplicate in this study.

165

5.2.6 Determination of the sensitivity of *B. subtilis* to UV light

In this study, the determination of the sensitivity of *B. subtilis* to UV light was very important to the BD experiments. The sensitivity, expressed as the UV fluence-response curve of *B. subtilis* spores, was determined as follows:

1. Exposure of the challenge microorganism for a period of time to UV light.

2. Incubation and enumeration of the UV-exposed sample.

3. Determination the log reductions of *B. subtilis* spores for various fluences.

A collimated beam apparatus with a 10 W low-pressure UV lamp was used for the determination of the UV fluence-response curves. The experimental procedures used to expose *B. subtilis* spore samples to UV light were same as those used for the exposure of free chlorine samples, which was described in Chapter 3. The irradiated challenge microorganism samples were incubated and enumerated according to the method stated above. In each run, based on the concentrations of *B. subtilis* spores before and after exposure to UV light, the log (decadic) reductions for various fluences were calculated. Then the UV fluence-response curve was plotted as log reduction versus the corresponding fluences.

5.3 Experimental system for the validation experiments

5.3.1 Introduction

The experimental system used for the validation experiments is shown in Figure 5.2. The water matrix was prepared according to the method given above and stored in the container C1 (200 L plastic barrel with a lid). The concentrated *B. subtilis* solution ($\sim 10^7$ CFU/mL) used in the BD experiments was stored in a C2 (Nalgene® round carboy

166

with spigot, 10 L, Fisher Scientific Co.) that was put on a magnetic stirrer to maintain sufficient mixing. Container C3 (200 L plastic barrel with a lid) was used to collect the effluent from the experimental system. Before being discharged, this biohazard effluent was treated by adding enough bleach solution (about 500 mg L^{-1}) and was stored for 2 to 3 days to make sure that all *B. subtilis* spores in the effluent were inactivated. A static in-line mixer (Model 3/4-40C-4-6-2, Koflo Corporation, Cary, IL) was installed before the validated UV reactor to make sure that the concentrated *B. subtilis* spores from C2 were sufficiently mixed with the water matrix from C1, and a flow meter (Model: 9904, Cole-Parmer Instrument Company, Concord, ON Canada) was used to measure the total flow rate in the experimental system. Two peristaltic pumps, P1 (Model No. 7591-60, Masterflex®, Cole-Parmer Instrument Company, Concord, ON Canada) and P2 (Model No. 7553-71, Masterflex®, Cole-Parmer Instrument Company, Concord, ON Canada), were used to pump the water matrix from C1 and *B. subtilis* spores from C2 flowing through the UV reactor. Some two-way valves (20.5″ DN15, U-PVC, Cole-Parmer Instrument Company, Concord, ON Canada) were used in the system to control the flow rate and the flow direction. Also, some pieces of IPS PVC pipe (6.2 mm ID, Cole-Parmer Instrument Company, Concord, ON Canada) and Fisherbrand® tubing (15.9 mm ID × 3.2 mm wall, Fisher Scientific Co.) were used to connect the parts (such as the UV reactor, pumps, and static mixer, etc.) in the system. In each experimental run, the water samples were taken from the sample ports, SP1 and SP2, as influent and effluent samples for the UV reactor.
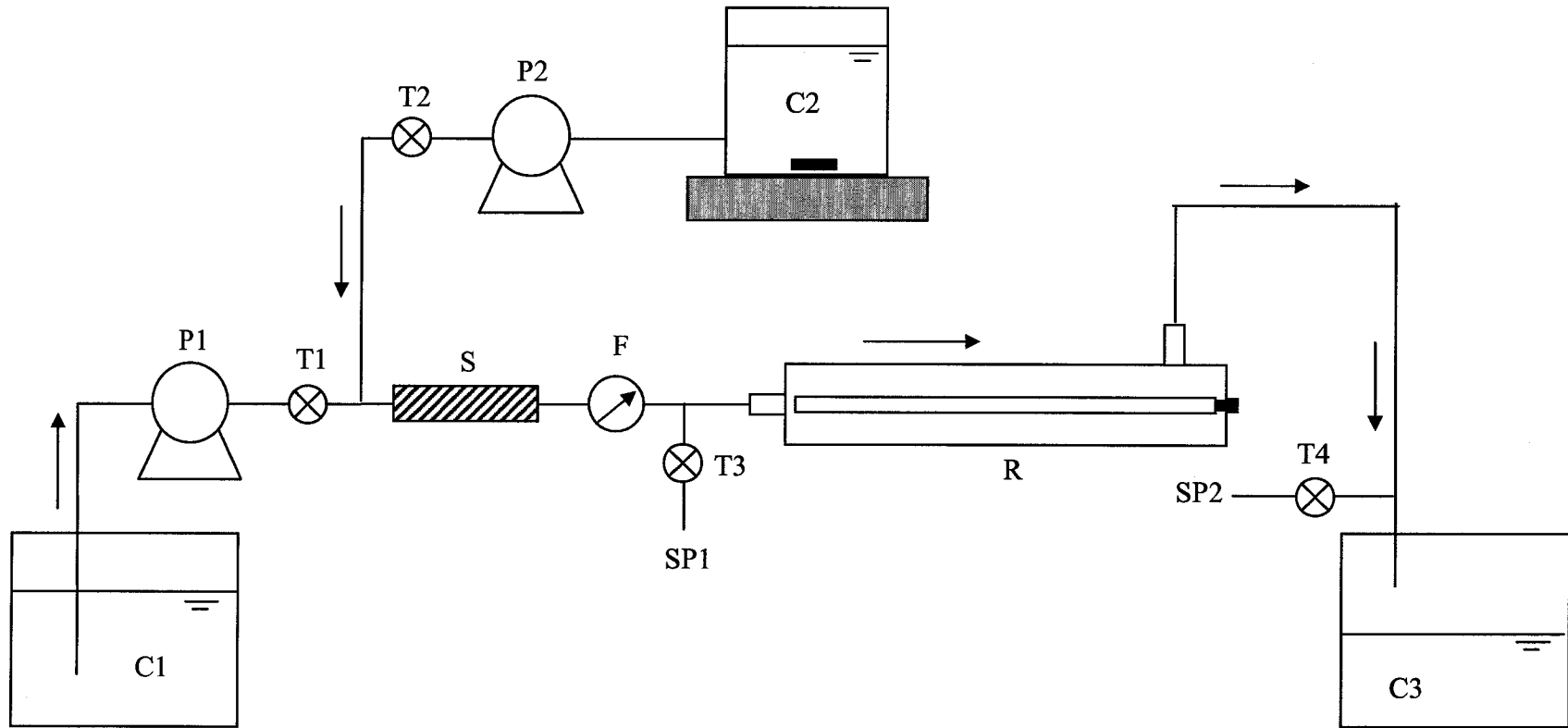
Figure 5.5 Schematic diagram of the experimental system (C1, C2 and C3 are the containers for the water matrix, concentrated *B. subtilis* solution and wastewater, respectively; P1 and P2 are peristaltic pumps; T1, T2, T3 and T4 are two-way valves; S is the static mixer; F is a flow meter; SP1 and SP2 are the sample ports; and R is UV reactor to be validated with a low-pressure UV lamp)

5.3.2 Experimental operation procedure

When the UV reactor was validated by biodosimetry, the water matrix and concentrated *B. subtilis* solution ($\sim 10^7$ CFU mL^{-1}) were first prepared and, respectively, put into reservoirs C1 and C2. Then, the pumps, P1 and P2, were adjusted to obtain the design flow rate, and to assure that the concentration of *B. subtilis* spores in the influent was in the range of 10^3 to 10^5 CFU mL^{-1}. The concentrations of *B. subtilis* spores varied according to the UV transmittance and the flow rate applied in the validation process. The clearer the test water and the slower the flow rate, the higher the concentration of *B. subtilis* spores was needed in the experiment. The UV lamp was switched on and subsequently, the pump P1 was turned on to pump the test water flowing from C1 through the validated UV reactor for about 10 minutes. When the hydraulic condition in the system and UV lamp working status were stable, the pump P2 was turned on and the *B. subtilis* spores were spiked into the influent. After pump P2 was operated for a while (~5 minutes), the water samples were taken from sample ports SP1 and SP2 every 3 to 5 minutes for 5 replicates. Finally, the absorbance of water samples at 254 nm and the log reduction of spores were determined based on the cell count levels for these samples. Then the fluence (UV dose) delivered in the experimental UV reactor was obtained according to the log reduction obtained against the fluence-response curve of the *B. subtilis* spores.

On the whole, the procedure of the validation experiments by the PFC method was very similar to that for the BD method, but the procedure was simpler. This was because a concentrated chlorine solution was usually added directly to the container C1; hence, pump P2 and container C2 were not used in this experimental process. When the

169

test water with free chlorine was ready, the validation experiment was started by pumping the free chlorine water sample from C1 flowing through the UV reactor to C3. The water samples also were taken from SP1 and SP2 every 3 to 5 minutes for 5 replicates. Then, the log decomposition of free chlorine was determined and the fluence (UV dose) delivered in the UV reactor was calculated.

5.3.3 Design of the validation experiments

In order to confirm the feasibility of the PFC method for UV reactor validation, three potential influencing factors, the water quality, the UV transmittance (T_{10}, %) and the flow rate, were considered in the experimental design. In order to compare the validation results and evaluate the proposed method, three validation methods, the BD method, a mathematical modeling model, and the PFC method were used in the validation experiment. For the mathematical modeling method, the *UVCalc* Software (Version 2.2.1, Bolton Photosciences Inc., Edmonton, AB Canada) was used for the calculation of the fluences delivered in the experimental UV reactor. For the BD and the PFC methods, the fluences delivered in the UV reactor were determined from the log inactivation of *Bacillus subtilis* spores or from the free chlorine photodegradation credit, respectively, as described in sections above. The following table shows the experimental runs that were performed:

170

Table 5.3 The factorial design for the validation experiment

Run #	Water quality	T_{10}, %	Flow rate, L/min
1			9
2		99%	8
3			6
4			4
5			9
6		90%	8
7			6
8	DI water (TOC: 0		4
9	to 0.4 ppm)		9
10		85%	8
11			6
12			4
13			9
14		80%	8
15			6
16			4
17			9
18		99%	8
19			6
20			4
21			9
22		90%	8
23			6
24	Synthetic water		4
25	(TOC: 3.4 ppm)		9
26		85%	8
27			6
28			4
29			9
30		80%	8
31			6
32			4

The UV reactor used in this study was validated by the PFC method under various operating conditions as listed in the above table. For the biodosimetry method, it also was

171

performed under the similar operating conditions in the validation experiment except that the factor of water quality was not involved. This is because it already proved that the biodosimetry method can work consistently in various water matircs with different qualities in many operations and studies. For the mathematical modeling method, one need only input variables or change some parameters in the *UVCalc* software and the fluence values of under various experimental conditions can be obtained[19]. In addition, the order of the 'Runs' in Table 5.3 is not the order in which the experimental runs were performed. By design, these runs were carried out randomly.

5.4 Results and discussion

5.4.1 Quantum yield for the photodegradation of free chlorine

The quantum yield of photodegradation of free chlorine in the test waters is very crucial for the UV reactor validation by the PFC method, as is the UV fluence-response curve of challenge microorganism for validation by the BD method. As discussed in Chapters 3 and 4, the quantum yield can be affected by many factors. For example, the pH and the initial concentration of free chlorine have some effects on the quantum yield for certain conditions; however, within the range of free chlorine concentration ($\sim$10 mg L^{-1}) generally applied in water treatment, these effects are not very significant. In addition, as discussed in Chapter 4, natural organic compounds and temperature also can affect the quantum yield of the photolysis of free chlorine. Since the temperature can change significantly on a seasonal basis, and the water quality also can vary significantly in different seasons and places, the quantum yields for the photodegradation of free

---

[19] The detailed calculation process is given in Appendix 5.1.

chlorine in these waters could be very different. Therefore, it is necessary to determine the quantum yield of the photodegradation of free chlorine carefully in the validation experiments.

In this study, two kinds of test waters with different qualities were used in the validation experiments. One is a synthetic drinking water, which was prepared to simulate the natural drinking water, and the other is the distilled water obtained from the local water supply system. The experiments were performed under ambient conditions $(21 \pm 2°C)$, and the pH of water samples used in each run was always adjusted to 7.2 ± 0.3. The concentration of free chlorine in the experiments ranged from 2.8 to 3.2 mg L^{-1}. At least 10 replicates were performed to determine the quantum yield of decomposition of free chlorine in each water matrix, and the average quantum yields obtained in this manner are listed in Table 5.4. These data were then used for the determination of the fluence (UV dose) delivered in the experimental UV reactor that was to be validated by the PFC method.

Table 5.4 Quantum yields of the photodegradation of free chlorine in the test waters used in the validation experiments

Water matrix	TOC level	Quantum yield
DI water	< 0.4 mg/L	1.1 ± 0.2
Distilled water	1.0 ± 0.2 mg/L	1.9 ± 0.2
Synthetic water	3.5 ± 0.3 mg/L	2.9 ± 0.3

5.4.2 UV fluence-response curve of *B. subtilis* spores

For the validation experiments using the BD method, the fluence (UV dose) is determined primarily based on the fluence-response curve of challenge microorganism (*B.*

173

subtilus spores were used in this research). Figure 5.3 shows the UV fluence-response curve of *B. subtilis* spores obtained in this study, which is the composite of data sets obtained from 5 replicate runs. It should be emphasized that these replicates were performed randomly over long time intervals. The results indicate that throughout the period of the validation experiments, the *B. subtilis* spores used in this study always had a consistent response to UV light at 254 nm.

As is known, the UV fluence-response curve of microorganisms in a semi-log (decadic) presentation can be expressed by the following equation:

[5.4] $$\log \frac{N}{N_0} = \log \left[1 - (1 - 10^{-kH'})^{10^d} \right]$$

where, N_0 is the number of microorganisms before exposed to UV irradiation, N is the number of surviving microorganisms after the exposure, k is the slope of the linear part of the survival curve in $m^2 J^{-1}$ (UV sensitivity), H' is the fluence delivered to microorganisms in $J\ m^{-2}$, and d is the distance between the intercept of the linear part with the ordinate and origin. For the spores of *B. subtilis*, the constants k and d should be in the following range according to ÖNORM (2003):

[5.5] $k = 0.0065 \pm 20\%\ m^2\ J^{-1}$ (i.e., $k = 0.0052$ to 0.0078)

[5.6] $d = 0.7 \pm 30\%$ (i.e., $d = 0.49$ to 0.91)

In this study, the parameters k and d were determined using the MS Excel™ "Solver" tool and had the values of $0.0083\ m^2\ J^{-1}$ and 0.63, respectively. Generally speaking, they fit into the above ranges (Eqs. 5.5 and 5.6) very well, although k is slightly out on the high side. A regression curve in Figure 5.3 was plotted using Eq 5.4 with the determined k and d values, and it was very consistent with the plots of the experimental data. In Figure 5.2, there is a shoulder on the survival curve when the fluence is in the

174

range of 0 to 11 mJ cm^{-2}, and the curve becomes linear when the fluence is more than 11

mJ cm^{-2}. However, a tail appears at the fluence of around 53 mJ cm^{-2} although this is not

very distinct in Figure 5.3. Therefore, in this study, in order to avoid the interruption of

errors, the linear part of the survival curve in the fluence range of 11 to 53 mJ cm^{-2} was

used for the determination of fluence (UV dose) in the biodosimetry experiments.
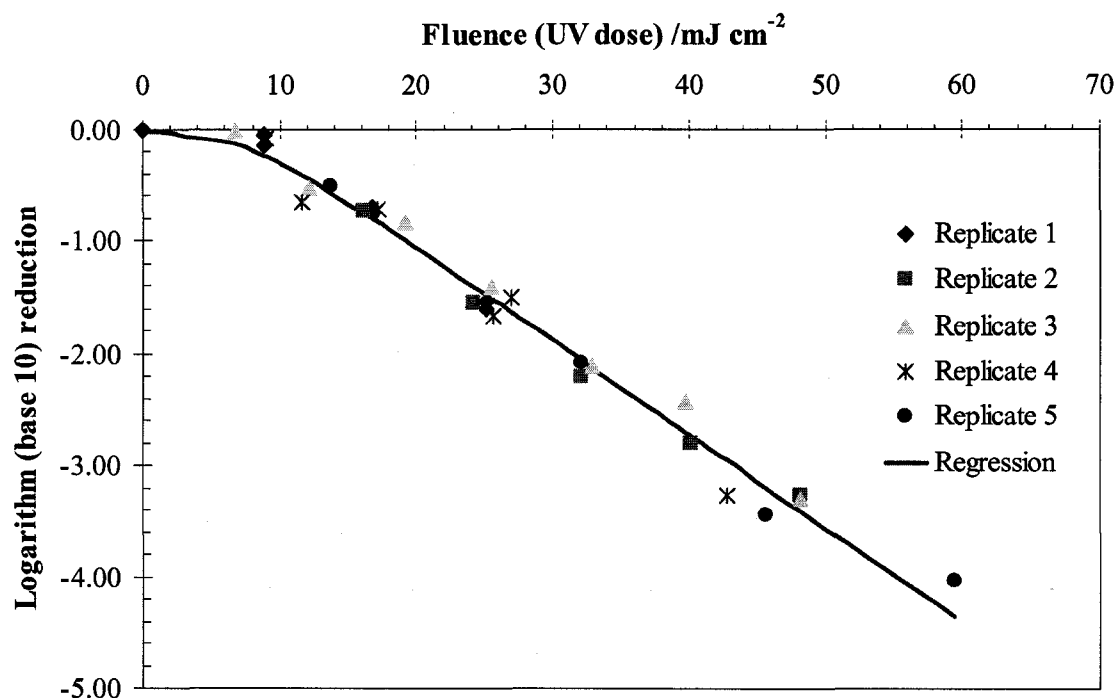
Figure 5.3 The UV fluence-response curve of *B. subtilis* spores exposed to 254 nm UV light. Five replicates (Replicate 1 to 5) were performed during the period of validation experiment and a semi-log (decadic) regression line was plotted with the constants *k* = 0.0083 m^2 J^{-1} and *d* = 0.63 (see Eq. 5.4).

5.4.3 The photodecomposition of free chlorine and the log reduction of *B. subtilis* spores

The fluence (UV dose) delivered by UV reactors is usually determined by the

reduction of challenge microorganisms in biodosimetry (the BD method); however, as

discussed above, it also could be determined by the photodegradation of free chlorine (the

175

PFC method). Figure 5.4 presents the correlation of the fluence (UV dose) determined from the PFC method and that determined from the BD method responding to the same fluences. The experimental data presented in this figure were measured using a bench-scale collimated beam UV apparatus. Firstly, the quantum yields for the photodegradation of free chlorine in three water matrixes with different TOC concentrations were measured and the log (naperian) reductions of *B. subtilis* spores at different fluences were determined. Then, the photodegradation of free chlorine corresponding to these fluences was calculated based on the quantum yields, using Eqs. 5.1 to 5.3. Figure 5.4 was plotted based on the photodecompositions of free chlorine and the reductions of *Bacillus subtilis* spores for the same fluences.

As discussed above and as shown in Figure 5.3, a shoulder and a tail characterize the fluence-response curve of *B. subtilis* spores. However, the photodegradation of free chlorine almost certainly follows first-order kinetics. Therefore, the plots in Figure 5.4 do not represent a linear increase in the shoulder and tail phases of *B. subtilis*. For the plots within the fluence range of 11 to 53 mJ cm^{-2}, the photodegradation of free chlorine has an essentially linear relation with the reduction of *B. subtilis* spores. This indicates that, in this study for this fluence range, there should be no difference between these two methods for the validation of the UV reactor. In addition, the slope of the plots depends on the TOC concentration in water matrixes. This is because the quantum yield of free chlorine varies with the TOC level. As discussed in Chapter 4, the higher the TOC concentration, the higher the quantum yield of photodegradation of free chlorine, and therefore more free chlorine will be decomposed for the same fluence. This is the reason that the slope of the plot of sample 3 (TOC 3.2 to 3.8 mg/L) is the largest among the three

176

plots in Figure 5.4. This also implies that TOC can increase the sensitivity of the PFC method for the validation of UV reactors. According to this figure, the TOC concentration is expected to be as high as possible in the validation of UV reactors by the PFC method, so that the sensitivity of this method can be improved.
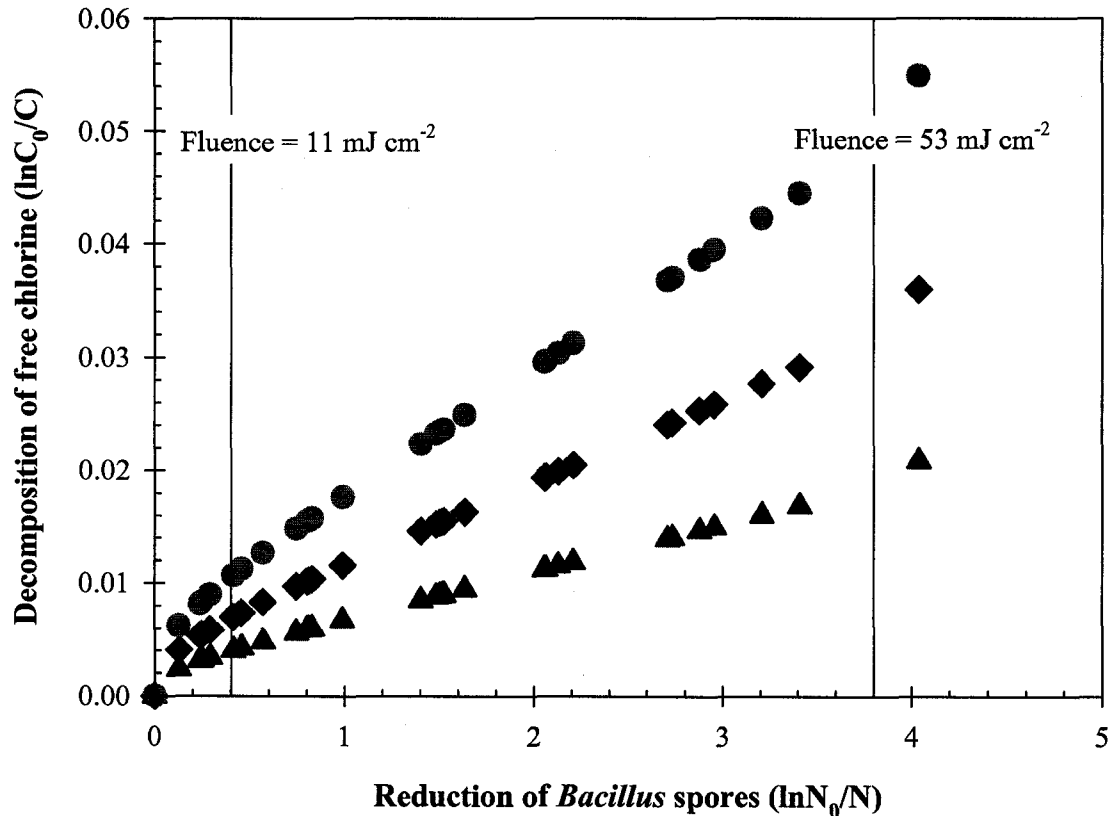
Figure 5.4 Comparison of the photodegradation of free chlorine and the reduction of *B. subtilis* spores for the determination of fluences in bench scale experiments. The concentration of free chlorine was 2.8 ± 0.4 mg Cl/L, the pH was 8.2 ± 0.4, and the temperature was (20 ± 2) °C. (▲ sample 1: TOC 0 to 0.4 mg/L, ♦ Sample 2: TOC 0.8 to 1.2 mg/L, and ● Sample 3: TOC 3.2 to 3.8 mg/L)

177

5.4.4 Comparison of the validation results obtained by the PFC method and the BD method

As we know, the purpose of validating a UV reactor is to provide confidence that the UV reactor can provide the level of inactivation required for a given application. Because the operating conditions of a UV reactor cannot be fixed as constants and always fluctuate within a range of conditions, validation testing must determine a set of operating conditions within which the UV reactor can be operated in practical operations. In this study, the flow rate, UV transmittance, and water quality were selected as the influencing factors for the operating conditions. A new UV lamp was used for the validation experiments and each run of the experiments was performed randomly, so the possible effect of lamp age can be eliminated. The lamp sleeve used in this research was also brand new, and it was removed from the UV reactor for thorough cleaning after each run. The validation experiments by either the PFC method or the BD method were performed under experimental operating conditions that were controlled by fixing one of the influencing factors (flow rate, UVT, and water quality) and changing the others. In addition, the ideal fluences delivered in the experimental UV reactor under these operating conditions were calculated from a mathematical method using *UVCalc* Ver. 2 (Bolton Photosciences Inc.). The fluences determined by the PFC method, the BD method, and the mathematical method using *UVCalc* Ver. 2 were analyzed in the following subsections for the various experimental operating conditions.

5.4.4.1 Same water quality, different UV transmittance and different flow rate

Figure 5.5 shows the comparison of fluences determined by the PFC, BD, and mathematical methods at flow rates of 6, 8 and 9 L min^{-1}. Distilled water was used as the

178

test water in these runs, and the UV transmittance was varied from 80 to 99%. From Figure 5.5, it can be observed that the fluences calculated by the mathematical method are always considerably higher than those obtained by the experimental methods (PFC and BD methods). This is reasonable because the fluences calculated using the mathematical method are based on the assumption of ideal plug flow with completely radial mixing in the validated UV reactor. The data determined by the experimental methods inherently account for the hydrodynamic status in the validated UV reactor. Therefore, they are smaller compared with the calculated data. As is known, the fluence (UV dose) is a function of UV transmittance, water depth, exposure time and the UV fluence rate. The results calculated using the mathematical method reflect the ideal relation of fluence with flow rate (exposure time) and UV transmittance. The higher the UV transmittance and the lower the flow rate (the longer the exposure time), the higher the fluence delivered in the UV reactors. It can be noticed in Figure 5.5 that the fluences measured by the experimental methods have a similar tendency with the calculated data, although they have a distinct offset. This also demonstrates that the PFC method can be used to reflect the disinfection behavior of the validated UV reactor authentically from another point of view. In addition, Figure 5.5 also illustrates that the fluences determined by the PFC method are very consistent with those determined using the BD method. Therefore, in this study, it can be concluded that the UV transmittance and flow rate do not have significant impacts on the reliability of the validation results determined by the PFC method, and, under these operating conditions, the two methods are interchangeable for the validation of the UV reactor.

179
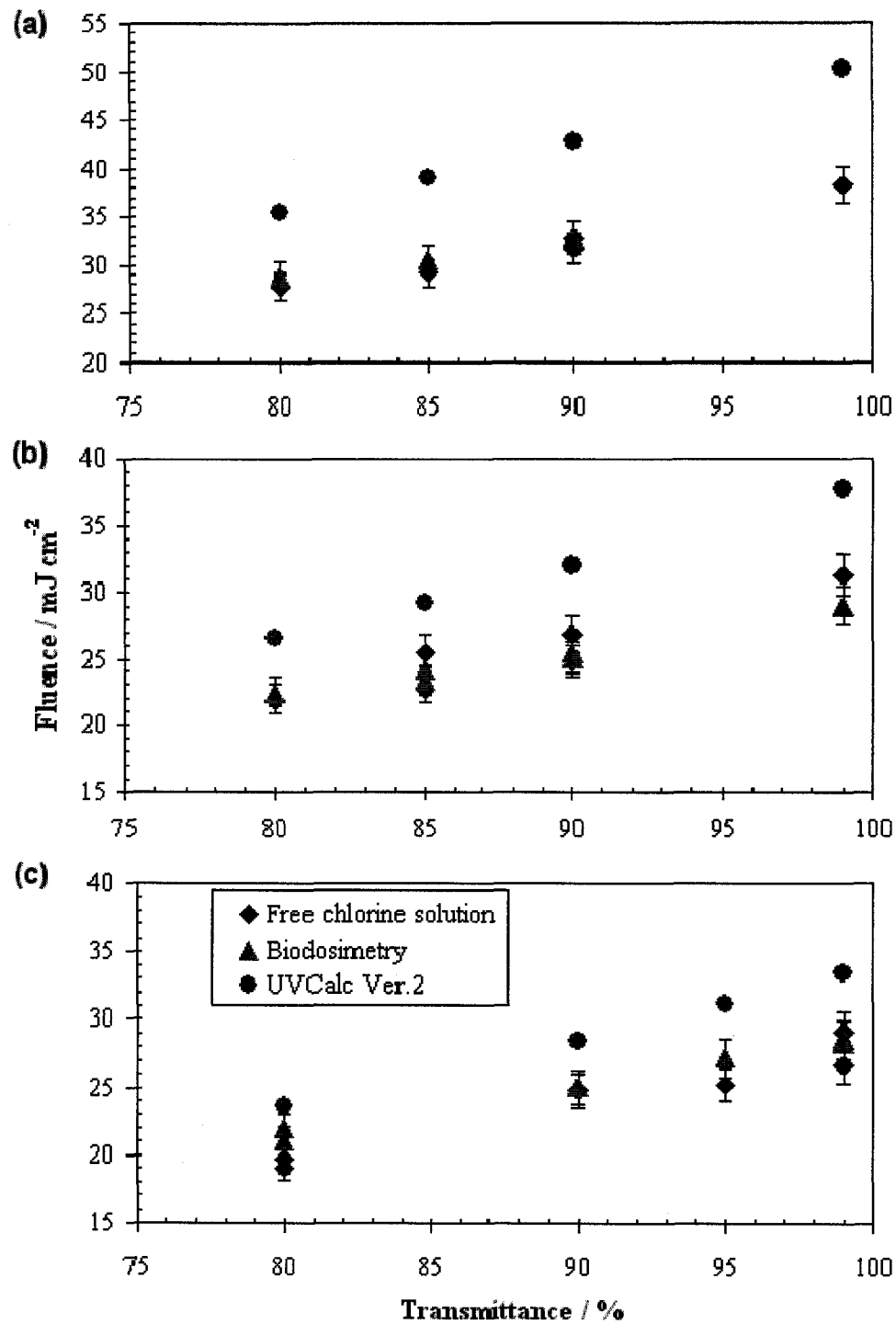
Figure 5.5 Fluences determined by the PFC method, the BD method and the mathematical method at flow rates of (a) 6 L min⁻¹, (b) 8 L min⁻¹ and (c) 9 L min⁻¹. Distilled water (TOC 0.8 ~ 1.2 mg/L) was used as the test water in the experiments and the experimental temperature was (21 ± 2)°C.

180

5.4.4.2 Same flow rate, different transmittance and different water quality

Figure 5.5 already demonstrates that for the same water quality matrix, the flow rate and UV transmittance have no impact on the proposed PFC method for the validation of the experimental UV reactor in this study. Since the quantum yield of the photodegradation of free chlorine in a given test water is a crucial parameter for the UV reactor validation by this proposed PFC method, and can be significantly influenced by water quality, it is very necessary to verify the reliability of this method using water matrices with different qualities. Figure 5.6 illustrates the effect of quality of the water matrix on the validation results determined by the PFC method. For the BD method, only distilled water (TOC ranges from 0.8 to 1.2 mg/L) was used as the water matrix in this experiment to perform the validation testing. The reason is that considerable applications have already proven that water quality (TOC) has no significant influence on the reliability of the BD method. However, two water matrices with different qualities, distilled water and synthetic drinking water (TOC ranges from 3.2 to 3.8 mg/L), were used in this experiment for the validation testing of the proposed PFC method. No parameters related to water quality needed to be adjusted; therefore, for different water qualities, the fluences calculated using the mathematical method are the same when the operating conditions are not changed.

The flow rate of water matrix in this experiment was set as a constant at 8 L min^{-1}, and the experimental temperature was always kept within the range of 19 to 23°C. Firstly, Figure 5.6 shows that the fluences determined by the various methods have a same increasing tendency with increasing UV transmittance. This is reasonable and can be explained by the Beer-Lambert Law. In some sense, this also reflects the reliability of

181

these methods for the measurement of the fluence delivered by UV reactors. Secondly, Figure 5.6 is similar to Figure 5.5, in that Figure 5.6 also indicates that the fluences calculated using the mathematical model are always higher than those determined by the experimental methods. The most important information derivable from Figure 5.6 is that there is no significant difference between the data sets, determined by the PFC method, for these two different test waters. In addition, these results are very consistent with those determined by the BD method. This means that the water quality does not influence the reliability of the validation results determined by PFC method, and hence, the proposed PFC method can be used as in place of the BD method for various water matrices.
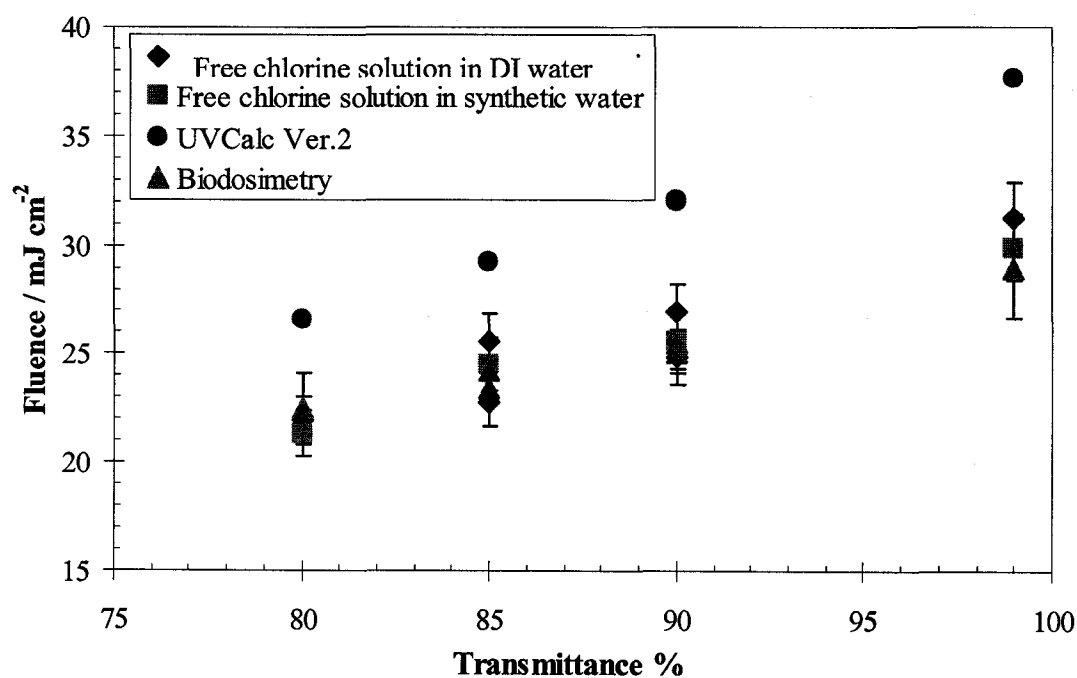
Figure 5.6 Comparison of the fluences determined by the PFC method, the BD method, and the mathematical method using different water matrices with various qualities. (Flow rate = 8 L min^{-1})

182

5.4.4.3 Same transmittance, different water quality and different flow rate

Figure 5.6 shows that the water quality has no influence on the validation results determined by the photolysis of free chlorine when the flow rate is constant (8 L min^{-1}). In real operations, the flow rate of a UV reactor could vary over a large range. Therefore, it is necessary to test the impact of water quality on the validation results determined by the PFC method for different flow rates. Figure 5.7 shows the fluences determined by the PFC method and the BD method at a UV transmittance of 90% and various flow rates. This figure shows that the fluence decreases with increasing flow rate. This is because the retention time (or exposure time) of water sample has a reciprocal relationship with the flow rate for a given UV reactor. Therefore, the higher the flow rate, the lower the fluence will be delivered in the UV reactor. Again, since they were calculated under ideal conditions, the data in Figure 5.7 obtained by the mathematical method are a little higher than the experimental data. However, it should be pointed out that in Figure 5.7 the difference between the theoretical maximum values (the calculated data) and the measured data by the experimental methods gradually decreases with increasing flow rate. This indicates that the mixing efficiency of the test water in the UV reactor increases with increasing flow rate, and thus the hydrodynamic status approaches that of the ideal condition with increasing flow rate. For example, at a flow rate of 9 L min^{-1}, the water sample in the UV reactor was almost completely mixed in the radial direction; therefore, at this point, as shown in Figure 5.7, the data calculated from the mathematical model were very close to those determined by experimental methods (PFC method and the BD method). Also, it should be clarified that the the difference of the fluences determined by the mathematical model and the experimental methods (PFC and BD) does not indicate

183

that the model (UVCalc) does not work very well. On the contrary, the decrease of the difference, as shown in Figure 5.7, reflects that this is a very useful model. Because in design and operation of UV reactors designers try to make the hydraulic condition in UV reactors as close as possible to the ideal mixing status (PF with completely radial mixing), the resuls obtained in Figure 5.7 expresses that the model (UVCalc) should be able to give a very good estimate of the fluences delivered in a UV reactor in practical applications. The important conclusion from this figure is that the fluences determined by the PFC method at various flow rates are independent of the quality of the water matrix. There is no significant difference between the validation results determined by PFC method at each flow rate using different water matrices and, at the same time, these results also are very consistent with the data determined by the BD method. Therefore, it can be concluded, according to these results, that the proposed PFC method can be used equally as well as the BD method for the validation of UV reactors for various flow rates and water qualities.
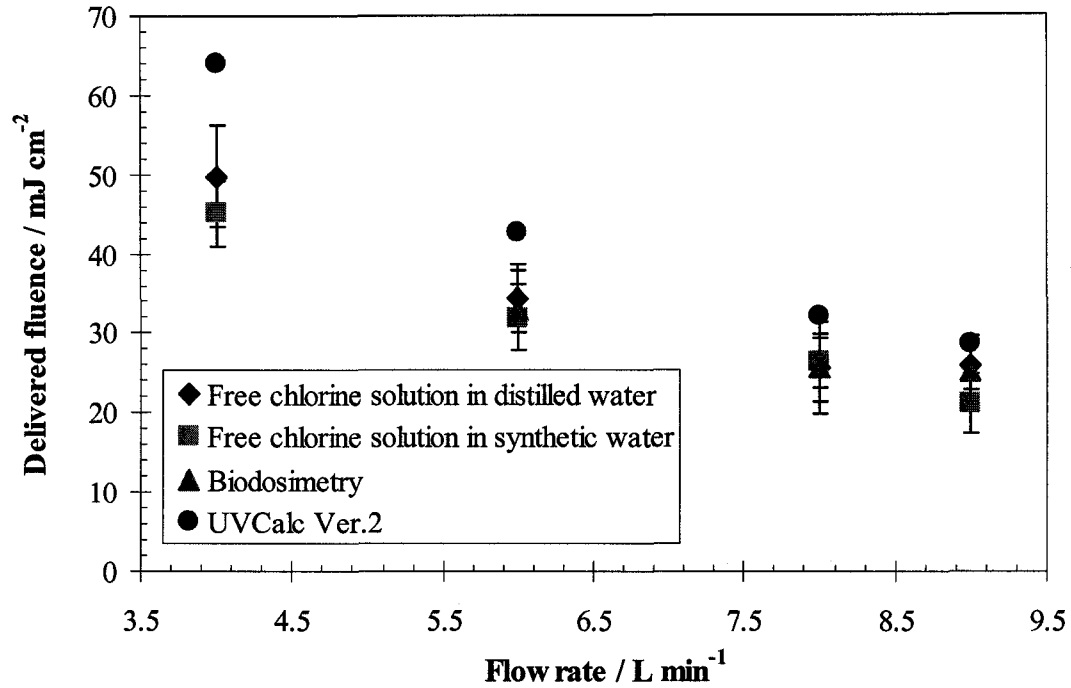
Figure 5.7 Fluences delivered in the experimental UV reactor determined by the PFC method and the BD method using *B. subtilis* for various flow rates. The experiment was performed under ambient conditions, and the UV transmittance of the test water was kept at 90%.

5.4.4.4 Mixing efficiency

As shown in Figure 5.7, the theoretical maximum UV fluence is always higher than the measured fluence, but the difference decreases with increasing flow rate. The ratio of UV fluence H' determined using the experimental methods (such as the PFC and BD methods) to the theoretical maximum UV fluence (H'_{max}) is called the 'mixing efficiency', namely

[5.7] $\text{Mixing efficiency} = \dfrac{H'}{H'_{max}}$

From its definition, the mixing efficiency accounts for the effect of the hydrodynamic status on the fluences delivered in the validated UV reactor. That is, the stronger the turbulence (induced by higher flow rates) in UV reactors, the closer the H' will be to the

185

H'_{max} and so, the closer the mixing efficiency will be to unity. However, according to its definition, in reality the mixing efficiency should be always less than unity because no real UV reactor operates under ideal mixing conditions.

Figure 5.8 shows the mixing efficiencies for the various flow rates obtained in the validation experiments using the PFC method and the BD method. In this figure, it is obvious that the mixing efficiency gradually increases from about 0.7 to 0.9, when the flow rate ranges from 4.0 to 9.0 L min^{-1}. This indicates that the mixing intensity of the test water in the validated UV reactor gradually increases with increasing flow rate. For a given flow rate, the mixing efficiencies obtained by the PFC method and the BD method show no significant differences. This also proves that under the same experimental operating conditions, the fluences (UV doses) determined by the PFC method are very close to those determined by the BD method, and there are no significant differences between these two validation methods.

186
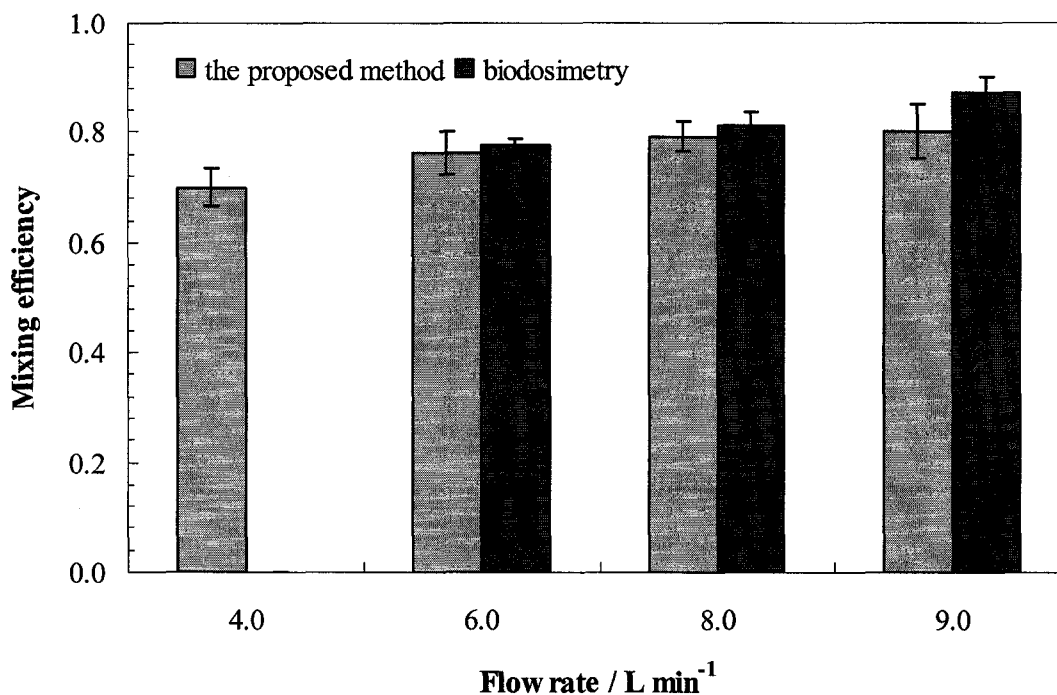
Figure 5.8 Comparison of the mixing efficiency for various flow rates as determined by the PFC method and the BD method.

5.4.5 Statistical analysis of the comparison of the PFC and BD methods for the validation of UV reactors

The experimental results presented above have shown visually that there is likely no significant difference between the proposed PFC method and the BD method for the validation of the experimental UV reactor used in this study. Figure 5.9 is a correlation chart of the validation results determined, under various experimental conditions, by the PFC method and the BD method, respectively. In general, the data obtained by these two methods show a linear relation, although there are some small deviations. In this figure, the 95% confidence intervals indicate a 0.95 probability of containing the mean of a fluence (UV dose) determined by the PFC method for a set of values at a specified fluence (UV dose) determined by the BD method. For example, in this study, if the

187

fluence (UV dose) determined by the BD method was 32 mJ cm^{-2}, there is a 95% probability that the fluence (UV dose) determined by the PFC method was in the range of 30 to 34 mJ cm^{-2}. The narrow confidence intervals indicate that there is a high correlation between these two methods. The 95% prediction intervals mean that for a specific fluence (UV dose) determined by BD method these intervals have 95% probability to contain all fluences (UV doses) that could be obtained by the PFC method. It is shown in this figure for a comparison with the 95% confidence intervals.
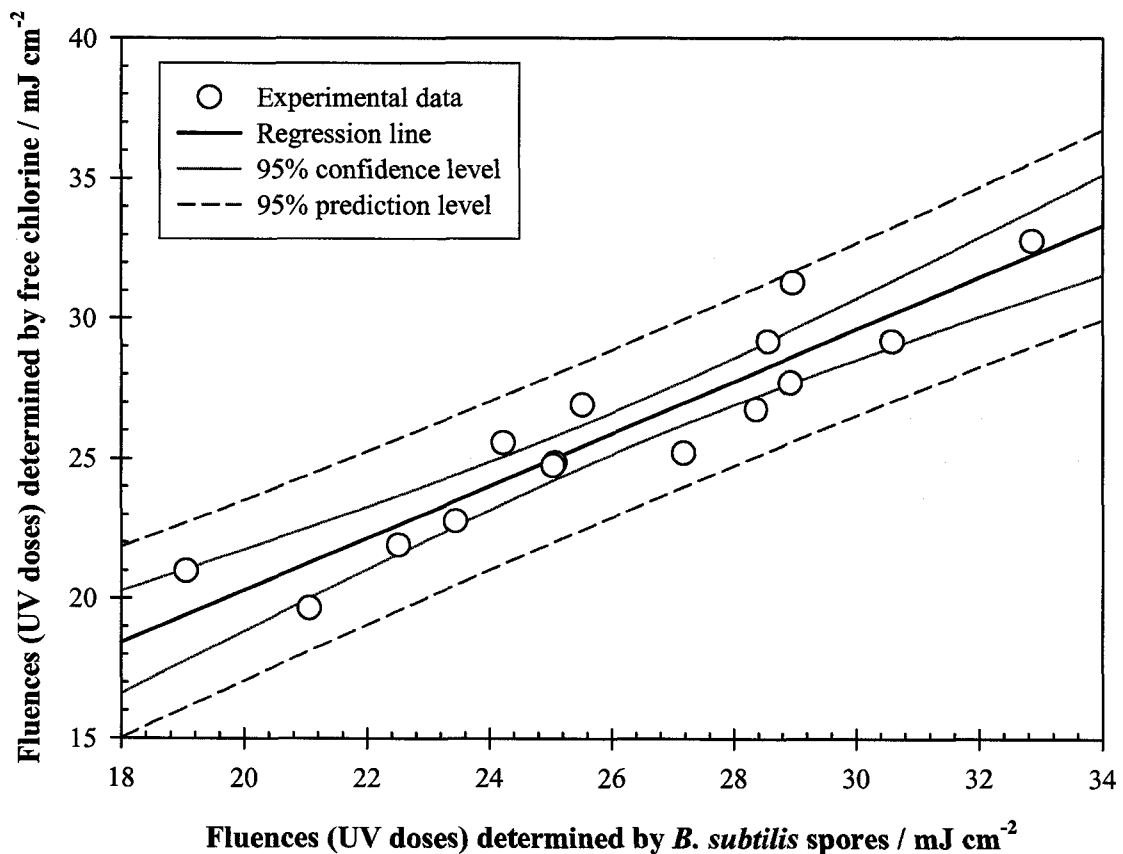
Figure 5.9 Correlation of the fluences (UV doses) determined by the PFC method and the BD method. The upper and lower limits for 95% confidence and prediction intervals are presented.

188

In addition, a t-test (paired two samples for means, confidence level 95%) was performed, based on the experimental results obtained in this study, using the "Data Analysis" of Microsoft™ Tools. The analysis results are summarized in Table 5.5. Because the validation experiments were performed for various operating conditions, the fluences (UV doses) varied in a large range. Therefore, the variance listed in Table 5.5 is very large. The Pearson Correlation Coefficient (0.93), which is very close to 1, indicates that there is a good linear relation between the validation results determined by PFC method and those determined by the BD method. In addition, at the confidence level of 95%, in this study the value of t-test statistic is always smaller than the t-test critical values (one- or two-tail), which means that at this confidence level, there is no significant difference between these two methods (PFC and biodosimetry) for the UV reactor validation. The big P-values (one- or two-tail) also illustrate this point.

Table 5.5 t-Test: Paired two samples for means (confidence level 95%)

	Free chlorine	*B. subtilis*
Mean fluence	25.96	26.09
Variance	13.90	13.95
Observations	15	15
Pearson Correlation	0.93	
Hypothesized Mean Difference	0	
df (degree of freedom)	14	
T Stat	−0.37	
P(T<=t) one-tail	0.36	
T Critical one-tail	1.76	
P(T<=t) two-tail	0.72	
T Critical two-tail	2.14	

189

5.5 Conclusions

UV disinfection has been recognized as an effective technology for drinking water disinfection and is widely employed to inactivate some refractory pathogens that are very resistant to traditional disinfection methods. In order to make sure that the target microorganism can be reduced to certain level, it is very important to determine the fluences delivered in the UV reactor under various operating conditions. Biodosimetry is the most widely used and reliable method for the validation of UV reactors, but it still has some disadvantages and limitations. For instance, it cannot be applied for online monitoring of the performance of UV reactors. Free chlorine is usually used in drinking water treatment for MOR treatment, and it can be decomposed by UV irradiation. According to the study on the quantum yield of the photolysis of free chlorine, it is possible to use free chlorine photodegradation as an indicator of the UV fluence delivery. Therefore, this study has investigated the feasibility of using the PFC method to determine the fluences delivered in UV reactors. In order to testify the reliability of the proposed PFC validation method, the flow rate, water quality (TOC) and UV transmittance were used as influencing factors, and the fluences determined by the PFC method, the BD method and the mathematical method under various operating conditions were compared and analyzed.

In the process of validation of a UV reactor by the PFC method, the quantum yield of photodegradation of free chlorine in the test water is as important as is the UV fluence-response curve of the challenge microorganism in the BD method. In this study, the quantum yields of photodegradation of free chlorine in DI water, distilled water and synthetic water were determined, and the results clearly demonstrate again that the water

190

quality (particularly the TOC) has a significant effect on the quantum yield, as has been observed in previous chapters.

B. subtilis spores were used as the challenge microorganism in the BD experiment. In this study, five (5) replicates were performed during the period of the validation experiments to determine UV fluence-response curve of the *B. subtilis* spore, and the results show that the sensitivity of *B. subtilis* spores throughout the experiment process was very stable. In addition, the parameters k and d of the UV fluence-response curve obtained in this study are also very consistent with those reported in previous studies.

By altering operating conditions, such as UV transmittance, water quality (TOC) and flow rate, the fluences delivered in an experimental UV reactor were determined by the PFC method, the BD method and the mathematical method, respectively. According to a comparison of these validation results, the analysis shows that the fluences determined by the proposed PFC method are very consistent with those determined by the BD method under various operating conditions, but the results calculated by the mathematical model are always higher. This indicates that the hydrodynamic status in the experimental UV reactor is not ideal, as is assumed in the mathematical model. With increasing flow rate, the difference between the fluences calculated from the mathematical model and those determined experimentally was observed to decrease gradually. This observation implies that the mixing intensity gradually increases with increasing flow rate, and the hydrodynamic status in the UV reactor also slowly moves toward the ideal condition. In general, the experimental results obtained in this study show that the reliability of the proposed PFC method for the validation of the experimental UV reactor is not affected by some operating factors (such as the flow rate,

water quality and UV transmittance) and that there is no significant difference in the fluences determined by this PFC method and those determined from the BD method. Therefore, it can be concluded that in this bench-scale study, the proposed PFC method and the BD method are interchangeable for the validation of UV reactors, and the PFC method works as well as the BD method under various operating conditions. However, a full scale study will be needed before it can be applied in practice and the experiments with medium-pressure UV reactors also are needed for extending the application of this method.

5.6 References

Blatchley, E.R. and Hunt, B.A. 1994. Bioassay for full-scale UV disinfection systems. *Wat. Sci. Technol.*, **30(4)**: 115–123.

Blatchley, E.R., Do-Quang, Z., Janex, M.L. and Laîné, J.M. 1998. Process modeling of ultraviolet disinfection. *Wat. Sci. Technol.*, **38(6)**: 63–69.

Bolton, J.R. 2000. Calculation of ultraviolet fluence rate distributions in an annular reactor: significance of refraction and reflection. *Wat. Res.*, **34(13)**: 3315–3324.

Bolton, J.R., Stefan, M.I., Cushing, R.S. and Mackey, E.D. 2001. The importance of water absorbance/transmittance on the efficiency of ultraviolet disinfection reactors. Proceedings first international congress on ultraviolet technologies, Washington, DC, June, 2001.

Cabaj, A., Sommer, R. and Schoenen, D. 1996. Biodosimetry: model calculations for UV water disinfection devices with regard to dose disitributions. *Wat. Res.*, **30(4)**: 1003–1009.

DVGW. 1997. Deutscher Verein des Gas- und Wasserfaches e.V. (1997). UV Systems for Disinfection in Drinking Water Supplies - Requirements and Testing (English version transferred and edited by J. R. Bolton). Postfach 14 01 51, D-53056 Bonn, Germany (1997).

Fenner, R.A. and Komvuschara, K. 2005. A new kinetic model for ultraviolet disinfection of grey water. *J. Environ. Engng.*, **131(6)**: 850–864.

Harris, G.D., Adams, V.D., Moore, W.M. and Sorensen, D.L. 1987. Potassium ferrioxalate as chemical actinometer in ultraviolet reactors. *J. Environ. Engng.*, **113(3)**: 612–627.

Lawryshyn, Y.A. and Cairns, B. 2003. UV disinfection of water: the need for UV reactor validation. *Wat. Sci. Technol.: Wat. Supply*, **3(4)**: 293–300.

Leighton, T.J. and Doi, R. H., 1971. The stability of messenger ribonucleic acid during sporulation in Bacillus subtilis. *J. Biol. Chem.*, **246(10)**, 3189–3195.

Linden, K.G., Soriano, G.S., Dodson, G.S. and Darby, J.L. 1998. Investigation of disinfection by-product formation following low and medium pressure UV irradiation of wastewater. In: Proc. WEF Disinfection Specialty Conference, Baltimore, MD.

Liu, W., Andrews, S.A., Bolton, J.R., Linden, K.G., Sharpless, C. and Stefan, M. 2002. Comparison of disinfection from different UV technologies at bench scale. *Wat. Sci. Technol.: Wat. Supply*, **2(5–6)**: 515–521.

Mackey, E.D., Hargy, T.M., Wright, H.B., Malley, J.P. and Cushing, R.S. 2002. Comparing Cryptosporidium and MS2 bioassays – implications for UV reactor validation. *J. AWWA*, **94(2)**: 62–69.

Munakata, N. and Rupert, C.S., 1972. Genetically controlled removal of "spore photoproduct" from deoxyribonucleic acid of ultraviolet-irradiated bacillus subtilis spores. *J. Bacteriol.*, **111(1)**: 192–198.

Nieminski, E.C., Bellamy, W.D. and Moss, L.R. 2000. Using surrogates to improve treatment plant performance. *J. AWWA*, **92(3)**: 67–78.

ÖNORM 2003. Austrian National Standard: prÖNORM M 5873-2 E. 2003. Plants for disinfection of water using ultraviolet radiation: requirements and testing. Austrian Standards Institute, Vienna, Austria, www.on-norm.at

Rahn, R.O., Bolton, J.R. and Stefan, M.I. 2006. The iodide/iodate actinometer in UV disinfection: determination of the fluence rate distribution in UV reactors. *Photochem. Photobiol.*, **82(2)**: 611–615.

Sasges, M. and Robinson, J. 2005. Accurate measurement of UV lamp output. *IUVA News*, **7(3)**: 21–25.

Severin, B.F., Suidan, M.T. and Engelbrecht, R.S. 1983. Kinetic modeling of UV disinfection of water. *Wat. Res.*, **17(11)**: 1669–1678.

Sommer, R., Cabaj, A., Schoenen, D., Gebel, J., Kolch, A., Havelaar, A.H., and Schets, F.M. 1995. Comparison of three laboratory devices for UV-inactivation of microorganisms. *Wat. Sci. Technol.*, **31(5–6)**: 147–156.

Sommer, R., T. Haider, A. Cabaj, W. Pribil and M. Lhotsky, 1998. Time dose reciprocity in UV disinfection of water. *Wat. Sci. Tech.*, **38(12)**: 145–150.

Stefan, M.I., Bolton, J.R. and Rahn, R.O. 2001. Use of the iodide/iodate actinometer together with spherical cells for determination of the fluence rate distribution in UV reactors: validation of the mathematical model. Proc., First International Congress on

Ultraviolet Technologies, Washington, DC, International Ultraviolet Association, PO Box 1110, Ayr, ON, Canada N0B 1E0

USEPA – US Environmental Protection Agency, 2003. Ultraviolet Disinfection Guidance Manual. EPA 815-D-03-007, June 2003 draft, 1200 Pennsylvania Avenue NW Washington, DC 20460-0001;

Wright, H. and Lawryshyn, Y.A. 2000. An assessment of the bioassay concept for UV reactor validation. Proc., Disinfection 2000: Disinfection of Wastes in the New Millennium, New Orleans, LA, March 15–18. Water Environment Federation, Alexandria, VA.

Appendix 5.1 Calculation of fluences delivered in UV reactors by

UVCalc Ver.2

In this research, in order to compare the validation results obtained by different

methods, the mathematic model, UVCalc Ver.2[20], was used for the calculation of the

fluences delivered in the experimental UV reactor in various operating conditions. As

---
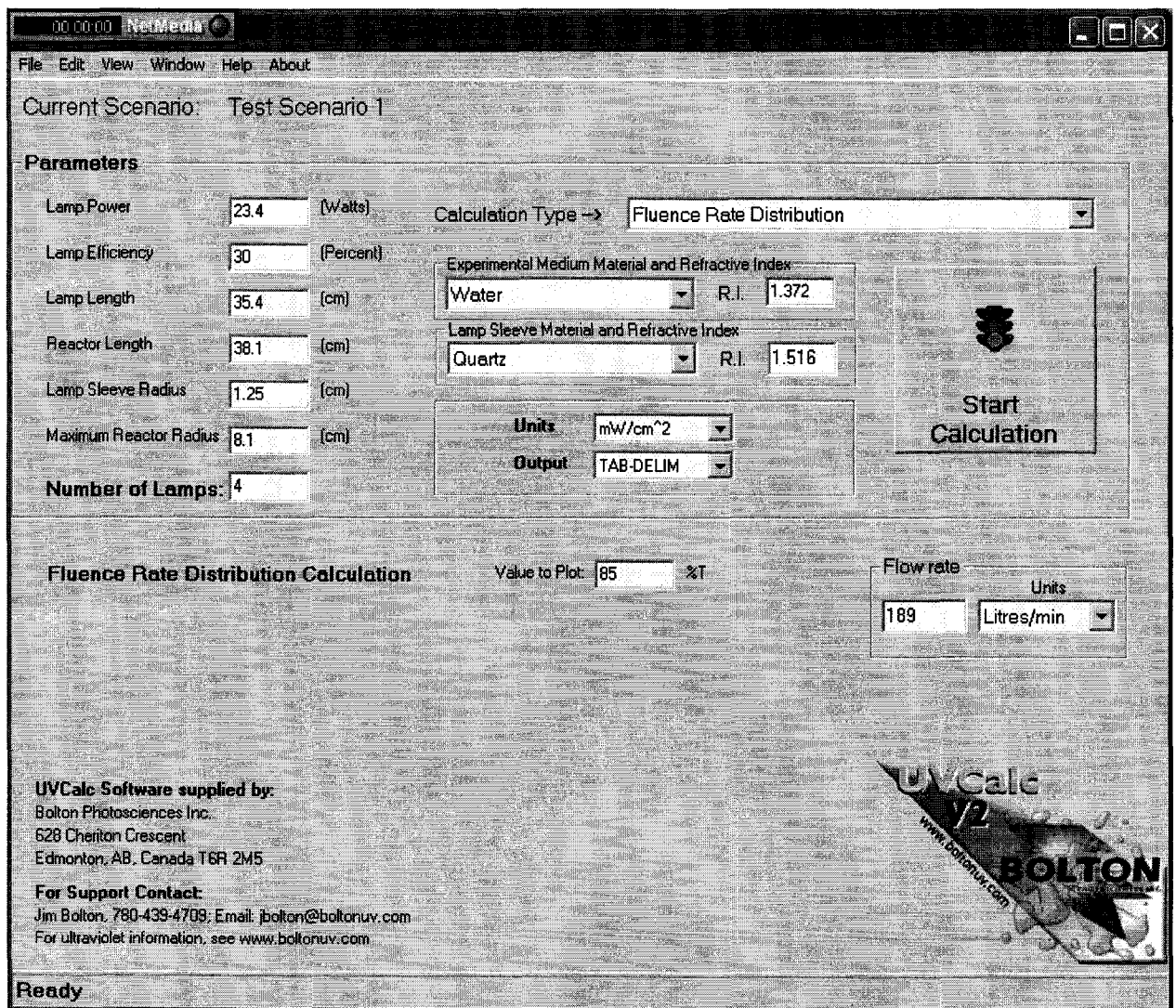
[20] The software is provided by Bolton Photosciences Inc., and the program of this software is based on the Multiple Cylindrical Segment Source Summation Method with full accommodation of reflection and refraction at the air/quartz/water interface (Bolton 2000).

shown in the screen image of the software above, the configuration of the validated UV reactor, the lamp power and efficiency, and some other data are required to input the software for the calculation. Therefore, in this study the fluences were calculated by UVCalc in the following steps:

1. Determine the configuration of the validated UV reactor, such as the reactor length and the maximum reactor radius;

2. Get the information of UV lamps in the reactor, such as the number of lamps, the power and efficiency of lamps, and the lamp length and its sleeve radius;

3. Select the calculation options. The UVCalc can provide two kinds of calculation option, "average fluence rate" and "fluence rate distribution". In this study, the "average fluence rate" option was used for the determination of the average fluence delivered in the experimental UV reactor;

4. Input other required calculation parameters, such as the materials and refractive indexes of experimental medium and lamp sleeve, the range of UV transmittance, and the flow rate; and

5. Press the calculation button and start the calculation.

In this research, the parameters used for the fluence calculation by UVCalc are summarized in Table 5.6.

Table 5.6 Summary of the parameters input the software (UVCalc Ver.2) for the fluence calculation

Parameters:	
Lamp power	1.84 W
Lamp efficiency	100%
Lamp length	36 cm
Reactor length	48 cm
Lamp sleeve radius	1.27 cm
Maximum reactor radius	9.0 cm
Number of lamps:	1
Calculation type:	Average fluence rate
Experimental medium material and refractive index:	Water/1.372
Lamp sleeve material and refractive index:	Air/1.000
UV transmittance:	70% to 99%
Flow rate:	4 to 9 L min^{-1}

It should be noted that the power of the original UV lamp supplied by Wyckomar Inc. with the experimental UV reactor is too high for this study. Accordingly, an opaque paper was used to cover the UV lamp so that a part of UV light can be cut down to reach the requirement of the experiment. The 'lamp power' listed in the above table is the result measured in the experiment according to the method described by Sasges and Robinson (2005). In the measurement of the 'lamp power', the paper covered UV lamp with the quartz sleeve was taken as an entire unit and the power of the UV light irradiating from the quartz sleeve was determined as the 'lamp power'. Therefore, the 'lamp efficiency' used in the calculation in this study is 100%, and for the same reason, the 'lamp sleeve material and refractive index' was set as 'air/1.000' in this study.

198

CHAPTER 6 GENERAL CONCLUSIONS AND

RECOMMENDATIONS

6.1 General overview

As discussed in the previous chapters, UV disinfection for drinking water treatment is becoming more and more popular day by day. In order to make sure the UV reactors are working properly to protect the public from harmful pathogens, the determination of fluences delivered in UV reactors for various operating conditions is a very crucial step in the design and operation of UV reactors. Biodosimetry, actinometry and mathematical models validated by biodosimetry are usually employed for the validation of the fluence delivery in UV reactors. As reviewed in Chapter 2, each of these methods has some disadvantages and limitations. For instance, the biodosimetry method cannot be used for online monitoring, the actinometers usually used are expensive and the test water could be contaminated by the added chemicals, and the mathematical models cannot be used for the UV reactor validation tests alone. Therefore, the primary purpose of this research is to look for an appropriate validation method that can work better than the current methods available.

Chlorination is the most widely used MOR treatment process for drinking water treatment at the present. Sometimes, the sequential treatment for MOR using chlorination and UV irradiation is also applied as multi-barrier approach for the drinking water safety. In many operations, it has been observed that free chlorine can be significantly decomposed by UV light. Accordingly, in this research free chlorine was selected for the measurement of UV irradiation. In the proposed validation process, the quantum yield of

199

photodegradation of free chlorine is a very important parameter, which is then utilized to determine the delivery of fluences in the validated UV reactor. Therefore, it is first necessary to carry out a detailed investigation of the quantum yield of photodegradation of free chlorine for various operating conditions and possible influencing factors from water quality parameters. In addition, in order to get a correct understanding of the photodegradation of free chlorine and to apply it properly for the validation of UV reactors, the photodegradation process and the photo-products of the free chlorine degradation are also important to provide a comprehensive and systematic study. The most important aspect is to examine the feasibility of this proposed method for the purpose of monitoring of the performance of UV reactors. That is, it is essential to test the reliability of the proposed method of the photodegradation of free chlorine for the measurement of fluences delivered in UV reactors under various operating conditions.

In this research, a through study was carried out concerning the quantum yield of the photodegradation of free chlorine and the influencing factors from water quality parameters. The photodegradation of free chlorine and its photo-products also were investigated. Compared with fluences obtained by biodosimetry (using *B. subtilis* spores) and a mathematical model (*UVCalc*) for various operating conditions, the reliability of the proposed validation method (the photodegradation of free chlorine) was thoroughly investigated.

6.2 Conclusions

Based on the experimental and theoretical studies, the conclusions of each subtopic of this research (such as the quantum yield of the photodegradation of free

200

chlorine, influencing factors, degradation products and the reliability of the proposed validation method) were obtained in the previous chapters. The following is a general summary of the whole research project, in which conclusions from specific chapters are again outlined.

6.2.1 Quantum yield of the photodegradation of free chlorine

The quantum yield of the photodegradation of free chlorine in DI water was investigated over a large range of free chlorine concentrations and pH values. At pH 5, the quantum yield of the photodegradation of free chlorine (primarily HOCl) was observed to be sensitive to the concentration of free chlorine. When the concentration was not very high (<71 mg L^{-1}), the quantum yield was approximately constant at 1.0 ± 0.1; otherwise, the quantum yield rose linearly with increasing free chlorine concentration at a rate of 0.0025 (mg Cl/L)$^{-1}$. However, compared with the HOCl, it was found, in this study, that the quantum yield photodegradation of free chlorine (OCl$^-$) at pH 10 was not significantly affected by the concentration of free chlorine over the investigated range of 3.5 to 640 mg L^{-1}. The photodegradation quantum yield for OCl$^-$ was always around 0.9 ± 0.1.

Based on the experimental results, a mathematical model (Eq. 3.18) was established to allow estimation of the overall photodegradation quantum yield of free chlorine by UV light at 254 nm in DI water. In this model, it was hypothesized that the photodegradation of HOCl and OCl$^-$ are two independent processes, and that interactions between these two processes are negligible. Compared with the experimental results measured at various pH values and free chlorine concentrations, the predictions calculated by this model agree quite well with the measured data. This indicates that the

201

model is useful for the estimate of the quantum yield of free chlorine decomposed, and the hypothesis of this model does not significantly affect its application.

In addition, three organic chemicals, *tert*-butanol, methanol and 1,4-dioxane, were respectively used to examine the effect of water quality on the quantum yield of the photolysis of free chlorine. It was observed that these organic compounds increased markedly the photodegradation quantum yield of free chlorine at pH 5. However, this study shows that the effects on the quantum yield vary for different organic compounds. For example, the photodegradation quantum yield at pH 5 is 2.4 ± 0.2 for a 6 mM free chlorine sample in DI water, but increases to 4.1 ± 0.5 for the same sample with 10 mM *tert*-butanol, to 7.0 ± 0.3 for 10 mM methanol and to 11.2 ± 0.5 for 10 mM 1,4-dioxane. But at pH 10, the addition of methanol was not observed to cause any rise of the photodegradation quantum yield as observed at pH 5. For instance, it was determined that the quantum yield at pH 10 was 1.2 ± 0.2 for a 6.0 mM free chlorine sample containing 50 mM methanol.

The photodegradation of free chlorine can be expressed as a first-order equation when its concentration is not very high. That is, the log decomposition of free chlorine exhibits a linear relation to the UV irradiation (fluence) absorbed. At a fluence of 400 J m^{-2}, the free chlorine is degraded only very slightly (~1%) in DI water when the concentration of free chlorine is not very high (~20 mg L^{-1}), but it can be distinctly consumed in the presence of some organics. Therefore, the presence of some organics in water could increase the sensitivity of free chlorine to UV light.

6.2.2 Factors influencing the quantum yield

In the study of the photodegradation quantum yield of free chlorine, it became clear that the quantum yield can be affected by organic materials, the pH and the concentration of free chlorine. However, in real operations, the concentration of free chlorine usually is not very high (~10 mg L^{-1}) and pH varies in the range of 6.5 to 8.5. Therefore, the effects of concentration and pH would not be quite significant. In order to make a detailed investigation on the photodegradation quantum yield of free chlorine, in this study, some other potential influencing factors on the quantum yield were examined.

Firstly, humic and alginic acids were used as TOC sources to simulate the natural organic materials (NOM) present in the influent of water utilities and the effect of the TOC on the quantum yield was examined again. With the TOC concentration ranging from 0 to 6.8 mg/L, it was observed that the quantum yield of free chlorine (3.0 ± 0.2 mg L^{-1}) increased from 1.1 ± 0.2 to 4.9 ± 0.4 under ambient condition. Obviously, the natural organic compounds also have a significant effect on the photodegradation quantum yield of free chlorine.

Due to the seasonal variation of the water temperature in most water utilities, the temperature also was studied as a potential influencing factor on the quantum yield of free chlorine decomposed. The experimental results obtained in this study show that the effect of temperature primarily depends on the water quality. When the free chlorine sample was prepared in DI water (with a TOC concentration <0.4 mg/L), the variation of temperature from about 2 to 22°C did not cause significant changes on the quantum yield of the photolysis of free chlorine. However, for the free chlorine sample with the TOC (humic acid and alginic acid) level of 3.4 mg/L, the quantum yield was observed to drop

203

from 3.4 ± 0.5 at 22°C to 1.7 ± 0.3 at 2°C. Thereby, it can be concluded that the experimental temperature has a significant effect on the photodegradation quantum yield of free chlorine when organic compounds are present;[21] otherwise, the effect is negligible.

For the consideration of using the proposed method in medium-pressure UV reactors, the dependence of quantum yield of free chlorine decomposed on the wavelength of UV light was investigated. In this study, it was found that the quantum yield did not change significantly for UV light ranging from 200 to 300 nm.

6.2.3 Photodegradation products in the photolysis of free chlorine

The disinfection by-products produced in the sequential process of chlorination and UV irradiation have been reported in abundant of studies, but few studies focused on the photodecomposition products directly generated from free chlorine. The time profiles of the photodegradation of free chlorine at pH 5 and pH 8.5 were performed and a chlorine (Cl) mass balance was examined. In this study, chloride (Cl^-) and chlorate (ClO_3^-) ions were detected in samples exposed to 254 nm UV light and the mass balance shows that they are the major photo-products. In the photodegradation of free chlorine in this study, no detectable chlorite (ClO_2^-) and perchlorate (ClO_4^-) were observed.

Some factors that may affect the photodecomposition of free chlorine were tested. When the concentration of free chlorine were altered from 3 to 55 mg L^{-1}, the photodegradation products (Cl^- and ClO_3^-) and their ratio (Cl^- to ClO_3^-) were independent of the change in concentration. However, it was observed that this ratio could be affected by the pH. In this study, when pH was varied from 5 to 10, the

---

[21] There could be exceptions for some organic compounds (e.g., acetate) which normally do not affect the photolysis of free chlorine.

204

production of chloride decreased from about 80 to 70% and that of chlorate correspondingly increased from about 20 to 30%. In addition, organic compounds present in the samples can also increase the production ratio of chloride for the photodegradation of free chlorine. Also, according to the photodegradation mechanism of aqueous OCl⁻ reported by Buxton and Subhani (1972), this study made a simple exploration concerning the photolysis of HOCl.

6.2.4 Validation of UV reactors by the photodegradation of free chlorine (PFC) method

In this research, the photodegradation of free chlorine (PFC) method was used to determine the fluences delivered in a bench-scale UV reactor for various operating conditions. The results were compared with fluences determined by the biodosimetry (BD) method using *B. subtilis* spores and a mathematical model (using the software *UVCalc*). Based on the experimental results, the reliability of the proposed PFC validation method was analyzed.

In general, in this research, the fluences obtained by the PFC method were very consistent with those obtained by the BD method. The operating conditions, such as the water quality (TOC), the UV transmittance and the flow rate, were not found to influence significantly the reliability of the proposed PFC method. The data obtained from the mathematical model usually were a somewhat larger than those obtained by the PFC and BD methods. The difference was observed to gradually decrease with the increasing flow rate. This reflected the hydrodynamic status in the experimental UV reactor. The higher the flow rate, the stronger the mixing intensity should be in the reactor. Generally speaking, the observations obtained in the bench-scale study indicate that the proposed

205

PFC validation method can account properly for the impact of the hydrodynamic status in UV reactors and works as well as the BD method for the validation of fluences delivered in UV reactors.

6.3 Recommendations

In order to examine the feasibility of the method using the PFC method to estimate the fluences delivered in UV reactors, this research investigated the photodegradation quantum yield of free chlorine for various conditions, the photodegradation products, and the reliability of the proposed PFC method. Based on the conclusions stated above, it is recommended that the following investigations should be performed in the further studies:

- Full-scale examination of the proposed PFC validation method. In this research, only a bench-scale UV reactor was used for the validation experiments, and the maximum flow rate tested in this research was about 9 L min^{-1}. However, in the real operations, the UV reactors should be much larger than the experimental one used here, and the flow rate also should be much higher than 9 L min^{-1}. The operating conditions in a full-scale application in practices could be more complex than those in laboratory bench-scale equipment. Accordingly, it is necessary to perform some full-scale examinations to test the effectiveness of the proposed PFC validation method before it can be employed to monitor the performance of UV reactors in water utilities.

- Application for the validation of medium-pressure UV reactors. In this research, a low-pressure UV reactor was used to examine the feasibility of proposed PFC method for the validation of UV reactors. Although UV wavelengths ranging

206

from 200 to 300 nm were studied for the effects on the photodegradation quantum yield of free chlorine, no tests on a medium pressure UV reactor were carried out. In practice, there are many water utilizes employing medium-pressure UV reactors for the drinking water MOR treatment. The working status of the medium-pressure UV reactors could have some differences (e.g., temperature and wavelength) from that of the low-pressure UV reactors. Thereby, it is important to perform a systematic study from bench-scale to full-scale to examine the suitability of the proposed PFC method for the monitoring of the performance of medium-pressure UV reactors.

- Application for the online monitoring of the performance of UV reactors. In this research, it was proposed that the PFC method could be applied for online monitoring of the performance of UV reactors; however, no experiments were performed to test this proposal. Since free chlorine is a common disinfectant and often found in the influent of UV treatment systems in drinking water treatment plants, and there is abundant commercial equipment available for the online monitoring of free chlorine concentration, the proposed PFC method should be readily applied for online monitoring of the UV fluence. In order to prove this supposition, one should establish an online validation system based on the proposed PFC method and carry out some experiments to verify the feasibility of this method.

- DBPs may be produced in the validation process by the proposed PFC method. Considerable studies have been reported about DBPs produced in the sequential disinfection process of chlorination and UV treatment. In addition, this study

investigated the photodegradation products directly generated from the photodegradation of free chlorine with 254 nm UV light. However, few researchers have examined the formation of DBPs in the pre-chlorinated UV irradiated water over long contact times. There are usually some natural organic materials present in the influent of water utilities, so the reactions occurring in the water pre-chlorinated followed by UV treatment would be very complicated. The rates of some reactions, which could result in some harmful DBPs, could be very slow. Therefore, considering that the drinking water may stay in the distribution system for several days after the water treatment process, it is necessary to determine the formation of DBPs in the pre-chlorinated UV irradiated water over a long contact time.